Dissecting the role of dimeric MukF in chromosome organisation by *Escherichia coli* MukBEF

Rachel A. Baker

Department of Biochemistry

The Queen's College

University of Oxford

Trinity 2019

This thesis is submitted to the Department of Biochemistry at the University of Oxford, in partial fulfilment of the requirements for the degree of Masters by Research.

Abstract

The organisation and segregation of chromosomes from all domains of life are mediated by the architecturally conserved Structural Maintenance of Chromosomes (SMC) proteins and their accessory factors. In *Escherichia coli*, the distantly related complex MukBEF retains the distinctive tripartite ring structure that has been proposed to topologically entrap DNA. Cyclical loading and unloading of DNA is regulated by ATP binding and hydrolysis, both of which are essential for SMC function. The kleisin MukF stimulates MukB ATPase activity. Uniquely, MukF forms stable dimers through the N-terminal Winged Helix Domain (WHD), thus potentially allowing for the formation of higher order complexes. Null mutations in any one of the *mukBEF* genes results in temperature sensitivity in rich media, disturbed organisation of the chromosome and anucleate cell production even under permissive conditions.

In this study a tripartite approach of biochemistry, genetics and *in vivo* imaging, provides insight into the functional importance of dimeric MukF. I have identified hydrophobic interactions between protomers that contribute to MukF dimerisation. *In vitro* assays show that full length MukF monomers are folded and stimulate MukB ATPase to wild type levels. However, *in vivo,* MukF dimerisation is essential for MukBEF function, as judged by the ΔMukBEF phenotype of temperature sensitivity in growth on rich media. Epifluorescence image analysis and Photoactivatable Localisation Microscopy (PALM) data indicate that chromosome interaction of MukBEF complexes formed with monomeric MukF is defective. Furthermore, an artificial dimerisation domain fails to rescue the ΔMukBEF phenotype. I propose that the formation of dimers of dimers is a prerequisite for the ability of MukBEF to transport chromosomal DNA by a “rope-climber” model and that the dimerisation domain may play a dynamic role in the coordination of MukBEF complexes.

Authorship Declaration

I declare that this thesis is entirely my own work except the cases described below and throughout the thesis. This thesis has not been submitted for any other degree at the University of Oxford or any other institution.

Experiments performed by others

SEC-MALS and CD was performed by Dr David Staunton, in-house Biophysics suite.

Mass Spectrometry was performed by Dr Sabrina Liberatori, in-house advanced proteomics facility.

PALM analysis and script by Dr Jarno Mäkelä.

Script for spot detection of epifluorescence images by Dr Jarno Mäkelä.

Constructs obtained from others

See Chapter 2, materials.

Acknowledgements

Over 25 years ago I vowed never to touch a pipette again, then, I arrived in Oxford and met Professor Sherratt, a renewed love for science began. Of course, I would like to start by thanking ‘The Boss’. Dave’s infectious enthusiasm, thirst for knowledge and much needed patience has been an incalculable influence on many great scientist’s careers and without whom this chapter in my life would have been impossible. It has been a privilege to be part of the Sherratt family, even more so, to be the last student...possibly?? I would also like to thank Lidia, whose support, both intellectually and personally is deeply appreciated. I have had the pleasure of working with many talented people and life has been enriched by cultures from all over the world. Sadly, I haven’t space to thank everyone, but Bernard, Bilou and family deserve a special mention, our children grew up together, we have great memories and I hope to make many more. Malcolm, I would have achieved more without you, but it would not have been as much fun. Vik, Heather and Batman!! I love you!...KK, you and your ‘Viking’ make a fabulous pair, thank you Jarno for remaining calm in the face of adversity! Kasia Z, the hottest ‘kochanie’ I have ever worked with, I owe you EVERYTHING. Gemma, I can never repay you for all your help, but I will try…many beers to come! You have become a great friend, split by a generation but joint in spirit. Finally, my family. Mamma e Papà, you are my foundation. James, Michelle, Grace and Jessica, the best! My children Emily and Josh, thank you, with Jason and Kate you have looked after me over the past year, I am SO proud of both of you. And most importantly, Simon, you are a tower of strength and calm, thank you for putting up with the tears and tantrums. Now… let’s PARTY!!!

List of Abbreviations

ABC	ATP-binding cassette
ADP	adenosine diphosphate
ATP	adenosine triphosphate
B. subtilis	*Bacillus Subtilis*
C. crescentus	*Caulobacter crescentus*
C. thermophilum	*Chaetomium thermophilum*
C-Ter	C-Terminal
Da	Dalton
DMSO	dimethylsulfoxide
DNA	deoxyribonucleic acid
dNTP	deoxyribonucleotide
DTT	dithiothreitol
dsDNA	double-stranded DNA
E. coli	*Escherichia coli*
EDTA	ethylenediaminetetraacetic acid
4HB	4-helix bundle
HEPES	4-(2-hydroxyethyl)-1-piperazineethanesulfonic acid
6xhis	6 X histidine tag
HPLC	high-performance liquid chromatography
IPTG	isopropyl β-D-1-thiogalactopyranoside
K_d	dissociation constant
LB	Luria Bertani
M	middle MukF domain

MALS	Multi-Angle Light Scattering
MukFd	Dimeric MukF (WT)
MukFm	Monomeric MukF
MukFsm	Single mutation in MukF dimerisation domain
MW	molecular weight
MWCO	molecular weight cut-off
NADH	nicotinamide adenine dinucleotide
N-Ter	N terminal
P. aeruginosa	*Pseudomonas aeruginosa*
OD_{600}	optical density at 600nm
ON	overnight
Ori	origin of replication
P*ara*	promoter inducible by arabinose
PALM	photoactivatable localisation microscopy
PCR	polymerase chain reaction
PAGE	polyacrylamide gel electrophoresis
PDB	Protein Data Bank
RT	room temperature
S. cerevisiae	*Saccharomyces cerevisiae*
SDS	sodium dodecyl sulfate
SDS-PAGE	sodium dodecyl sulfate polyacrylamide gel electrophoresis
SEC	Size Exclusion Chromatography
SMC	Structural Maintenance of Chromosomes
ssDNA	single-stranded DNA

TAE	Tris, acetic acid and EDTA buffer
ter	terminus
TopoIV	topoisomerase IV
Tris	tris(hydroxymethyl)aminomethane
WHD	Winged Helix Domain
WT	wild-type

Table of Contents

List of Figures

List of Tables

Chapter 1

Introduction

1.1 Life requires order

All life requires genetic information to be faithfully transferred from mother to daughter. In the turbulent environment of the cell, DNA needs to be organised and compacted in a way that ensures functionality is preserved and processes such as replication and transcription are unimpeded. Electron microscopy images of gently lysed *Escherichia coli* cells have demonstrated that the nucleoid is packaged in a non-random fashion (Kavenhoff and Bowen, 1976). These observations inspired a 'scaffold' model whereby the *E. coli* chromosome is organised into a series of loops anchored by a central proteinaceous core (Saitoh *et al*. 1995). Numerous Nucleoid Associated Proteins (NAPS), able to bend and bridge DNA and are expected to stabilise chromosomal loops (Browning *et al.* 2010). However, random collisions cannot explain the fundamental question of how chromosomes remain discrete structures. It was therefore suggested that the chromosome is somehow 'reeled' in by an active process, so forming a series of loops. This process is now thought to be performed by a group of proteins known as the Structural Maintenance of Chromosome proteins (SMC), which are ubiquitous across all domains of life (Hirano, 1999).

SMCs and their accessory proteins have key roles in chromosome management. They have been shown to be involved in processes such as regulation of gene expression and DNA repair, as well as longitudinal chromosome compaction and individualisation (Nasmyth and Haering, 2005). SMCs are large elongated proteins that form v-shaped dimers; the extreme N- and C- termini come together to form a globular ATP-binding 'head'. The intervening helical polypeptide is hinged centrally by a dimerisation domain, the 'hinge', and folds back upon itself to form an antiparallel coiled-coil, typically 50nm in length (Niki *et al.* 1991, 1992:

Hirano and Mitchison, 1994; Melby *et al.* 1998; Haering *et al*. 2002; Hirano and Hirano 2002) (Figure 1.i). The SMC heads are bridged by a member of the kleisin superfamily, which binds asymmetrically, resulting in a closed ring-like structure typical of all SMC complexes (Schleiffer *et al.* 2003). Upon ATP binding to the SMC heads, the kleisin facilitates head engagement and thus the two composite sites become catalytically active (Hirano *et al.* 2001). Subsequently, the head domains separate upon ATP hydrolysis (Hirano 2006; Ivanov and Nasmyth 2005). A large body of evidence has suggested that both the topological entrapment and the release of DNA by SMC complexes are dependent on cycles of ATP binding and hydrolysis (Arumugam *et al.* 2003; Haering *et al*. 2002; Gruber *et al*. 2003; Haering *et al.* 2008; Nasmyth, 2001; Wilhelm *et al.* 2015).

The large proteinaceous SMC ring is then bound by other non-SMC proteins that predominantly interact with the central region of the kleisin. Together these accessory factors seem to regulate and direct the function of SMCs (Yamazoe *et al.* 1999; Ono *et al.* 2003; Haering *et al*. 2002). The HAWK complex (HEAT repeat subunits containing proteins associated with kleisins) associates with eukaryotic SMCs whereas KITE proteins (kleisin interacting winged-helix tandem elements) interact predominantly with archaeal and bacterial SMCs and the eukaryotic Smc5-6 complex (Palecek and Gruber, 2015; Wells *et al.* 2017).

Most evidence for chromosome management has come from eukaryotic systems where SMCs are heterodimeric. Along with their subunits, SMCs form three types of complexes: cohesin; condensin and Smc5-6 complexes, each of which have evolved with different functions. Cohesin is responsible for holding sister chromatids together whilst they align during metaphase (Michaelis *et al.*1997). Additionally, cohesin complexes accumulate at insulator sights and support gene

regulation during interphase. This is a process of dynamic compartmentalisation of the chromosome into topologically associated domains (TADS) (reviewed in Merkenschlager and Nora, 2016). Condensin has been identified as essential for chromosome compaction and individualisation during mitosis (Ono *et al.* 2003) as well as being involved in gene regulation, the DNA-damage response and DNA repair (Hirano, 2012). Finally, the Smc5-6 complex is involved in double-stranded break repair by homologous replication and resolution of topological entanglements resulting from replication (Lehmann *et al.* 1995; Jeppsson *et al.* 2014).

In contrast to their heterodimeric eukaryotic counterparts, prokaryotic SMCs or SMC-related proteins are homodimeric and to date three families of condensin-like complexes have been identified. Most bacteria encode for the protein Smc (Strunnikov *et al.* 1993) which is bridged by the kleisin ScpA (Segregation and condensation protein A) and KITE ScpB (Mascarenhas *et al*. 2002; Soppa *et al*. 2002; Bürmann *et al.* 2013). These complexes are required for the resolution and segregation of newly replicated sister origins (Wang *et al.* 2014).

In *E. coli* and related γ-proteobacteria, the condensin-like MukB shares an operon with its accessory factors MukE (KITE) and MukF (kleisin) (Niki *et al.*1991, 1992; Yamanaka *et al*. 1996). More recently, a novel family of SMC-like proteins have been described. Unlike *E. coli* and *Bacillus subtilis* that either encode MukBEF or SMC-ScpAB respectively, *Pseudomonas aeruginosa* carries two condensins, the canonical SMC-ScpAB and a novel family, identified as MksBEF (MukBEF-like SMC) (Pertushenko *et al*. 2011). The *mks* locus has the same operon organisation as MukBEF. The distantly related MksBEF is thought to have a complementary role in chromosome management.

1.2 MukBEF is different to other SMC complexes

The *E. coli* SMC MukB was first identified by Niki *et al.* (1991) and in common with other SMCs, the N- and C-terminal domains of MukB contain the Walker A and Walker B motifs respectively, which once juxtaposed, form ATP binding sites on the surface of the globular 'head' (Woo *et al.* 2009). Despite low primary sequence homology with other SMCs, MukBEF complexes share the distinctive SMC complex architecture, with one striking difference. Curiously, and unique amongst the kleisins, MukF forms stable dimers through its N-terminal domain (Schleiffer *et al*. 2003; Fezzie-Fennell *et al.* 2005) so potentially facilitates the dimerisation of the total MukBEF complex (Figure 1.i). In this work, a tripartite approach of biochemistry, genetics and *in vivo* imaging provides insight into the functional importance of dimeric MukF.

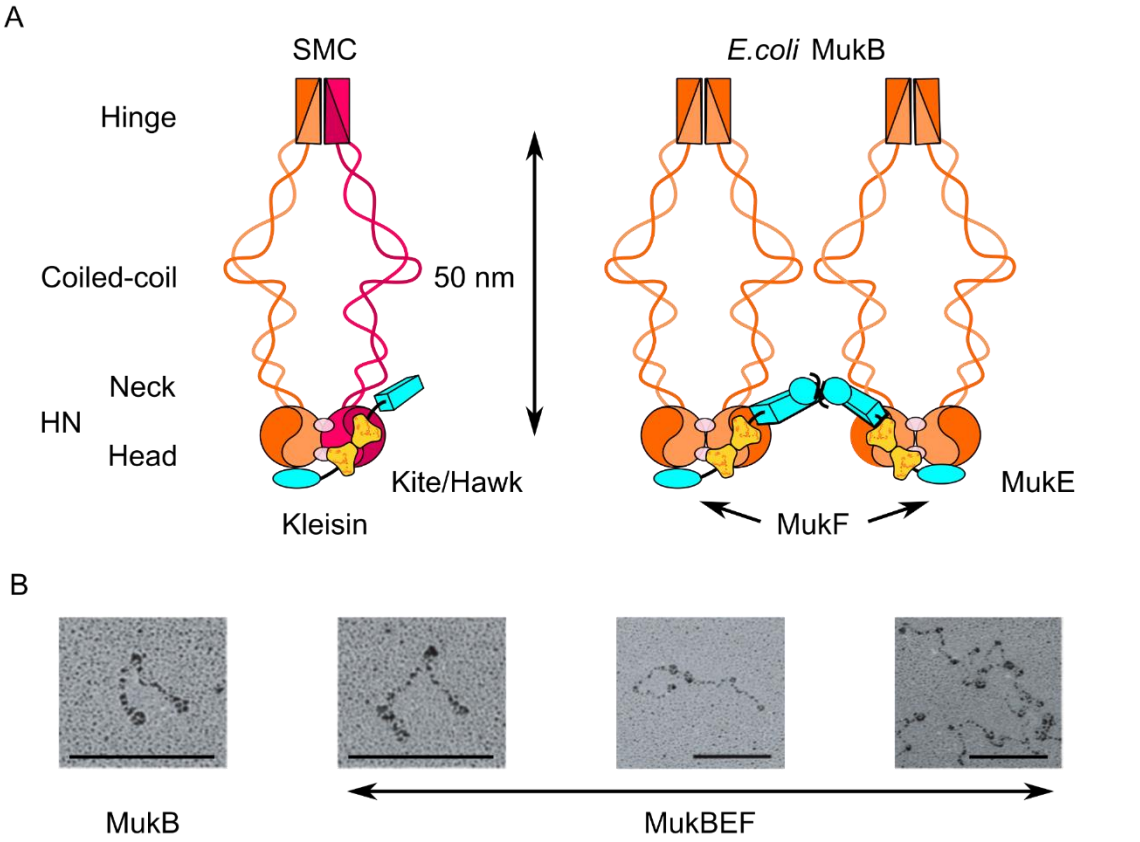

Figure 1.i - A. Schematic of generic SMCs and MukBEF. B. Electron microscopy images of MukB and MukBEF.

Exclusive to MukF orthologs, the dimerisation domain allows for oligomerisation of MukBEF complexes. Scale bars represent 1000 Å. Images were taken in the absence of DNA and ATP. In ~1% of MukB molecules, i-shaped structures were observed which were about half the length of MukB homodimer, suggesting self-folding. This is discussed further in Chapter 6. Adapted from Matoba *et al*. 2005.

Electron microscopy has revealed that MukBEF complexes can form multimers resulting either in fiber- or rosette-like structures (Figure 1.i) (Matoba *et al.* 2005). The formation of oligomeric MukBEF complexes or “dimer of dimers” has been supported by evidence from *in vivo* work (Badrinarayanan *et al.* 2012a) as well

as *in vitro* data (Rajasekar *et al*. 2019). So how does the dimer of dimers relate to function?

In wild type *E. coli* cells, the 4.6 Mbp circular chromosome is replicated bi-directionally, from a unique origin of replication (*oriC*) located at the mid-cell and terminating at a broad terminus region (*ter*) which is diametrically opposite (Niki and Hiraga, 1998). Genetic loci occupy specific addresses within the cell and these move during the cell cycle (Wang *et al.* 2005). Post replication, daughter *oriC*s move to the cell quarter position followed by the remaining chromosome. Left and right replichores, or 'arms', occupy separate halves of the cell (Niki *et al.* 2000). Null mutations in any one of the *mukBEF* genes results in inviability at higher temperatures in rich media, as well as increased production of anucleate cells in permissive growth conditions and a global disorganisation of the chromosome (Niki *et al.* 1991; Yamanaka *et al*. 1996; Britton *et al* 1998, Danilova *et al.* 2007). The transverse Left-Right organisation is disrupted in MukBEF mutants, resulting in arms that are extended from pole to pole with the *ori* region located at the old pole (Fig.1.ii). Ohsumi *et al.* (2001) observed that MukBEF complexes form discrete foci, dependent on the expression of MukB, MukE and MukF. This prompted further investigation into the relationships between specific genetic loci positioning and MukBEF complexes (Danilova *et al*. 2007). This study concluded that MukBEF is not simply involved in the topological re-modelling required for efficient segregation but may also be important in positioning the *oriC* region, either by chance, or, by active, directional translocation (Hofman *et al*. 2018; Mäkelä and Sherratt, 2019).

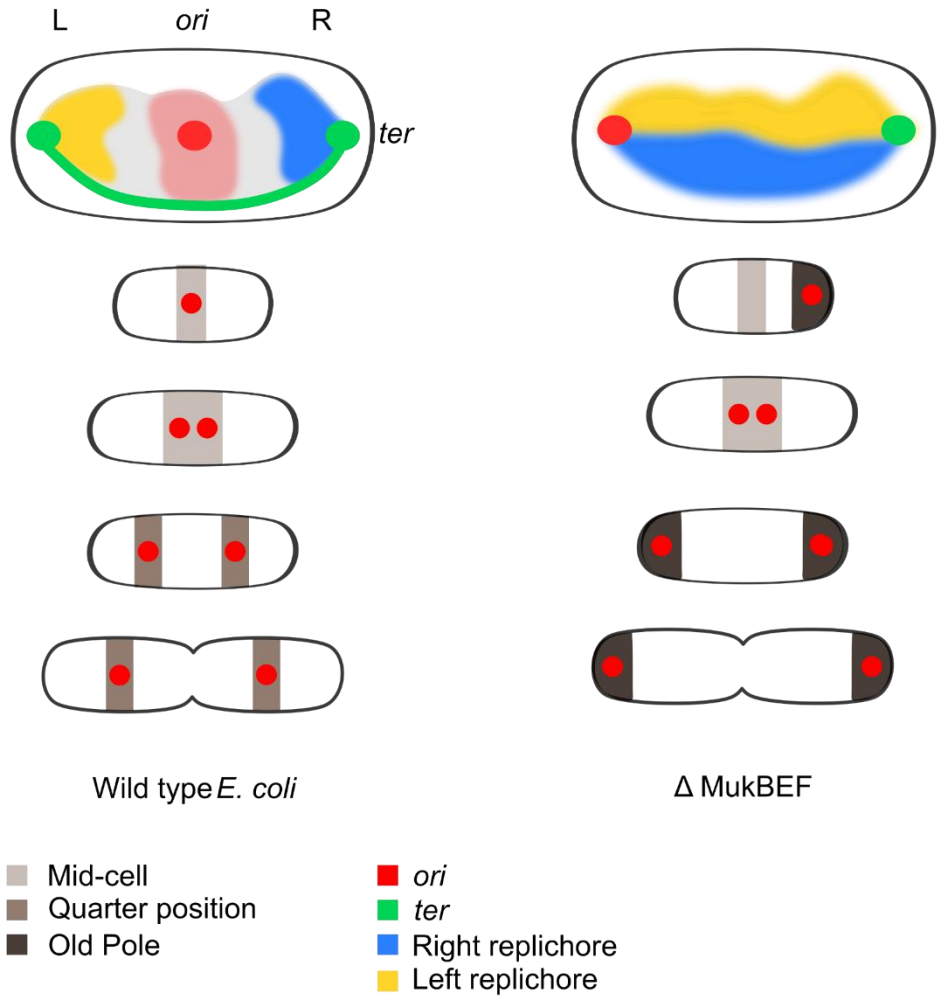

Figure 1.ii - Schematic of macrodomain organisation and ori positioning during division of wild type *E. coli* and cells deleted for *mukBEF*.

Adapted from Danilova *et al*. 2007 and Reyes-Lamothe and Sherratt 2019.

Bacterial species that have MukBEF rather than the canonical SMC complexes also encode for MatP, suggesting a co-evolutionary pressure. MatP is known to bind to *mat*S sites in the chromosome replication terminus (*ter*) (Mercier *et al.* 2008) and is thought to displace MukB from this region (Mäkelä and Sherratt 2019). Ancient interactions between MukBEF, MatP and the decatanase Topoisomerase IV demonstrate a functional interplay between chromosome

organisation and topological simplification (Nolivos *et al.* 2016; Nicolas *et al.* 2014; Zawadzki *et al*. 2015).

The question is...how do these complexes manage chromosomes and is there a unifying mechanism reflected by the universal architecture observed amongst SMC complexes throughout all domains of life? I don't *think* the answer is 42… (Adams 1979).

1.3 The art of loop extrusion

Arguably the most efficient way of compacting DNA in a manner that maintains longitudinal order is described by the 'loop extrusion' model. A segment of DNA is captured and by a mechanism that is dependent upon ATP hydrolysis, a loop is processively enlarged so that distant loci are brought together.

SMCs and their accessory factors have been implicated in loop forming activities across chromosomes, with an ever-mounting body of evidence gathered from *in vivo, in vitro and in silico* studies (Nasmyth, 2001; Alpour and Marko, 2012; Wang *et al.* 2017; Terawaka *et al*. 2017; Ganji *et al.* 2018). Other models such as stochastic crosslinking have been proposed whereby segments of DNA in close proximity are bridged (Thadani *et al*. 2012), however, simple bridging is unable to recapitulate the behaviour of SMC complexes in chromosome organisation (Mäkelä and Sherratt, 2019). Although likely a part of the story, if SMCs made exclusively stochastic contacts between DNA segments, complexes would be observed throughout the chromosome. The observation that SMCs localise suggests that these complexes either interact with specific DNA binding sites or have an ability to translocate. Furthermore, random topological entrapments

would result in *in trans* interactions that would prevent chromosome segregation. So how are loops formed?

Dwell times and processivity vary, dependent upon the velocity of extrusion and potentially the number of complexes involved, be it as oligomers or multiples of individual complexes. SMC complexes exhibit a low rate of ATP hydrolysis compared to other DNA translocating motors, note MukBEF hydrolyses ATP at a rate of ~0.3 ATP molecules/s (Zawadzka *et al*. 2018), versus the bacterial translocase Ftsk which hydrolyses 2.600 ATP molecules/s (Graham *et al*. 2010). This makes it difficult to reconcile the high distances covered in the short time required for propagation. Hi-C data show, *in vivo*, that bacterial SMCs manage DNA organisation at a rate of up to 600 bp/s (Wang *et al*. 2017)**.** External motors such as RNAPs have been implicated in providing the driving force, however, evidence that TADs are formed in the absence of transcription, suggests that although a possibility, this is not exclusively the case (Vian *et al*. 2018). Furthermore, transcription cannot give the rates that have been inferred. So how do modest ATPase levels translate into global chromosome management?

Although the loop extrusion model is considered universal, several mechanisms have been suggested and are thought to differ between complexes (Figure 1.iii).

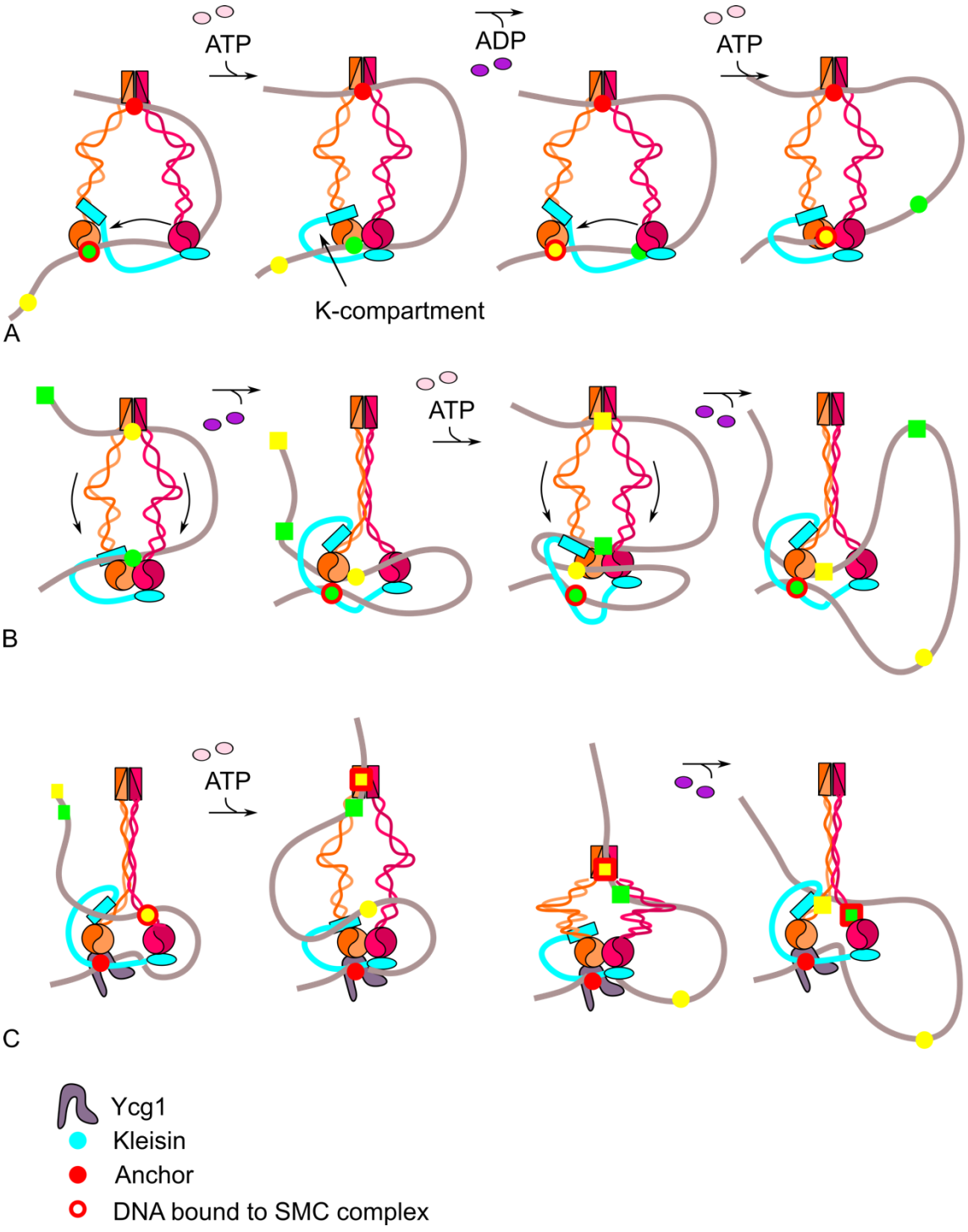

Figure 1.iii - Models proposed for active SMC-driven loop extrusion.

Model **A**- **'Walking'** model. Model **B**- **DNA pumping / segment capture** (Minnen *et al*. 2016; Diebold-Durand *et al*. 2017) requires the ATPase dependent zipping up of the coiled-coils, so pushing the entrapped DNA into the K-compartment through the disengaged heads. The second round of hydrolysis then enlarges the loop. Model **C**- **Extended scrunching**. This model relies on two DNA binding sites at the SMC heads

and at the hinge made accessible through ATPase-dependent conformational changes in the coiled-coils. The folded SMC (Bürmann *et al*. 2019) passes DNA from the hinge to head proximal DNA binding sites. Anchored by the Brn1-Ycg1 condensin complex subunits, the condensin then drags in the DNA loop as it translocates (Kschonsak *et al*. 2017). A, B and C Adapted from Hassler *et al*. (2018).

All SMCs are thought to use ATP binding and hydrolysis to induce the conformational changes required for loop processivity. These variations in processivity are dependent upon ATP turnover and the stability of complexes on DNA. Members of the kleisin superfamily and their associated HAWK/KITE complexes are considered to regulate both ATP turnover and DNA interactions (summarised by Haering and Gruber, 2016). Terawaka *et al.* (2017) have shown *in vitro* that condensin purified from *S. cerevisiae* can travel ≥10 kb in an ATP-dependent and step-wise manner (~30 bp per molecule of ATP). The step sizes measured are comparable to the length of its coiled-coil and produced a rate of movement of 60 bp/s along doubly-tethered DNA. The 'sequential walking' model (Fig3.iiiA) may account for stepped translocation observed, one SMC head attaches to the DNA allowing for the second head to reach and bind a distant segment. Subsequent conformational changes release the first head, allowing it to 'step' forward analogous to cytoskeletal protein models (Peterson, 1994). Further investigations whereby a second DNA molecule was provided *in trans* led the authors to propose that DNA transport can give rise to the formation of loops. Direct contacts between the SMC complex and the DNA, anchors the base of the loop, then one piece of DNA is moved relative to the other (Terawaka *et al.* 2017). The 'DNA pumping' model proposed (Figure 3.iii B) suggests that a segment of DNA is pseudo-topologically captured and pushed into the second compartment

by the ‘zipping up’ of the coils upon ATP hydrolysis. A second round of ATP binding engages heads and coils are parted so capturing a second segment of DNA. ATP hydrolysis again results in the coils being ‘zipped up’, which allows the second segment to join the first loop that is confined by the engagement of ATP bound SMC heads and the kleisin (Diebold-Durand *et al*. 2017). The ‘extended scrunching’ model (Figure 3.iiiC) takes into consideration the alternative view that the coils are highly flexible (Ryu *et al.* 2019), adopting a rod or collapsed and open conformation dependent upon ATP hydrolysis. An anchor site formed by the kleisin and HAWK ensures DNA is reeled into a loop as it translocates.

Could MukBEF complexes also transport DNA, in a step-wise manner dependent upon MukF dimerisation, described by the ‘rope-climber‘ model (Badrinarayanan *et al.* 2012a)? In such a case, as in the ‘walking model’, one MukBEF complex would be tethered to DNA allowing for the second complex to trap a distant segment of the chromosome (Figure 1.iv).

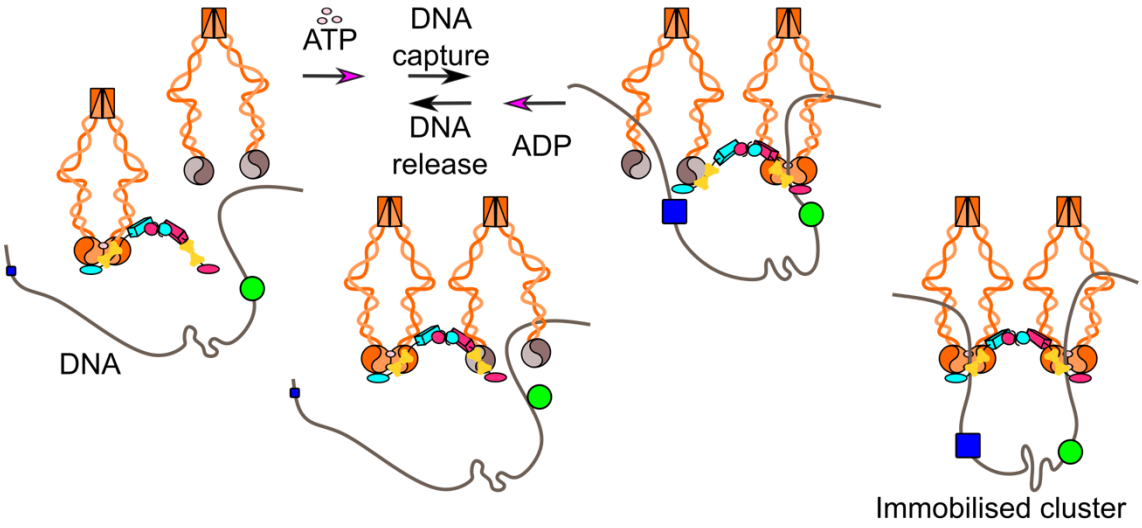

Figure 1.iv - Rope-climber model.

Dimeric MukF allows for the binding of a second MukB dimer. Upon DNA 'loading' a second DNA segment can then be captured so bringing together distant chromosomal loci (Badrinarayanan *et al.* 2012a). Sequential ATP binding and hydrolysis of two complexes allows clusters to form. Orange MukB heads show ATP bound state, fawn MukB heads show no nucleotide or ADP bound.

1.4 The aim of this thesis

Through the disruption of MukF dimerisation, I hoped to gain further insight into the mechanisms by which MukBEF complexes manage the chromosome, thereby allowing for faithful replication and efficient segregation. It is potentially through the dimerisation of MukF that multimerisation of MukBEF complexes, referred to as the formation of 'dimer of dimers', is permissible. I also explored the potential coordination of MukBEF complexes through dynamic interactions directed by the dimerisation domain.

1.5 The structure of MukF, the obligate dimer

In common with all other SMC complexes, the kleisin MukF bridges the MukB heads asymmetrically to form a proteinaceous ring (Burmann *et al.* 2013; Gligoris *et al*. 2014; Gligoris and Löwe, 2016; Gruber *et al.* 2003; Haering *et al.* 2004; Huis in't Veld *et al.* 2014). However, striking structural features set it apart from other SMC complexes and suggest a model of chromosome management that may be exclusive to MukBEF. The N-terminal region, spanning residues 1-287, whose structure was solved by Fennell-Fezzie *et al.* (2005), demonstrates a high structural homology between MukF and other kleisins. However, unique to MukF orthologs, there is an extended N-terminal helix α1, and beta strand β1 which together stand alone. These are followed by a Winged Helix Domain (WHD), which shows structural similarity to the C-terminal domain of Scc1 (cohesin-associated kleisin). A doubly domain swapped quaternary arrangement ensures the stability of a highly entwined pair of protomers, suggesting that an obligate dimer is required for function.

MukF comprises four distinct domains, an N-WHD, (residues 1-120), a four-helix bundle (residues 121-291), a middle region (residues 292-354) and finally a C-terminal WHD (residues 355-440) (Fezzie-Fennell *et al.* 2005; Woo *et al*. 2009) (Fig. 1.v). Helix α1 makes no intramolecular contacts and by cupping the N-WHD of its partner subunit, it buries a portion of helix α2 so burying the hydrophobic core of this domain. The following β1 strand forms an antiparallel beta sheet with its partner protomer. Adjacent to the C-terminal of the N-WHD, a second domain swap leads to a 4-helix bundle (4-HB), known to interact with the coiled-coil proximal region of MukB C-terminal head 'neck' and participate in stimulation of

MukB's ATPase activity (Zawadzka *et al*. 2018) (Figure 1.vi). This interaction does not interfere with the stable dimerisation of MukF.

The middle region of MukF is composed of an α helix, two β strands and a flexible linker. The acidic middle region (M) interacts avidly with the dimeric *E. coli* KITE, MukE (Yamazoe *et al.* 1999; Petrushenko *et al.* 2006; Gloyd *et al.* 2007; Rajasekar *et al.* 2019), with the effect of elongating the MukF molecule and stabilising the binding of MukF in a *trans*- configuration to two MukB globular heads. Co-crystals of MukE and MukF (Woo *et al.* 2009) show that MukE binds asymmetrically. The first MukE (a) interacts extensively with the middle region of MukF, whereas the second MukE (b) has limited interactions with strand β5. C-terminal to the flexible linker, a globular WHD has been shown to interact with MukB 'cap' or C-terminal globular domain, distal to the emerging coil-coiled (Figure 1.vi) (Woo *et al*. 2009; Zawadzka *et al.* 2018).

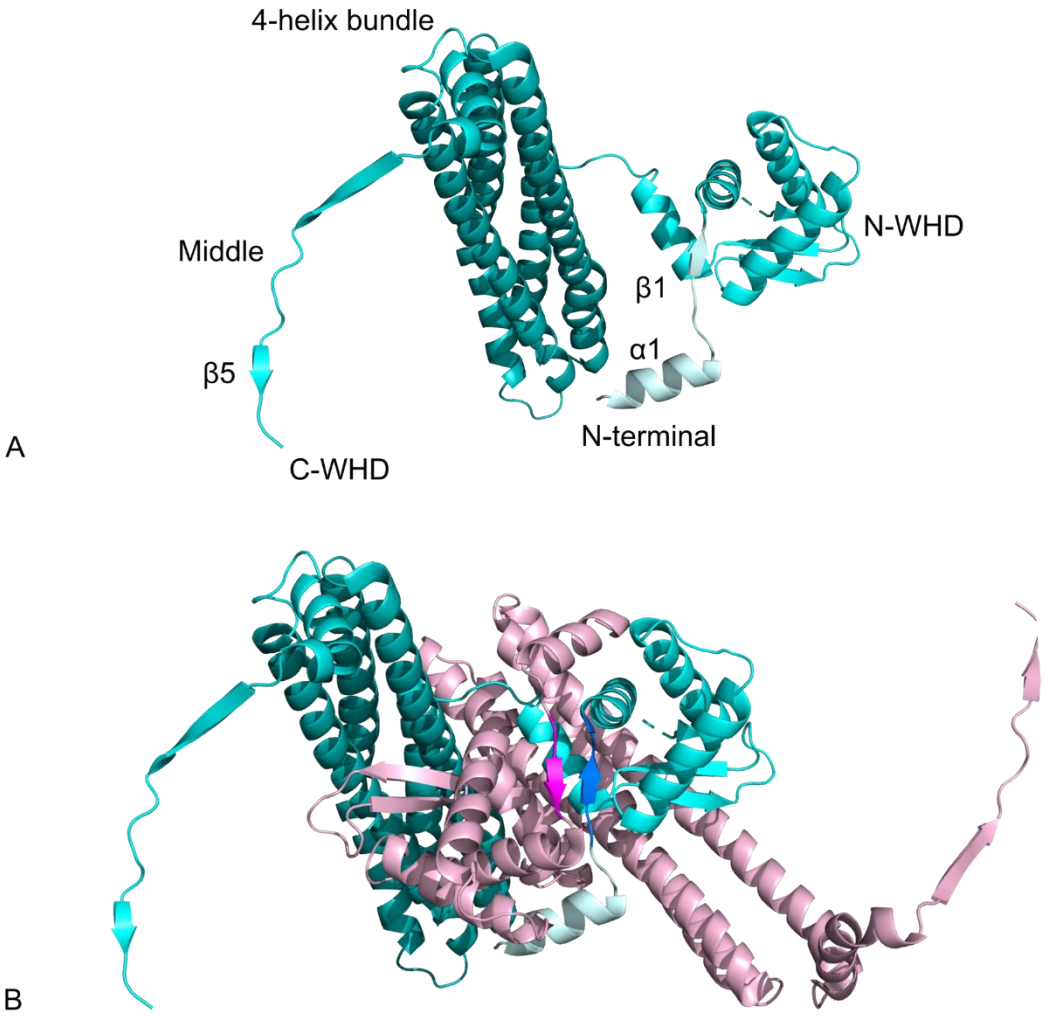

Figure 1.v - A. Crystal structure of a single MukF protomer. B. Entwined dimer showing one protomer in cyan and its partner in pink.

The antiparallel β sheet between the two MukF monomers is shown in magenta and marine. Adapted from Woo *et al*. 2009 using PDB entry 3EUH.

MukF stimulates the ATP hydrolysis activity of MukB. Upon ATP binding and head engagement, the MukF C-terminal WHD is sterically occluded and displaced by the linker, with the effect of transiently opening the MukBEF ring. In turn, this potentially allows for topological entrapment of DNA. Interactions of the MukF N- and C-terminal domains with MukB are broken and reformed during cycles of ATP binding and hydrolysis. This sequence of events is crucial for

formation of MukBEF clusters on the chromosome (Badrinarayanan *et al.* 2012a; Zawadzka *et al*. 2018).

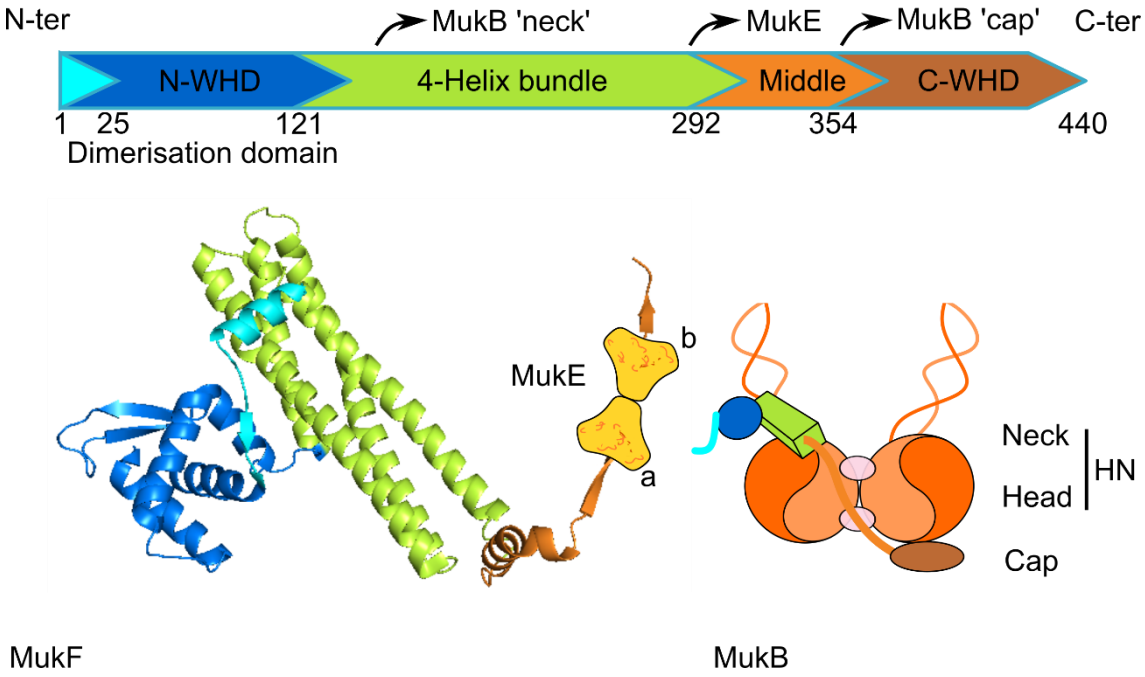

Figure 1.vi - Cartoon of MukF and its four distinctly folded domains.

Structural information derived from co-crystals of MukB, MukE and MukF from Haemophilus ducreyi, an organism that has >60% sequence identity to E. coli. Adapted from Woo *et al*. 2009 using PDB entry 3EUH. The MukF 4-HB and C-WHD interact with the MukB neck and cap, respectively.

1.6 Summary

In this work I address the question of whether the management of the *E. coli* chromosome by MukBEF is reliant upon the kleisin MukF being dimeric. I demonstrate that MukF dimerisation is essential. In allowing for the formation of dimers of dimers, I suggest that MukF dimerisation is a prerequisite for the step-wise transport of DNA by MukBEF complexes and so promotes long-range chromosome interactions. In turn, correct positioning of chromosomal loci and

promotion of orderly topological simplification, ensures that factors involved in the faithful propagation of genetic material proceed efficiently. Furthermore, I propose that through the dimerisation domain of MukF, ATPase events catalysed by MukB may result in sequential conformational changes that coordinate MukBEF complexes.

In Chapter 3, I isolate and characterise monomeric MukF. In Chapter 4, I describe the perturbed interaction of monomeric MukF with the chromosome. Chapter 5 explores the possibility of a dynamic functional role by the introduction of a synthetic dimerisation domain.

Chapter 2

Materials and Methods

2.1 Strains

All strains that were used in this work are *Escherichia coli* background and AB1157 derived unless stated otherwise. Strain C3013I was used for recombinant protein expression, and NEB5α for cloning and DNA propagation.

Table 2.i - List of derivatives and strains constructed for this work

Strain	Genotype	Origin
Derivatives and strains used for recombinant overexpression and cloning		
Ab1157	*thr-1, araC14, leuB6(Am), Δ(gpt-proA)62, lacY1, tsx-33, qsr'-0, glnV44(AS), galK2(Oc), LAM-, Rac-0, hisG4(Oc), rfbC1, mgl-51, rpoS396(Am), rpsL31(strR), kdgK51, xylA5, mtl-1, argE3(Oc), thi-1.* K12 derivative	Bachmann, 1972.
C3013I	*MiniF lysY lacIq(Cam^R) / fhuA2 lacZ::T7 gene1 [lon] ompT gal sulA11 R(mcr-73::miniTn10--TetS)2 [dcm] R(zgb-210::Tn10--TetS) endA1 Δ(mcrC-mrr) 114::IS10*. BL21 derivative	NEB
FK01	T7 Express *lysY/I^q mukB*-3XFLAG-kan C3031I derivative	Zawadzka *et al.* 2018
C2987H	*fhuA2 Δ(argF-lacZ)U169 phoA glnV44 Φ80 Δ(lacZ)M15 gyrA96 recA1 relA1 endA1 thi-1 hsdR17. DH*5α	NEB
Strains for complementation assays		
Ab233b	Δ*mukF*::kan *mukB*-GFP	Nolivos *et al.* 2016
Strains for microscopy		

SN182	*ori1 (lacO), ter3 TetR*-mCerulean and *LacI*-mCherry. *mukB Ypet* Kn^R	Nolivos *et al.* 2016
Ab256	PAmCherry-*mukF*	Anjana Badrinarayanan
Background and strains constructed for this work		
BL05	PAra-*mukF* cat:: Δ *argE*	Rodrigo Reyes-Lamothe
RRL252	Δ*mukF*::Kan PAra-*mukF* cat::Δ *argE*	Rodrigo Reyes-Lamothe
Ab238	PAmCherry-*mukB*	Anjana Badrinarayanan
KK132	*mukB-yPet, Kn^R-PAmCherry-mukFmono*	Kasia Ginda-Mäkelä
RAB02	Δ*mukF*::Kan PAra-*mukF* cat::Δ *argE* *mukB*-PAmCherry	This work
RAB03	Δ*mukF*:: Kan *mukB*-PAmCherry	This work
RAB05	Δ*mukF*:: Kan *mukB* ^{EQ} PAmCherry	This work

2.2 DNA reagents for mutagenesis and recombineering

2.2.1 Oligonucleotides

All oligonucleotides (written 5'-3' orientation) were sourced from Eurogentec and purified by reverse phase chromatography (RP-cartridge Gold™). For site directed mutagenesis, oligonucleotides were designed using the NEBase ChangerTM tool designed for Q5® Site-Directed Mutagenesis Kit (NEB E0554).

Table 2.ii - List of oligonucleotides used in strain construction and site-directed mutagenesis

Name	Description	Sequence
KK08	*mukB* 3921Fw	CTTCTCGGAAGCGCTGGCGA
KK17	*mukB*NOSTOP-contr	ACTCGCCTGAGAAGGCGCTTC
KK21	*mukB* 3791Fw	GTATCGTTTGGTCAGGTGAACAG
KK27	(*SmtA*)KnLredFw	GTTATATTCATGTCACCGCGCGCAAACCGCAGCAAGGATAAAGTATGACGATTGTGTAGGCTGGAGCTGCTTC
KK29	*mukF* Rv	TCAATATTTGTCGATGACATGCGC
KK42	(pnat)*smtA*ENDFw	TCAGAAAACGTCTTAGCCAACCGGTGGAGAAAGCATGAATTAGAAACGCGTTATTGCCG
KK58	*mukE*end Rv	TCAACGATGAAACCGAAGAGAATCA
JMP11	*mukB* C-ter Fw	AATTGTGTGAGCGTTTGCAAATGCA
JMP12	Down *mukB* C-term	GTACAACGCCAATACTCACGAAAGT
Site-directed mutagenesis		
RB01	sFIT22TFw	GACTTCTCCACCTCGCTGCCG
RB02	sFIT22TRv	ATTTTTTCTGGCCCAGGCAAC
RB03	*mukF*22T24N26TFw	CCCGACCGACCGACTCTCTTTTCTG
RB04	*mukF*22T24N26TRv	TTCGAGGTGGAGAAGTCATTTTTTCTGG
MukF constructs		
RB05	4HB-M-C-WHDNheI Fw	CGATTCGCTAGCCAGCGCGAGTTTTCTACGCTGCGT
RB06	4HB-M-C-WHD BamHInostop Rv	GCTCGAATTCGGATCCGCACTATATTTGTCGATGACATGCG
RB07	4HB-M Fw	CGATTCGCTAGCCAGCGCGAGTTTTCTACGCTGCGT

RB08	4HB-M Rv	GCTCGAATTCGGATCCGCACTAAACTCTTCGTATTCCAGATCC
		Rapamycin construct
RB09	NdeIF Fw	GACAGTATCATATGATGGAACTGATTCGTGTTGC
RB10	BamHIF Rv	TCGCGCTGGGATCCCTGCTTTGAGATACGGCGG
RB11	NdeIFKBP Fw	GACAGTATCATATGATGGGCGTTCAAGTCG
RB12	BamHIFKBP Rv	CGCGCTGGGATCCCTGTTCCAGTTTCAGCAGTTCC
RB13	BamHIlinkerNheI	GACAGTATGGATCCGGTGGTGGCGGCGGTTCGAGGGCGGTGGTTCAGAAGGCGGTTCCGGTTCTAG AGAGGGCGGTGGTTCAGAAGGCGGTTCCTCCGCTAGCCAGCGCGA
RB14	BamHIlinkerNheI	TCGCGCTGGCTAGCGGAGGAACCGCCTTCTGAACCACCGCCCTCTCTAGAACCGGAACCGCCTTCTGAACCACCGCCCTCGGAACCGCCGCCACCCCGGATCCATACTGTC

2.2.2 Plasmids

All constructs were verified by sequencing through the Source Bioscience Oxford facility and analysed using SerialCloner 2-6-1.

Table 2.iii – List of derivative plasmids and those constructed for this work

Plasmid	Source	Description
		Commercial
pET-21a(+)	Novagen	T7 (N-ter), His (C-ter) T7 promoter expression vectors, Ampicillin^R
pET-28a(+)	Novagen	N/C-ter His Tag T7 lac T7 promoter expression vectors,

		Kanamycin^{R}
pETDuet-1	Novagen	The Duet vectors are T7 promoter expression vectors, each designed to co-express two target proteins in *E. coli*. Ampicillin ^{R}
pBAD24	Guzman *et al*. 1995	Tight regulation, modulation, and high-level expression by vectors containing the arabinose pBAD promoter. Ampicillin^{R}. *ara* promoter, *araC*, 4542 bp
pKD46	Datsenko *et al.* 2000	Lambda Red recombinase expression plasmid includes 2154 nucleotides (31088-33241) of phage Lambda, which includes the terminator downstream *frp*, *exo*, tL3 and a small ORF. GenBk-AY048746 encodes for lambda red Exo- 5-3 ds DNA exonuclease, Beta- protects ss DNA produced by *exo*, Gam– protects linear ssDNA from RecBCD and SbcCD nucleases).
pKD4	Datsenko *et al.* 2000	Template plasmid for frt-flanked *kan* cassette
pCP20	Datsenko *et al.* 2000	pCP20 has the yeast *Flp* recombinase gene, FLP, chloramphenicol and ampicillin resistant genes, and temperature sensitive replication.
		Gifted Plasmid DNA
pKZ02	Zawadzka *et al.* 2018	MukB pET-21a C-ter-His_6 tag
pKZ54	Zawadzka *et al.* 2018	MukE +9 pET-21a C-ter- His_6 tag

pKZ05	Zawadzka *et al.* 2018	MukB E1407Q pet-21a C-ter- His_6 tag
pKZ14	Zawadzka *et al.* 2018	MukB Head-Neck pET-21a C-ter- His_6 tag
pKZ17	Zawadzka *et al.* 2018	MukF N-ter WHD pET-28a C-ter- His_6 tag
pKZ33	Zawadzka *et al.* 2018	MukF M-C-WHD pET Duet-1 C-ter- His_6 tag
pKZ46	K. Zawadzka	MukB CAP interaction mutant C-ter- His_6 tag
pKZ77	Zawadzka *et al.* 2018	MukB LKLK Neck interaction mutant C-ter- His_6 tag
pKZ111	Zawadzka *et al.* 2018	MukF N-ter WHD- 3X FLAG pBAD24
	Davis *et al.* 2011	pBluescript-pTac::FRB-eYFP kindly gifted by DR T.A Baker
	Davis *et al.* 2011	pKT100-*pLac*::*luxAB*-FKBP kindly gifter by T.A Baker
Plasmids constructed in this work		
pRBMukFm	This work	MukF I22T,L24N,V26T pET-21a His_6 tag
pRBMukFsm	This work	MukF I22T pET-21a His_6 tag
pRB4HBMCWD	This work	MukF 4HB-M-C-WHD pET-21a His_6 tag
pRBMCWHD	This work	MukF M-C-WHD pET-21a His_6 tag
pRBFN2tm	This work	MukF N-ter WHD I22T,L24N,V26T pBAD24
pRAB01	This work	FRB -4HB-M-C-WHD pET-21a His_6 tag
pRAB02	This work	FKBP- 4HB-M-C-WHD pET21a His_6 tag

pRAB03	This work	FRB and FKBP -4-HB-M-C-WHD pETDuet-1 His_6 tag
pRAB05	This work	FRB- MukF pET21-a His_6 tag
pRAB06	This work	FKBP- MukF pET21-a His_6 tag
pRAB07	This work	FRB and FKBP- MukF pETDuet-1 His_6 tag
pRAB08	This work	FRB -MukFm pET21-a His_6 tag
pRAB09	This work	FKBP -MukFm pET21-a His_6 tag
pRAB10	This work	FRB and FKBP- MukFm pETDuet-1 His_6 tag

2.3 DNA preparations

2.3.1 Site directed mutagenesis

The design of amino acid substitutions was informed by the interactions at the interface between two monomers of MukF (PDB entry 3EUH, Woo *et al*. 2009). Amino acid substitutions were either invariant or highly conserved amongst MukF proteins across bacterial species. Mutations were made in plasmid-encoded genes by Q5® site-directed mutagenesis kit (NEB) in accordance with the manufacturer's protocols. Primers were designed by NEBase Changer (Table 2.ii) and reaction conditions followed as suggested. Plasmids were isolated using Qiagen miniprep kits and mutations confirmed by sequencing (DNA sequencing services by Source Bioscience, Oxford). Analysis used SerialCloner 2-6-1.

2.3.2 Design and preparation of truncated MukF variants

Design of truncations was according to previously described (Fennie-Fezzel *et al.* 2005) and characterised MukF domains (Zawadzka *et al.* 2018). Primers were designed so that amplified products contained different 3′ and 5′ restriction digestion sites allowing for subsequent ligation into parent expression vectors

(Table 2.iii). PCR products were checked for size by agarose gel electrophoresis with a 1% (w/v) agarose and run at a constant 100 V. All constructs were confirmed by sequencing as above.

2.3.3 Construction strategy for synthetic dimerisation

The entire coding regions of FRB and FKBP were codon optimised for expression in *E. coli* and cloned into pBluescript- pTac::Ω -eYFP and pKT100-pLac::luxAB-Ω, respectively, to produce the plasmids pBluescript-pTac::FRB-eYFP and pKT100-pLac::luxAB-FKBP. Courtesy of Dr T.A Baker (Davis *et al*. 2011).

FRB and FKBP genes were amplified by PCR using Q5® High-Fidelity DNA Polymerase according to manufacturer's instructions, with appropriate unique restriction sites for subsequent subcloning into pET21-a. This produced amplicons of NotI-FRB-BamHI (333 bp) and NotI-FKBP-BamHI (356 bp). Oligonucleotides encoding for a flexible linker (GGGGGSEGGGS EGGSGSREGGGSEGGS) with appropriate flanking restriction sites (BamHI-NheI) were reconstituted in annealing buffer to 100 µM (10 mM Tris-HCl pH 8.0, 50 mM NaCl and 1 mM EDTA). An equi-molar -volume was mixed and heated to 95 ºC for 15 minutes in a C1000 Touch 2X48 well thermal cycler and over 750 cycles, the temperature was reduced by 0.1 ºC every cycle. The annealed duplex DNA was then ligated to FRB and FKBP and then ligated to the NotI-NheI sites of pET21-a. FRB and FKBP tags with linkers were then amplified and ligated into pET Duet-1 (Figure 2.i). The strategy was repeated for MukF and MukFm.

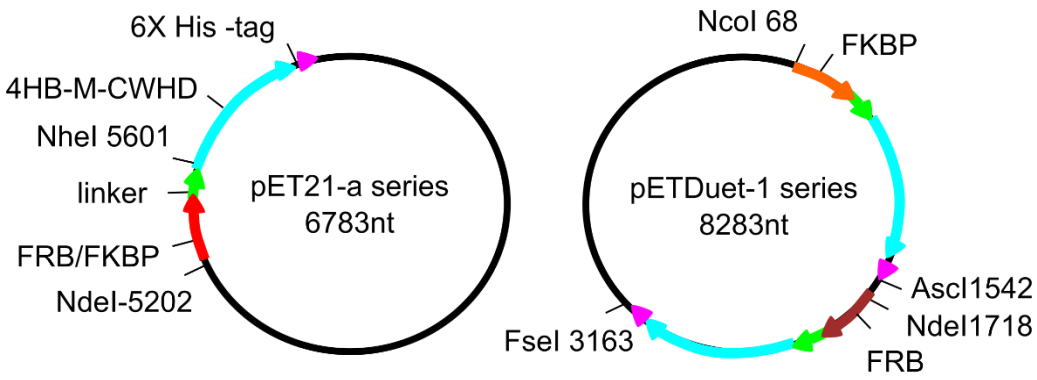

Figure 2.i - Schematic of strategy for expression of FRB and FKBP12 tagged MukF. Tagged MukF variants with unique flanking restriction sites were cloned into the pETDuet-1 dual expression system.

2.4 *In vitro* analysis

2.4.1 Protein expression and purification

All proteins were expressed and purified as described (Zawadzka *et al*. 2018) on an Äkta purifier with Unicorn manager software. All samples were analysed for size and purity by SDS polyacrylamide gel electrophoresis using Novex WedgeWell 4-20% Tris-Glycine Mini Gels (Life technologies) and stained using Instant Blue Coomassie stain. Samples were quantified using a Thermo scientific NanoDrop™ One/OneC Microvolume UV-Vis Spectrophotometer**.**

2.4.2 Native polyacrylamide gel electrophoresis

All native gels prepared were 6% in Tris buffer pH 8.8. As described in Rajasekar *et al*. 2019, samples were equilibrated and mixed in 50 mM HEPES pH 7.5, 100 mM NaCl and 1 mM DTT. Relative values of band intensities were calculated using a ChemiDoc XRS+ System and Image Lab software.

2.4.3 Size Exclusion Chromatography and Multi-Angle Light Scattering (SEC MALS)

Proteins were mixed to the ratios indicated and equilibrated in 50 mM HEPES pH 7.5, 100 mM NaCl and 1 mM DTT. Each sample volume was 100 µL and all samples were spun for 20 minutes at 100,000 rpm in an Optimax Max-XP Ultracentrifuge to remove aggregates before applying to a 24 ml Superdex™ 200 Increase 10/300 column at a rate of 0.5 ml/minute. SEC MALS was collected in collaboration with an in-house biophysics suite managed by Dr David Staunton using Wyatt Heleos8+ and T-rEX detectors and a Shimadzu chromatography system. Subsequently, data was analysed using Astra6 software (Wyatt Technologies).

2.4.4 Circular Dichroism (CD)

CD was performed in collaboration with Dr David Staunton, at our in-house biophysics suite using a Jasco J-815 Spectropolarimeter. Samples were prepared as follows: with a total protein concentration in the range of 0.1-0.05 mg/ml, approximately 200 µl sample volume suitable for a 1 mm cuvette and equilibrated in a buffer comprise of 10 mM phosphate buffer and 20 mM NaCl.

2.4.5 Mass Spectroscopy (MS)

MS was completed in collaboration with our in-house advanced proteomics facility, Dr Sabrina Liberatori. Samples were prepared by excising single bands from polyacrylamide gels, or from solution following purification. In both cases a 30 min gradient was used and protein identification

2.4.6 ATP hydrolysis assays

All samples were prepared and analysed as described in Zawadzka *et al.* 2018. Briefly, steady state reactions were prepared using an EnzChek Phosphate Assay Kit (Life Technologies Ltd) and assayed using a BMG Labtech PHERAstar FS next-generation microplate reader. Analysis used PHERAstar FS control software and the MARS data analysis. The final volume of samples was 150 µL, with the following final protein concentrations: MukB at 0.5 µM, MukF and variants at 1.25 µM and MukE at 5 µM, supplemented with 1.33 mM Tris-buffered ATP.

2.5 *In vivo* analysis

2.5.1 Strain construction

Bacterial strains and primers as listed in tables.

The RAB02 and RAB03 strains were generated using parent strains RRL252 and Ab233b, respectively. The 3.66 kbp PCR product was amplified with primers KK21 and JMP12 against PAmCherry-*mukB* from strain Ab238 and was introduced by λ-red recombination. The generated chromosomal locus was then transferred by P1 transduction into BL05 (Para-*mukF* cat:: Δ *argE*) and AB1157 resulting in strains RAB02 and RAB03, respectively.

Strain RAB05 (Δ*mukF*:: Kan *mukB*^{EQ} PAmCherry) was constructed by removing the *kan* resistance gene from parent strain RAB02 using Flp recombinase and introducing the following construct (PCR III) by λ-red recombination:

- PCR I: Fragment of MukB^{EQ} carrying the mutation (pKZ05) was amplified using primers KK08 (Fw) and KK27 (Rv). This generated a product of approx. 500 bp.

- PCR II: The MukB C-terminal PAmCherry fragment was amplified from Ab238 strain (MukB PAmCherry) using JMP11 (Fw) and JMP12 (Rv).
- PCR III: Using the products of PCR I and PCR II as a combined template, a fragment carrying both was produced – using primers KK08 (Fw) and JMP12 (rev).

The generated chromosomal locus was then transferred by P1 transduction into AB1157. All genetic modifications were verified by PCR and sequencing. The Muk- phenotype was verified by temperature sensitivity of growth on rich media.

2.5.2 Functional complementation analysis *in vivo*

This assay exploited the ability of MukF variants to rescue temperature sensitivity of growth in rich media of a Δ*muk*F strain as described in Rajasekar *et al.* 2019. For synthetically induced dimerisation, cells were allowed to recover following transformation with the plasmid carrying tagged MukF variants for 8 hrs in the presence or absence of 100 nM rapamycin (Rapamycin (Sirolimus), Stratech Scientific). Cells were then plated onto LB agar containing carbenicillin (100 µg/ml), +/- 100 nM rapamycin. For expression and purification of the tagged MukF constructs, a protocol was followed as above (Zawadzka *et al.* 2018). Cells were grown in liquid culture in the presence of 100 nM rapamycin.

2.5.3 Epifluorescence microscopy

As described in Rajasekar *et al.* 2019. Images were acquired using NIS-Elements software (Nikon). Cell segmentation and spot detection from fluorescent channel were performed using Supersegger (Stylianidou *et al.* 2016). Thresholds were

maintained for all samples and cells containing one or more spots were calculated using a custom MATLAB (MathWorks) script adapted by Dr Jarno Mäkelä.

2.5.4 Photo-activated localisation microscopy (PALM)

All PALM analyses were performed in collaboration with Dr Jarno Mäkelä. Cells were grown in M9 glycerol (+/- arabinose or rapamycin as described in Chapter 4), diluted ~1000-fold and when at an OD_{600} of 0.1, were spotted onto agarose pads. Cells were imaged with a PALM microscope every 15.48 ms (exposure time 15 ms) for 21,000 frames for adequate sampling. To analyse the single molecule data, cells' area were first segmented followed by linking of single molecule localisations into a track. Criteria for linking was that localisations appeared in consecutive frames or with 1 frame gap, within a window of 5 pixels, equivalent to 0.48 µm. The mobility of each molecule was then estimated by calculating the apparent diffusion coefficient (D*) from the mean-square displacement of tracks relating time to distance travelled over tracks with a length of four (Stracy *et al.* 2019).

Finally, to estimate the fraction of immobile molecules, the measured distribution of D* was fitted to an analytical 2-state model of single-molecule diffusion (mobile and immobile state) with free parameters of fractions and D* of mobile fraction. D* of immobile molecules was set to 0.05 according to previous estimates.

Chapter 3

In vitro characterisation and identification of monomeric MukF

3.1 Introduction

Kleisins are a superfamily of eukaryotic and prokaryotic proteins that, despite low sequence homology, show structural similarities reflecting a common asymmetric interaction with SMC dimers (Schleiffer *et al.* 2003). The kleisin C-terminal globular domain interacts with the C-terminal head domain of their cognate SMC at a site distal to the coiled-coil polypeptide, termed 'CAP', whereas the kleisin's 4-helix bundle binds the coiled-coil domain, 'NECK', proximal to the head of a partner SMC molecule thereby creating a characteristic ring-like structure (See Figure 1.i).

Apparently unique amongst kleisins, MukF has an N-terminal region extended by a Winged Helix Domain (WHD). Analysis of the crystal structure of the N-terminal 287 amino acids of MukF, (Fennell-Fezzie *et al.* 2005), reveals an intimately entwined dimer, with the N-terminal Winged Helix Domain (N-WHD), which is absent in non-MukBEF kleisins (Fig. 3.i), creating an interface predicted to be essential for dimerisation. Previously Size Exclusion Chromatography (SEC) has shown MukF to be dimeric in solution and analytical ultracentrifugation confirms monodispersity (Woo *et al.* 2009, Gloyd *et al.* 2007), however, the physiological relevance of dimeric MukF has not hitherto been investigated.

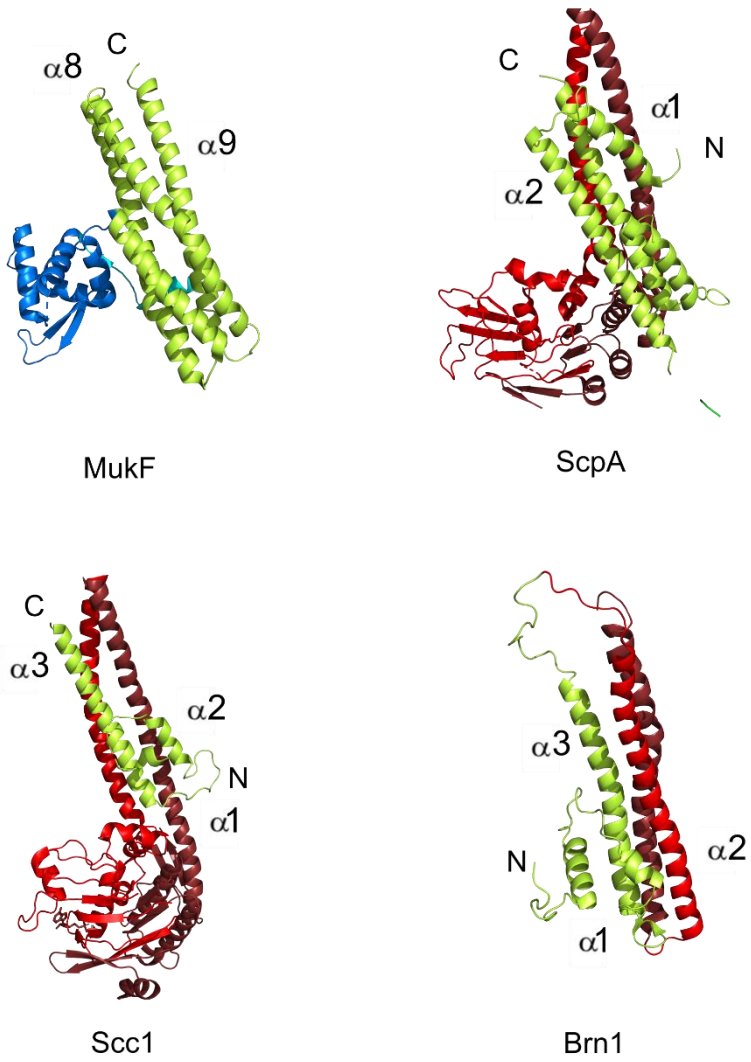

		core		kleisin	accessory	
	E. coli	MukB		MukF	MukE	
	B. subtilis	SMC		ScpA	ScpB	
Cohesin	*S. cerevisiae*	Smc1	Smc3	Scc1	Psd5	Scc3
Condensin	*C. thermophilium*	Smc2	Smc4	Brn1	Ycs4	Ycg1

Figure 3.i - A comparison of crystal structures of N-terminal domains of kleisins bound to their cognate SMC.

The domains of bacterial SMC (SMC:ScpA- adapted from PDB entry 3ZGX; Bürmann *et al.* 2013), yeast cohesin (SMC3:Scc1-adapted from PDB entry 4UX3; Gligoris *et al.* 2014) and thermophile condensin (SMC4:Brn1- adapted from pdb entry 6Q6E), which

interact with coiled-coil proximal region of SMC head, demonstrates structural similarities with the MukF 4-helix bundle. The MukF Winged Helix Domain in blue highlights this unique dimerisation domain.

3.2 Results

3.2.1 Disruption of hydrophobic interactions between protomers formed by the β1 strands monomerises MukF

An alignment of the extreme N-termini of select MukF proteins shows considerable sequence homology (Fig.3.ii). Strand β1, C-terminal to the first helix, forms an antiparallel sheet with its partner protomer. This flat hydrophobic surface appears to be a strong candidate for interactions that would lead to dimerisation and directed a structurally-led rationale for mutagenesis. Conserved hydrophobic residues predicted to contribute to dimerisation in strand β1 were identified and mutated to polar residues whilst maintaining structural integrity.

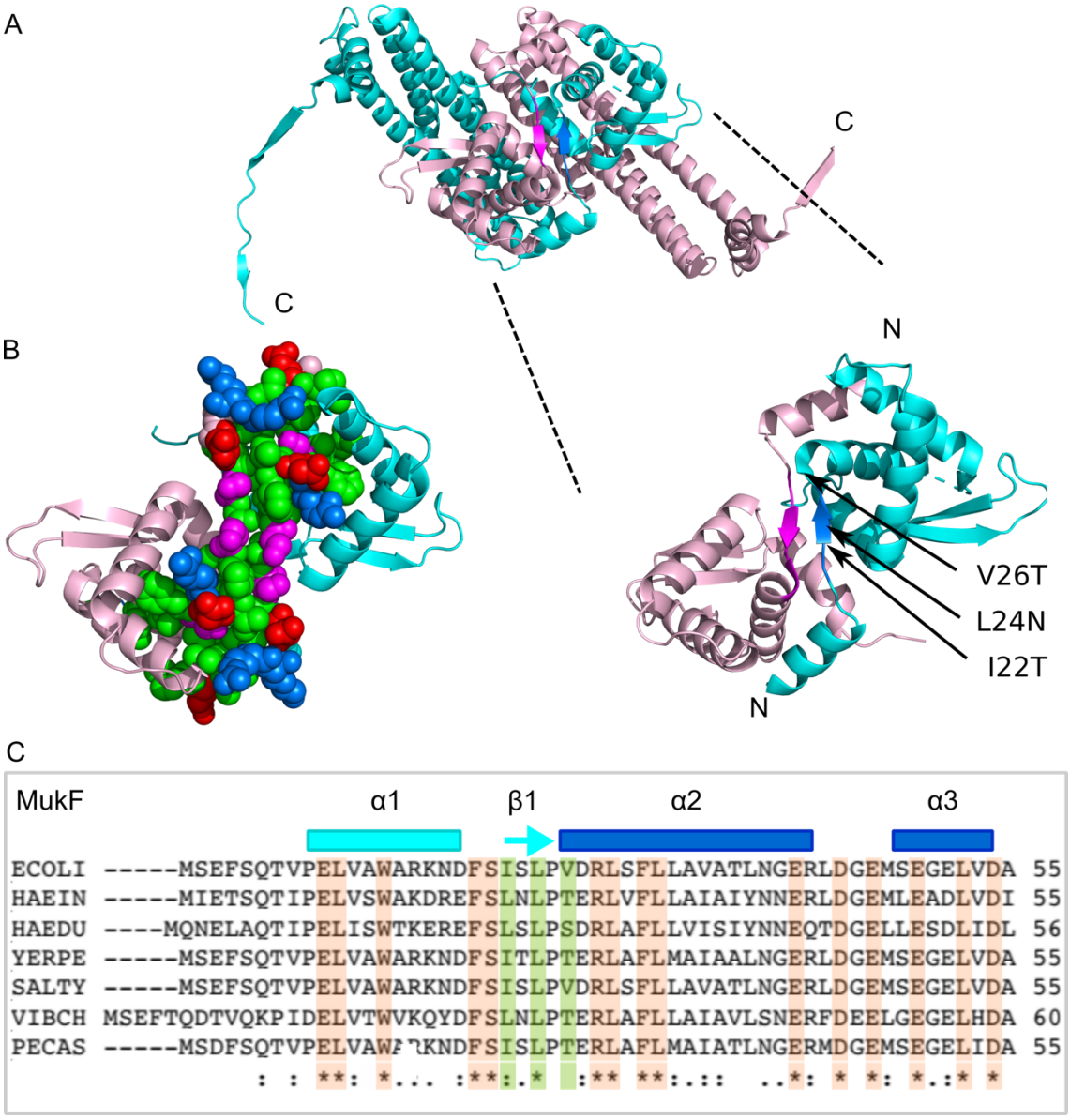

Figure 3.ii - Crystal structure of dimeric MukF with N-terminal alignments highlighting conservation within the dimerisation domain.

A-The first protomer is coloured in cyan and its partner in pink. **B-**The expanded view of the dimerisation domain indicates those residues substituted for effective monomerisation, and the properties of residues residing at the dimerisation interface. Hydrophobic residues are highlighted in green, charged residues in blue (+ve) and red (-ve), and polar residues are depicted in magenta.**C-** Invariant (**) and highly conserved (*) residues are highlighted in orange. Substituted residues are highlighted in green. Adapted from PDB entry 3EUH Woo *et al.* 2009.

A single mutation, I22T, was sufficient to monomerise MukF (MukFsm). Chromosomal substitution at this residue rendered cells temperature-sensitive (see Chapter 4). However, this variant didn't purify well and tended to aggregate, several impurities or proteolysis products co-purified and possible traces of dimer could be seen according to SEC, native gels and SEC-MALS (Fig.3.iii). A triple residue substitution (I22T,L24N,V26T), was therefore introduced by Q5 site-directed mutagenesis (See chapter 2). This putative monomeric MukF variant (henceforth MukFm) was successfully overexpressed and purified to homogeneity. Analysis by SDS PAGE confirmed that upon denaturation, both dimeric, wild type (MukFd) and MukFm ran with an apparent mass of ~50 kDa.

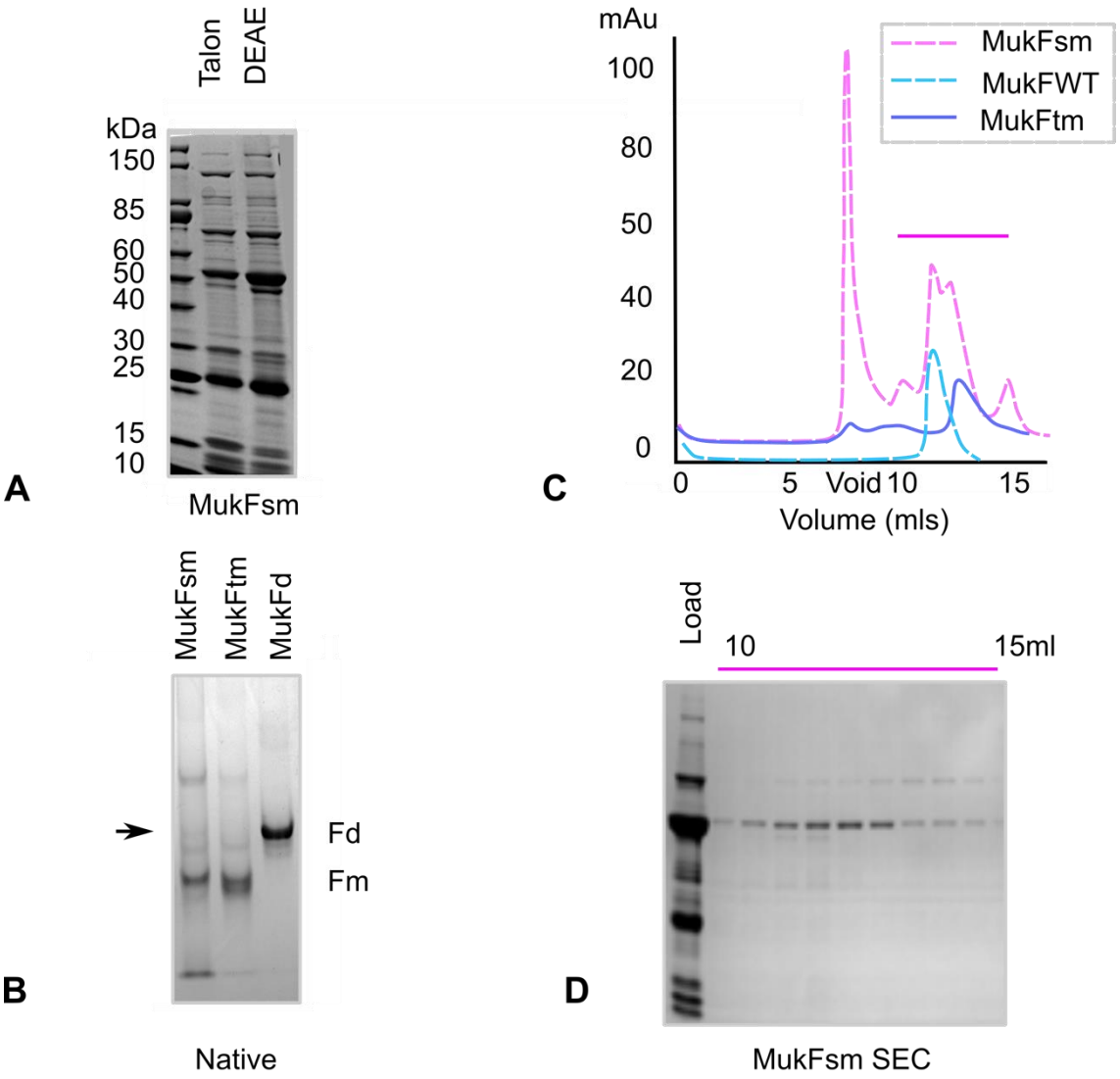

Figure 3.iii - Single residue substitution at position I22 is sufficient to perturb dimerisation of MukF.

A - Purification prior to SEC. **B** - Native PAGE confirms MukF dimerisation has been disrupted. **C** - SEC traces show wild type MukF as a dimer and the single and triple substituted variants as monomers. Large peak close to void possibly due to increased aggregation. **D** - Monomeric and dimeric species were separated according to size on a Superdex 200 HR10/30 column and demonstrated to be ~50 kDa upon denaturation.

To purify the triple residue substituted mutant further and remove endogenously expressed MukF dimers, MukFm was applied to a gel filtration column and its

elution profile was compared to the wild type MukFd. Size exclusion chromatography coupled with Multiple Angle Light Scattering (SEC-MALS) confirmed that the purified variant was a stable monomer in solution (Fig. 3.iv)

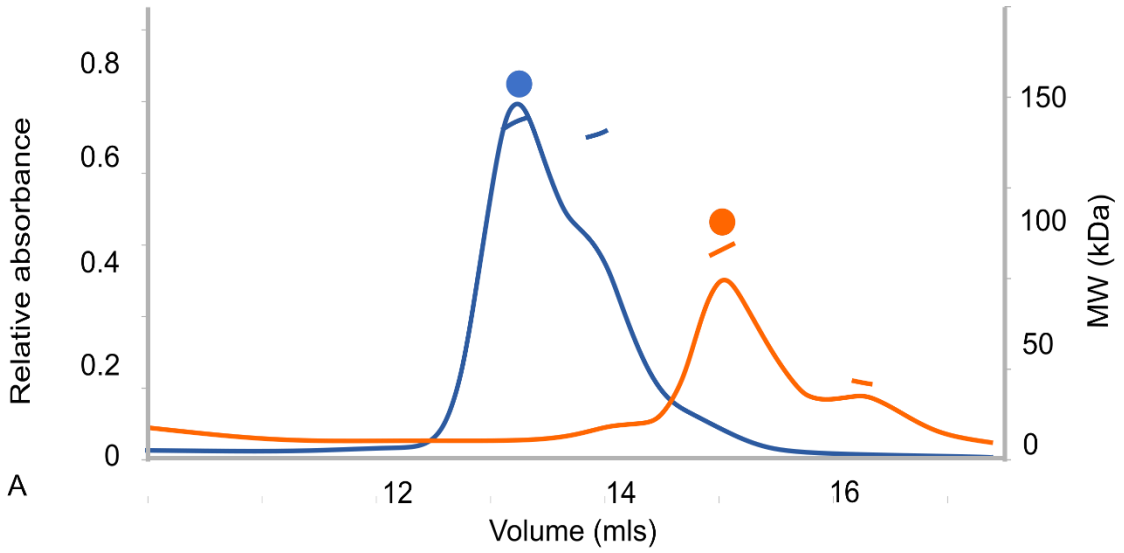

A

		Complex	Predicted (kDa)	Observed (kDa)
●	MukFd	2F	105.4	99.2 ± 3
●	MukFm	1F	52.7	57.3 ± 3

B

Figure 3.iv - SEC with triple residue substitution forms stable monomers of MukF. **A** - Elution profiles from a Superdex200 column of MukFd and MukFm. **B** - In the MukFm sample, the major peak corresponds to a mass consistent with monomeric MukF. Shoulders on both dimeric and monomeric profiles are due to proteolytic degradation as seen in previous studies (Rajasekar *et al.* 2019).

3.2.2 MukF variants with the triple residue substitution are folded

To ascertain whether monomeric MukF remains folded, two strategies were employed. First, a truncated MukF variant containing the N-terminal Winged Helix Domain (N-WHD) and 4-Helix Bundle (4HB) (Zawadzka *et al*. 2018) was monomerised by triple residue substitution (Nm-WHD-4HB) and compared to the dimeric version (Nd-WHD-4HB) by Circular Dichroism spectroscopy (CD). The spectra and melt profiles of Nd-WHD and Nm-WHD were comparable indicating that the N-terminal domains have remained folded following the triple residue substitution (Fig 3.v).

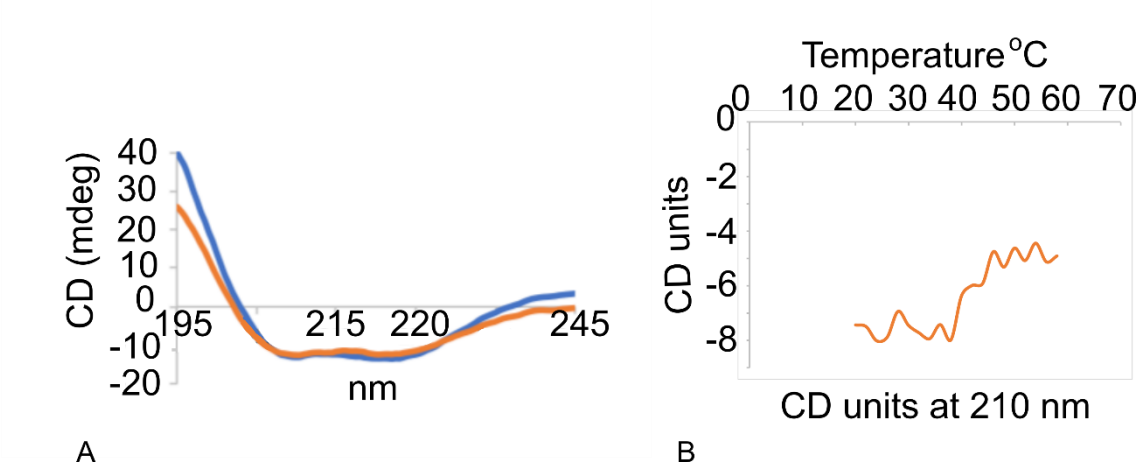

Figure 3.v - Circular dichroism spectroscopy of N-terminal MukF variants.

A - Overlay of traces from the monomerised N-terminal WHD and 4-helix bundle (Nm-WHD-4HB) variant and the dimeric wild type protein. **B** - The distinct step in the melt at ~40°C profile indicates Nm-WHD-4HB remains folded.

The second approach used, was to test whether the monomer variant could still bind to MukE through the middle flexible linker of MukF. The *E. coli* kite protein, MukE, reversibly dimerises (K_d~18 µM) through its N-WHD domain (Gloyd *et al*. 2007) and binds asymmetrically to the acidic, middle flexible region of MukF with

a K_d of ~7 nM (Yamazoe *et al*. 1999, Petrushenko *et al*. 2006a, Gloyd *et al*. 2007, Rajasekar *et al*. 2019). The binding of MukE to monomerised MukF (Fig. 3.vi) supports the assumption that this region remains folded.

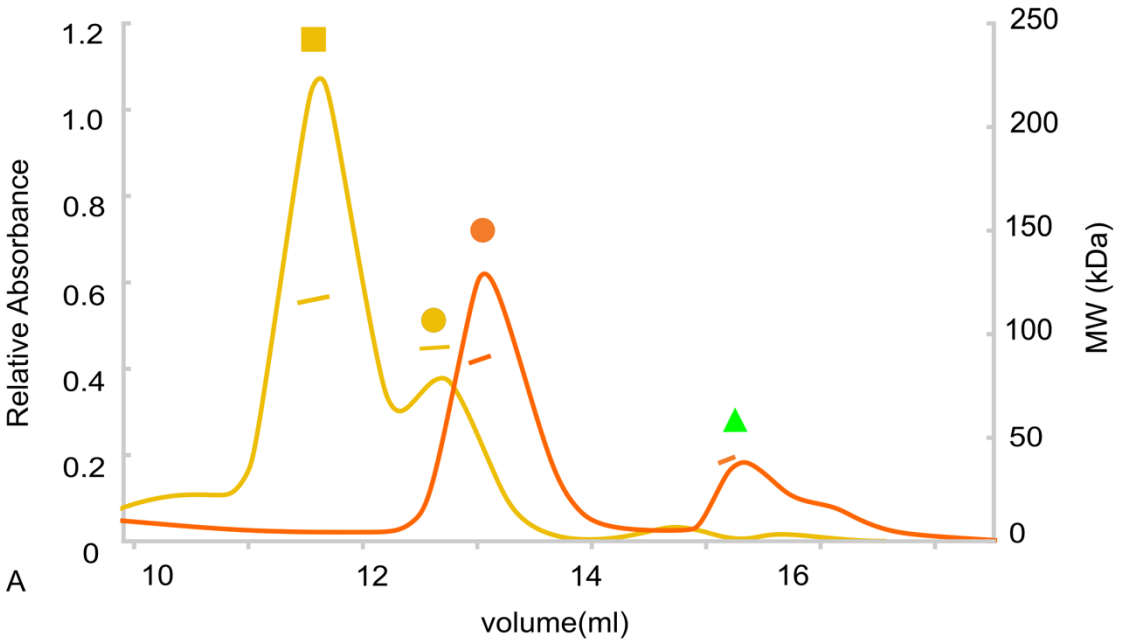

A

		Complex	Predicted (kDa)	Observed (kDa)
●	MukFd & MukE	2F-2E	164.2	148.0 ± 3
■		2F-4E	223.0	209.1 ± 1
●	MukFm & MukE	1F-2E	111.5	116.8 ± 5
▲	MukE	2E	58.8	44.5 ± 4

B

Figure 3.vi - *In vitro* analysis of MukFm confirms correct folding of MukF with triple substitution.

A - SEC MALS trace shows dimeric MukE binding to the middle flexible region (M) of MukFm. **B** - Tabulates predicted sizes along with those observed. Discrepancies in observed and predicted masses are consistent with previous work (Rajasekar *et al.* 2019) and is most likely due do an equilibrium mixture of MukE monomers and dimers MukE.

3.2.3 Both N-terminal deleted MukF and C-terminal deleted variants with triple residue substitution are monomeric

In common with other members of the kleisin superfamily, MukF bridges the head domains of MukB. To further investigate the functionality of the N- and C-terminal domains, a triple residue substitution was introduced into C-terminal truncated MukF variants along with deletions of the N- and C-WHD (Fig. 3.vii).

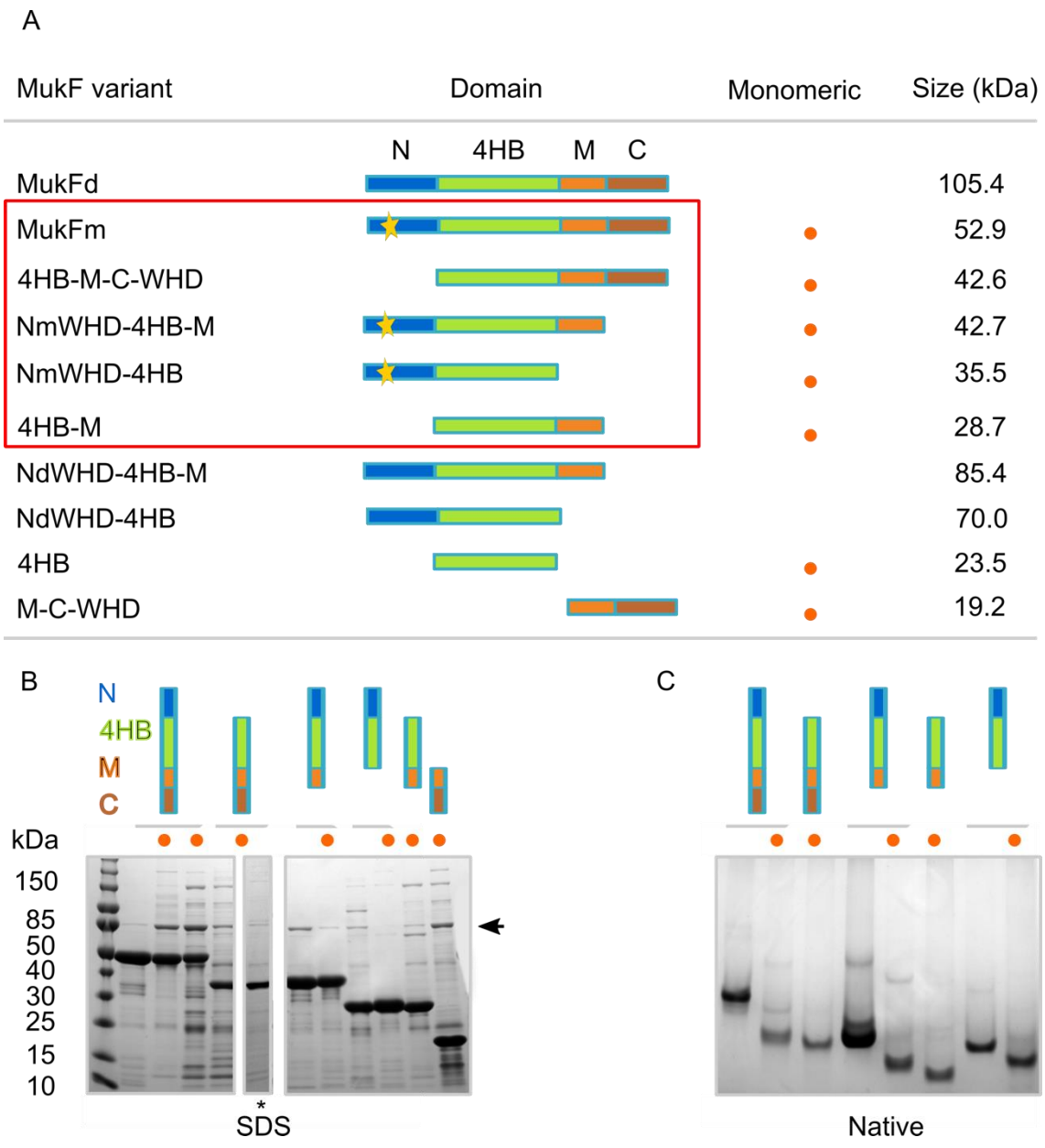

Figure 3.vii - Cartoon of monomeric variants, their purification and native PAGE.

A - Variants constructed for this study are boxed in red, others have been characterised previously (Zawadzka *et al*. 2018). **B** - SDS-PAGE shows proteins purified using a His-tag affinity and ionic exchange chromatography. An asterisk denotes purification of the 4HB-M-C-WHD variant before and after SEC. Arrowed contaminant with a mass of ~85 kDa that seemed to consistently co-purify was sent for Mass Spectroscopy (MS) analysis (outcome pending). **C** - Native PAGE demonstrates monomerisation of truncated MukF variants.

3.2.4 MukF monomer stimulates MukB ATPase activity to wild type levels

The globular head domains of all SMCs harbour two ATP binding pockets that form composite catalytically active ATPase sites upon ATP binding and head engagement. The field is now beginning to dissect the specific role of each site in the regulation of DNA entrapment and transport by SMC class proteins (Hassler *et al.* 2019).

The N-terminal domain contains the Walker A ATP binding motif and the C-terminal domain contains the Walker B and ABC signature motifs (Fig 3.viii). Crystal structures show that ATP is bound to the Walker A and B motifs of one head and the signature motif of the partner head. The binding of ATP brings the two heads together (Hirano and Hirano 2004: Moody *et al.* 2002: Woo *et al.* 2009), ATP hydrolysis results in the heads being driven apart (Hirano 2006: Ivanov and Nasmyth and Haering 2005).

Interaction through MukF 4-HB and C-WHD stimulates MukB ATPase activity both independently and additively (Zawadzka *et al*. 2018). Activity of both domains are essential for MukBEF function, suggesting that ATPase events may be alternating where only one molecule of ATP is hydrolysed at a time, rather

than sequentially when binding of one ATP powers the conformational change allowing the second hydrolysis event.

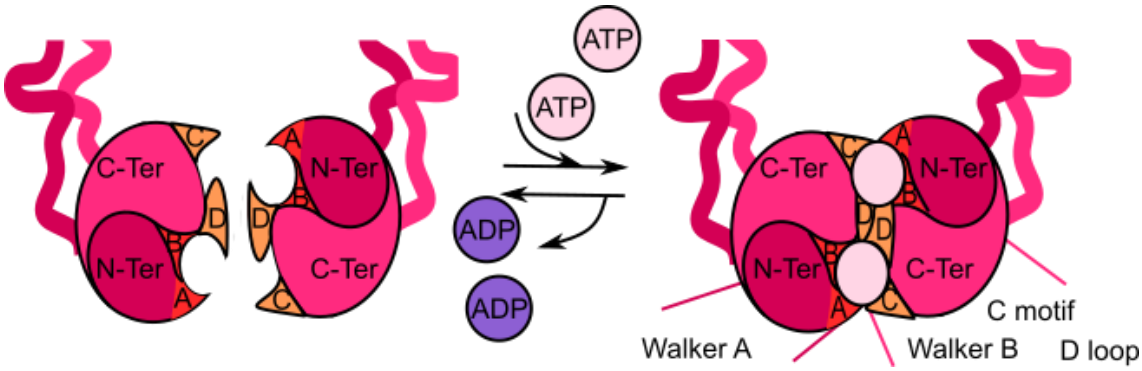

Figure 3.viii - Schematic of ATPase sites in the MukB head domain.

Conserved ABC-like ATPase binding domains are formed upon juxtaposition of the N- and C-terminal globular domains of two MukB heads. (**A**: Walker A, **B**: Walker B, **C**; Signature motif, **D**: D loop) Adapted from Nolivos and Sherratt, 2014.

In steady-state assays where MukF is in 2.5 molar excess over MukB, full length MukFm stimulated MukB ATPase activity to wild type levels (Fig.3.ix). Furthermore, removal of the entire N-WHD showed no reduction in stimulation of MukB activity mediated by the interaction of the 4HB domain with the MukB neck. Variants 4HB-M-C-WHD and 4HB-M were further purified by size exclusion chromatography and their size was estimated by SEC-MALS. Both variants were confirmed to be monomeric. Purified samples were also analysed by MS, which showed that peptides unique to full length endogenous MukF were 1000X fold less abundant than that of the overexpressed variants. Therefore, it can be assumed that this wild-type-like stimulation of MukB ATPase activity is not the result of co-purification with endogenous MukF

Previously characterised (Zawadzka *et al*. 2018), variant M-C-WHD, expressed and purified well, and stimulated MukB ATPase activity to levels in excess of 50% that of wild type MukF (Fig.3.ix). This is in good agreement with activity levels published by Zawadzka *et al.* (2018). Variant M-C-WHD lacks the 4HB and N-WHD, this variant is therefore intrinsically monomeric. Further characterisation of truncated MukF variants containing the triple substitution in strand β1 shows that the monomeric variants with the C-WHD deleted are severely defective in MukB ATPase stimulation (Fig. 3.ix).

MukF variant	Domain	ATP hydrolysed /MukB dimer/min	% activity
MukFd		23.3 ± 1.50	100
MukFm		20.9 ± 0.89	90
4HB-M-C-WHD		22.2 ± 2.86	95
NdWHD-4HB-M		7.5 ± 0.15	32
NdWHD-4HB		6.7 ± 0.72	29
M-C		13.9 ± 0.72	60
NmWHD-4HB-M		1.6 ± 0.61	7
FmWHD-4HB		1.2 ± 0.71	5
4HB-M		1.9 ± 0.80	8
4HB		2.5 ± 1.04	11

Figure 3.ix - Comparison of MukB ATPase activity stimulated by full length and truncated monomeric MukF variants.

Full-length MukFm and N-terminal WHD deleted MukF showed ATPase stimulation to WT levels. Monomeric variants lacking the C-terminal WHD were severely deficient in stimulation of MukB ATPase.

To further confirm the existence of variations between the MukB cap and neck interactions with monomeric MukF, the ATPase activity of MukB mutants that were defective in each MukF interaction were investigated (Fig.3.x). Previously characterised substitutions which led to defective N-terminal (neck) (L1219K L1226K) and C-terminal (cap) (F1453S, H1458A, R1465A) interaction with the MukF 4HB and CWHD, respectively, were used (Zawadzka *et al* 2018). MukB proteins harbouring the MukB cap mutation were unstable so reliable conclusions could not be made; however preliminary results show that the MukB cap interaction with MukF monomer is essential, lending further support to results shown in Figure 3.ix.

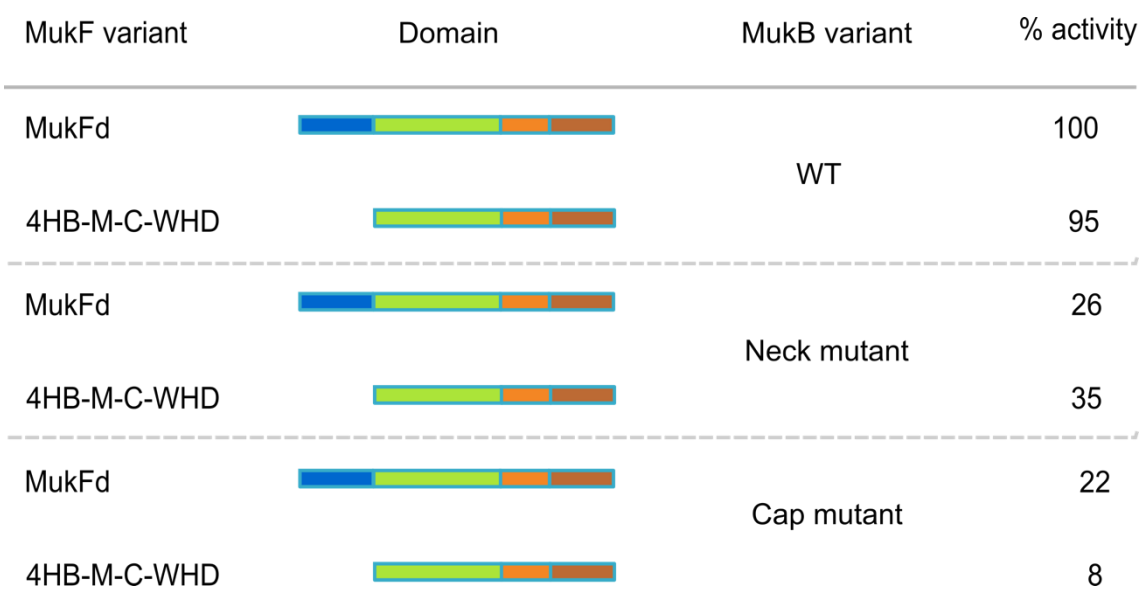

Figure 3.x - Comparison of MukB variant ATPase activity stimulated by full length and N-WHD deleted monomeric MukF.

Defective MukB neck interaction (L1219K L1226K) results in similar levels of reduced activity with WT MukF and N-terminal deleted monomer, however 4HB-M-C-WHD MukF has severely reduced ATPase activity when MukB cap (F1453S, H1458A, R1465A), interaction is perturbed.

The 4HB-M-C-WHD MukF variant showed a severe reduction in ATPase stimulation of the MukB cap mutant (Fig.3.x). This reduction in stimulation was equivalent to monomeric variants lacking the C-WHD, whereas activity of this variant showed a reduction comparable to MukFd with the MukB mutant deficient in 4HB interaction. This leads to the conclusion that monomeric N-terminal ATPase stimulation requires an intact MukF C-terminal. However, C-terminal activation is independent of the MukF4HB interaction with MukB neck.

3.3 Conclusions

The severely reduced ATPase activity observed with monomeric MukF variants upon disruption of C-terminal interaction with MukB may suggest that this domain acts as an ‘anchor’, stabilising the 4HB interaction with MukB neck. Other systems have shown that conformational changes arising from one ATP hydrolysis event allows hydrolysis of the second ATP (Hassler *et al*. 2019). ATPase activation by MukF C-WHD may be essential for any putative conformational changes needed to stabilise the MukF 4HB and MukB neck interaction necessary for a second ATP hydrolysis event. In the following chapter I explore the *in vivo* consequences of MukF monomerisation.

Chapter 4

Chapter 4

In vivo and *in vitro* analysis of MukBEF complexes formed with monomeric MukF

4.1 Introduction

Cells harbouring null mutations in any of the *mukBEF* genes have a characteristic phenotype. When grown in rich LB media, Muk$^-$ cells are temperature sensitive at 37°C, and at 22°C, produce a significant percentage of anucleate cells per generation (Niki *et al.* 1991, Danilova *et al.* 2007). Furthermore, under permissive conditions in minimal medium, cells have a disturbed organisation of the chromosome, with replication origins positioned towards the old poles rather than mid-cell/cell-quarter positions. Segregation of newly replicated origins is delayed. Deletions in other bacterial SMCs may share some, if not all, of these characteristics (Table 4.i).

Organism	Δgene	ts	Anucleate cells	Disorganised chromosome	Cell morphology	Ref
E. coli	Δ*mukB/E/F*	yes	5%	yes	filamentous	1,2,3,
P. aeruginosa	Δ*smc*	no	2.5%	yes	WT	4
P. aeruginosa	Δ*mksB*	no	1.2%*	no**	WT	4
C. crescentus	Δ*smc*	yes	0.1%	yes	no division	5,6
B. subtilis	Δ*smc*	yes	10%	yes	elongated	7,8,9

Table 4.i - Overview of phenotypes resulting from deletion of SMC or SMC-like proteins.

Temperature-sensitivity (ts) of growth in rich media. Chromosome organisation is determined with reference to positioning of genetic loci and *smc* deletions. *Only in M9 at 37˚C. Table adapted from Nolivos and Sherratt (2014). **Longitudinal organisation of the chromosome in Δ*mksBEF* remains unaffected, however timing of the segregation of chromosome loci is disturbed (Zhao *et al*. 2016). Refs **1**. Niki *et al.* (1991); **2**. Yamanaka

et al. (1996); **3**. Danilova *et al.* (2007); **4**. Petrushenko *et al.* 2011; **5**. Jensen and Shapiro (1999,2003); **6**. Schwartz and Shapiro (2011); **7**. Britton *et al.* (1998); **8**. Moriya *et al.* (1998); **9**. Lindow *et al.* (2002).

In order to investigate whether the dimerisation of MukF is an essential prerequisite for MukBEF function *in vivo*, cells expressing monomeric MukF were tested for Muk^+/Muk^- phenotypes.

4.2 Results

4.2.1 Cells expressing monomeric MukF are temperature-sensitive

Temperature-sensitivity provides a tool for the rapid initial screening and identification of variants that may disrupt MukBEF function. Basal expression from pET-21a expression vectors carrying *mukF* is sufficient to rescue defective growth of Δ*mukF* strains at 37°C on LB (Zawadzka *et al*. 2018). In this study cells deleted for MukF were transformed with pET-21a carrying wild type MukFd (dimeric MukF) or monomeric variants. Following an 8-hour recovery at room temperature, a 10-fold dilution series were spotted onto plates and then incubated at 22°C or 37°C. An empty vector was transformed as a control (Fig.4.i).

Cells expressing wild type MukF complemented the Δ*mukF* strain, however, cells expressing monomeric MukF remained temperature-sensitive on rich media. A single MukF mutation, I22T, which compromises but does not abolish dimerisation (Chapter 3), was sufficient to incur temperature-sensitivity, demonstrating that robust dimerisation of MukF could be essential for MukBEF function.

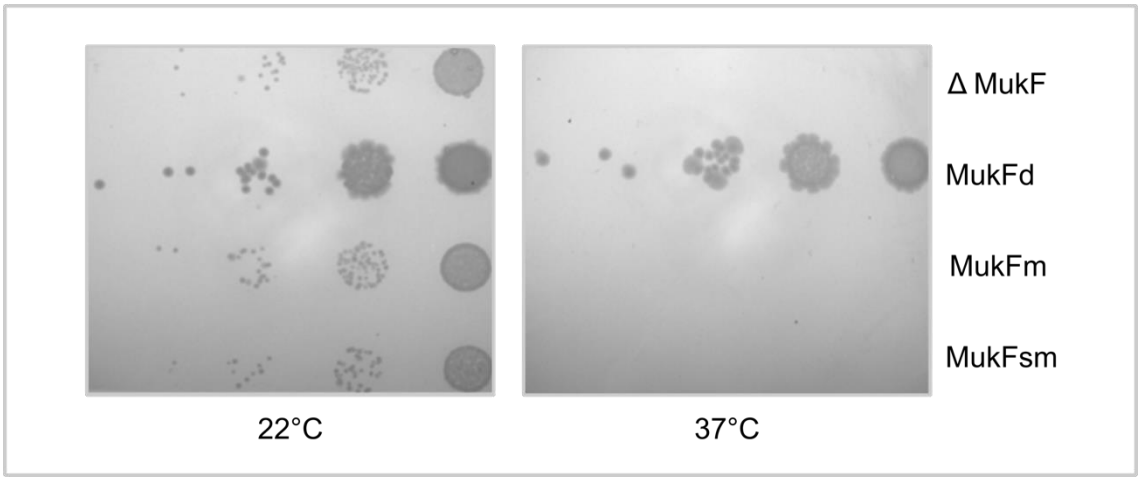

Figure 4.i - Complementation assay demonstrating Muk- phenotype.

Strain RAB02 (ΔMukF MukBpAMcherry P*ara*MukF) was transformed with a plasmid containing wild type MukFd or MukFm and grown overnight at 37°C or for 3 days at 22°C in the presence of glucose to repress expression from an inducible ectopic *mukF*. Basal expression was sufficient for levels of MukF expression to be reached that can rescue temperature sensitivity.

4.2.2 Cells deleted for MukF but expressing monomeric MukF mutants fail to form MukBEF clusters *in vivo*.

In vivo activity of MukBEF, like other bacterial SMCs, is required for chromosome management throughout the cell cycle (Badrinarayanan *et al*. 2012b). Images of cells undergoing a single round of replication produced foci containing clusters of 8-10 complexes (Badrinarayanan *et al*. 2012a) which have been shown to co-localise with the origin of replication (*ori*) and are independent of DNA replication. To investigate the importance of the dimerisation of MukF in the formation of functional MukBEF clusters, epifluorescence images of Δ*mukF* cells expressing MukFm and carrying a functional MukB-GFP fusion, were analysed. The presence of foci would indicate an ability of MukBEF complexes formed by

monomeric MukF bridging MukB heads, to stably associate with the chromosome and potentially direct the positioning of *ori*.

Images were taken of Δ*mukF* cells transformed with pET-21a carrying MukFd, MukFm or an empty vector (as described for the complementation assays). In cells expressing MukFm, fluorescence was diffuse throughout the cell, with foci only seen at levels equivalent to that observed in Muk- cells (Fig. 4.ii).

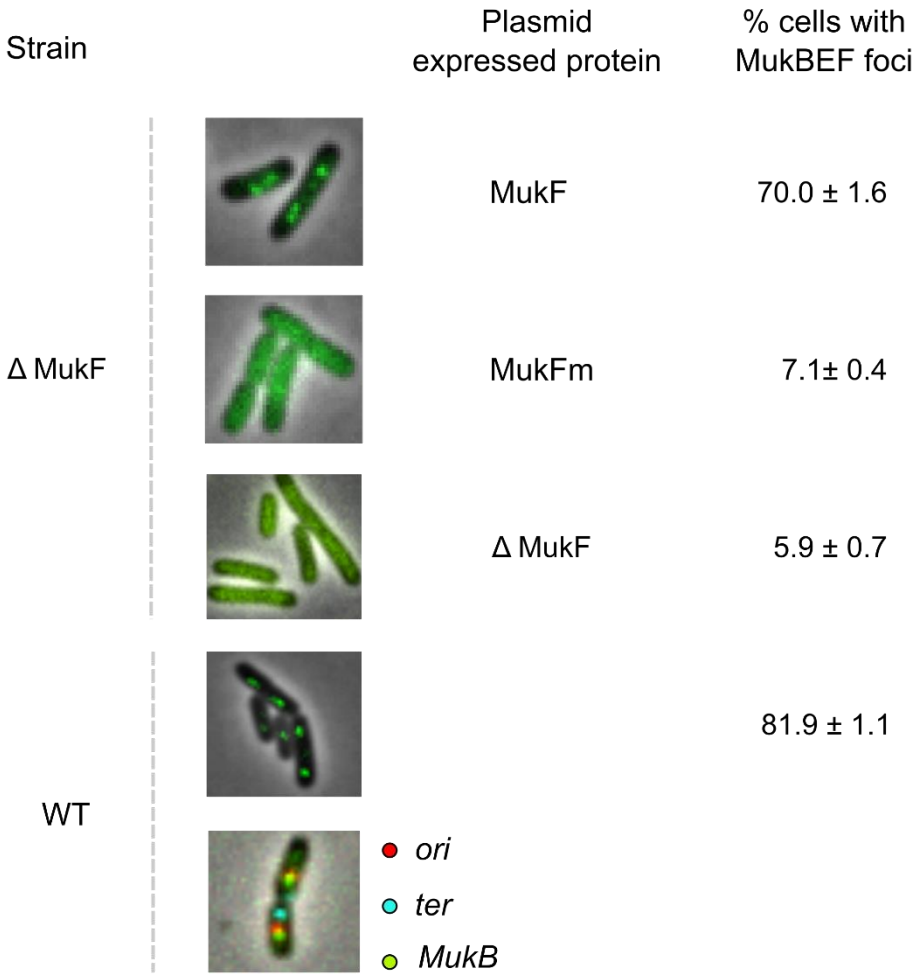

Figure 4.ii - Epifluorescence microscopy.

Ab233 (Δ*mukF*::Km *mukB*-GFP::Cm, Badrinarayanan *et al*. 2012a), transformed with pET-21a carrying MukF or variants, were grown to an OD_{600} of 0.2 in M9 glucose (1% v/v) and spotted onto agarose pads. Images were collected and percentages of cells

containing 1 or more spots were calculated using a custom MATLAB script. SEM is shown from 3 independent repeats. An additional control of WT cells expressing endogenous MukF with functionally labelled MukB-YPet. Overlays show co-localisation of MukB with *ori* SN192, (from Nolivos *et al.* 2016).

This suggests that either MukBEF complexes are unable to form in the presence of MukFm or that MukBEFm complexes are unable to form stable associations with the chromosome. This could be the result of perturbed interactions or due to increased off-rates for the MukBEF proteins. An alternative explanation may be that MukBEFm complexes are formed and *do* associate with the nucleoid, however oligomerisation of MukBEF complexes and the ability to form clusters has been lost by the disruption MukF dimerisation, and so foci are not detected.

4.2.3 Single molecule tracking shows that MukBEFm fails to form stable complexes on the chromosome

To analyse further properties of MukFm *in vivo*, a higher resolution technique, Photoactivatable Localization Microscopy (PALM) was used to track the movement of single MukBEF complexes and test whether transient interactions are being made between these complexes and DNA. PALM is a single-molecule approach that allows for live cell visualisation of the behaviour of individual MukBEF complexes by observing apparent diffusion coefficient in a single focal plane (Kapanidis *et al*. 2018). The observed diffusion coefficient is dependent on multiple factors including, interactions with other molecules such as protein partners or DNA. Such interactions can be detected whether they be transient or specific.

The fluorescently labelled proteins are known to be fully functional and the fluorescent domains do not significantly affect the diffusion or localisation on the chromosome (Badrinayanan *et al*. 2012a). Previous work has shown that apparent diffusion coefficients for MukB, E and F were all similar despite their size and shape differences, and therefore assumptions can be made that they are components of the same complex (Badrinayanan *et al*. 2012a).

In a strain where endogenous MukF had been deleted and replaced with an inducible ectopic *mukF* (Badrinarayanan *et al.* 2012b), MukB was tagged with PAmCherry, by lambda Red recombineering (RAB02). Strain RAB02 was transformed with pET-21a carrying Mukd, MukFm and empty vector to test the mobility of complexes formed with Mukd or MukFm. Cells carrying chromosomal PAmCherry-*muk*F with a single mutation (I22T; KK132: courtesy of Dr Kasia Ginda- Mäkelä) were also analysed. In the presence of arabinose, ectopic MukF could be induced in strain RAB02, repletion of MukFd allows for internal controls alongside a strain carrying functional PAmCherry-*muk*F expressed endogenously (Ab256-see chapter 2; Badrinarayanan *et al*. 2012a).

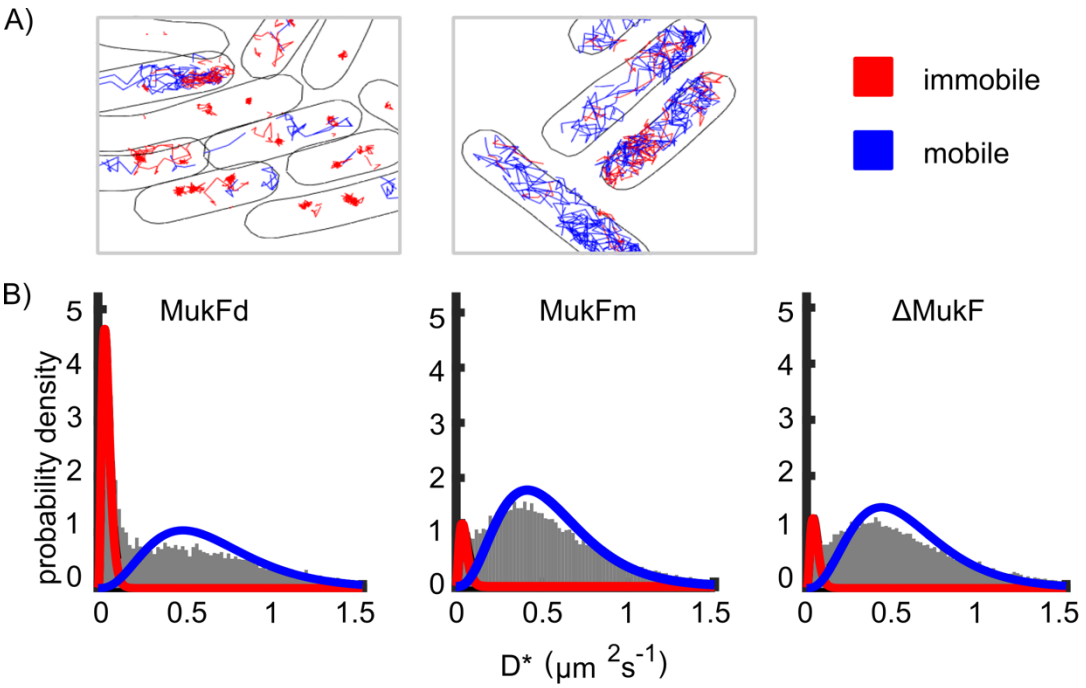

C)

Plasmid expressed MukF variant	% of immobile molecules at D=0.05 glucose	arabinose
MukFd	24.8 ± 1.3	36.8 ± 0.1
MukFm	5.5 ± 2.0	32.8 ± 1.9
MukFsm	7.6 ± 2.0	34.6 ± 1.8
ΔMukF	5.5 ± 1.0	34.6 ± 1.6
strain		
KK132 (MukFsm)	5.0 ± 0.7	-
Ab256 *(ΔmukF para mukF)*		42.1 ± 2.0

Figure 4.iii - Single molecule tracking of MukB-PAmCherry from cells expressing MukFd (WT) and ΔMukF cells expressing MukFm.

A - Examples of tracks in segmented cells. **B** - Measured apparent diffusion coefficients and fits to 2-state models of single- molecule diffusion (Stracy *et al.* 2019). Fraction of immobile molecules (fitted D*=0.05) in cells deleted for MukF with an ectopic MukF under arabinose inducible promoter were transformed with pET-21a carrying a MukF variant.

C- Error estimate is SEM of 3 independent experiments. Data acquired and analysed in collaboration with Dr Jarno Mäkelä.

In cells expressing dimeric MukF, the immobile fraction corresponded to ~30% of all cells (Fig4.iii). In cells deleted for MukF expressing MukFm, either with a single or triple residue substitution, only ~5% of MukBEF molecules were immobile. Upon repletion of MukFd the immobile fraction was similar to that seen at wild type levels.

If MukBEF complexes are being formed containing MukFm they are unable to form a stable association with the chromosome. Observations that diffusion rates are similar to those seen in ΔMukF cells suggest that transient interactions may be abolished.

4.2.4 An ATP hydrolysis deficient MukB mutant binds the chromosome in the absence of MukF

To attempt to test whether MukBEFm complexes were able to transiently associate with DNA, a strain was constructed with a mutation in the Walker B motif of MukB, rendering it ATP hydrolysis deficient (MukB-PAmCherry E1407Q). These cells were also deleted for endogenous *mukF* and carried an inducible ectopic *mukF*. This residue substitution is well characterised and is based upon similar constructs made within the same active domain of ABC-type ATPases (Moody *et al*. 2001, Hirano and Hirano, 2004, Arumugam *et al.* 2003, Badrinarayanan *et al.* 2012a). In this variant, ATP binds, but hydrolysis is impaired, in effect, stabilising head engagement, which is known to be essential in localised spot formation (Arumugam *et al*. 2003; Weitzer *et al*. 2003;

Badrinarayanan *et al.* 2012a). Any transient association of MukBEFm complexes with the chromosome would therefore be trapped.

As expected, cells harbouring MukB^{EQ} in a m*ukF*- strain were temperature sensitive on rich media and this phenotype could only be rescued by transforming with pET-21a carrying WT MukB and concomitantly inducing expression of an ectopic wild type MukF by growth in the presence of arabinose. Intriguingly, the E1407Q mutant protein formed immobile complexes at wild type levels, even in the absence of MukF, indicating that the ATP-dependent head engagement of this protein in the cell can lead to stable chromosome association even in the absence of MukF (Fig 4.iv).

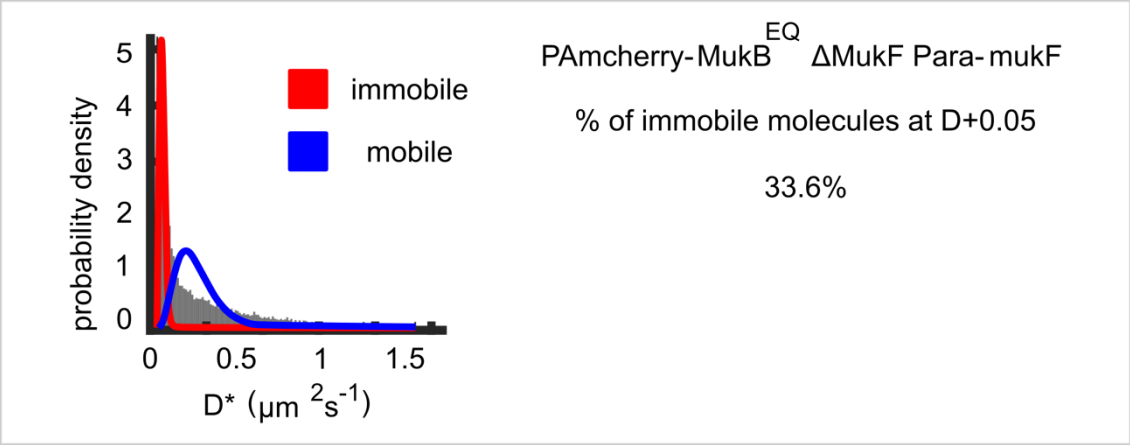

Figure 4.iv - MukB^{EQ} diffusion rates without MukF are similar to wild type MukBEF complexes.

In the strain carrying PAmCherry-*muk*B^{EQ} Δ*muk*F P*ara-muk*F, the percentage of immobile molecules at D*=0.05 was equivalent to that seen in wild type cells at 33.6%.

4.2.5 MukF monomeric variants lacking their C-terminal domain are compromised in binding to MukB

To gain insight into why a Muk- phenotype was observed *in vivo* when dimerisation of MukF was perturbed, I investigated how the formation of MukBEF complexes could be affected by the monomerisation of MukF. The N- terminal 4HB and C- terminal domains of MukF are known to interact with the MukB neck and cap, respectively (See Introduction Figure1.i) and impairment of these interactions leads to complexes being released from the chromosome to give a ΔMukBEF phenotype. Therefore, testing the binding affinity of truncated monomeric MukF variants to MukB *in vitro* may have provided further insight into the dynamic nature of the interaction between MukF and MukB.

For subsequent *in vitro* analyses a truncated variant of MukB (Head/Neck) subsequently abbreviated to $MukB_{HN}$) was used. In this variant the N- and C-terminal ATPase domains are linked through ~30% of their coiled-coils that bind the 4-helix bundle domain of MukF (4HB) (Zawadzka *et al.* 2018). This 91.5 kDa variant is monomeric as it lacks the hinge domain and provides a tool whereby smaller complexes formed by interactions between $MukB_{HN}$ and its binding partners can be resolved by SEC-MALS and native PAGE.

SEC-MALS data from previous studies has shown that full length MukF monomer in the presence of MukE is able to bind to two $MukB_{HN}$ molecules, (Rajasekar *et al.* 2019). However, binding is poor. No complexes with a single $MukB_{HN}$ were observed, indicating that the same $MukB_{HN}$ molecule is unlikely to bind simultaneously to the MukF monomer C-ter and 4HB due to the steric constraints of the elongated MukEFm complex (Woo *et al*. 2009). Higher levels of MukBEFm

complexes were seen in the Walker B mutant, $MukB^{EQ}$, compared to levels seen in the presence of ADP where MukB heads were expected to be unengaged.

A dimeric N-terminal MukF truncation containing the N-terminal WHD and 4-helix bundle (NWD-4HB), has been shown to bind $MukB_{HN}$ with a stoichiometry of $1B_{HN:}2F_{NWHD\text{-}4HB}$. In the presence of an excess of $MukB_{HN}$, low levels of complexes with 2 $MukB_{HN}$ molecules bound were observed (Zawadzka *et al*. 2018). In this study monomeric NWHD-4HB (NmWHD-4HB) was mixed in varying ratios with $MukB_{HN}$. SEC-MALS of the monomeric truncation lacking the middle MukF binding region and C-terminal WHD revealed no detectable binding to $MukB_{HN}$ (Fig. 4.v).

A)

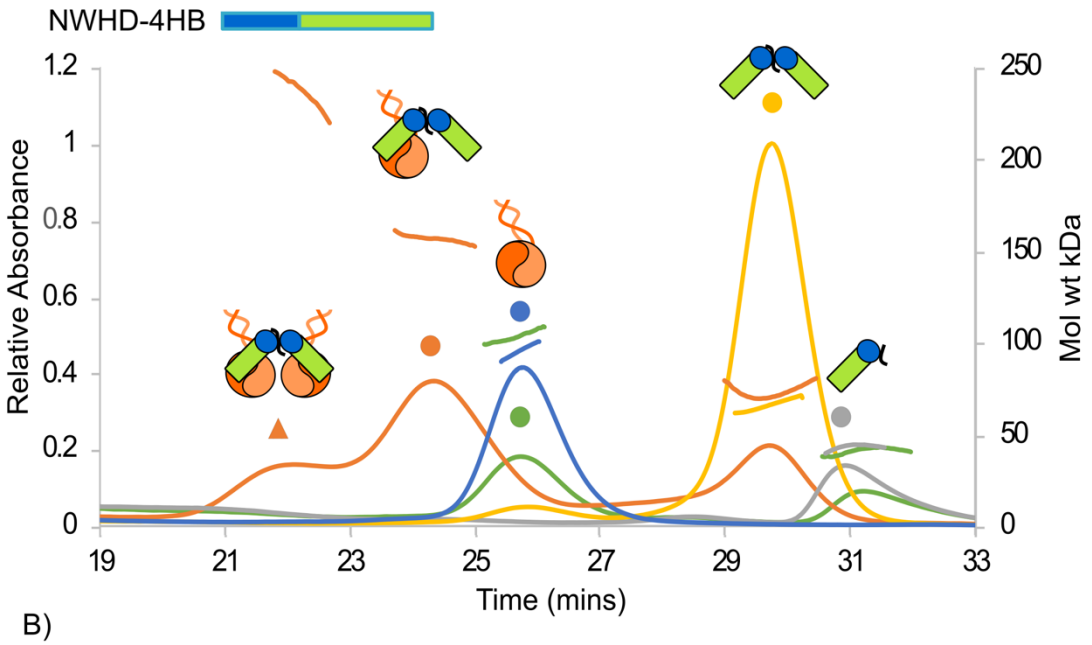

B)

		Complex	Predicted (kDa)	Observed (kDa)
●	NmWHD-4HB:HN	1F-1HN	125	100± 2 *
●	NdWHD-4HB:HN	2F-1HN	162	155± 3
▲		2F-2HN	253	231± 6
●	NmWHD-4BH	1F	34	41± 4
●	NdWHD-4HB	2F	69	72± 6
●	HN	1HN	92	99± 4

Figure 4.v - Binding of monomeric MukF lacking C-terminal to MukB$_{HN}$(HN) is perturbed.

A - SEC-MALS traces with S200 Superose column showed that in excess of MukB$_{HN}$ dimeric NWHD-4HBd is able to bind 2 MukB$_{HN}$ molecules as previously described (Zawadzka *et al.* 2018). **B** - Tabulates predicted and observed complex molecular weights, monomeric NWD-4HBm showed no detectable binding to MukB$_{HN}$ (*).

To further investigate whether transient interactions could be made, MukB$_{HN}$ and NWHD4-HB variants were incubated a room temperature for 30 minutes and then

resolved by native PAGE with the view that this approach could potentially visualise unstable complexes (Fig.vi).

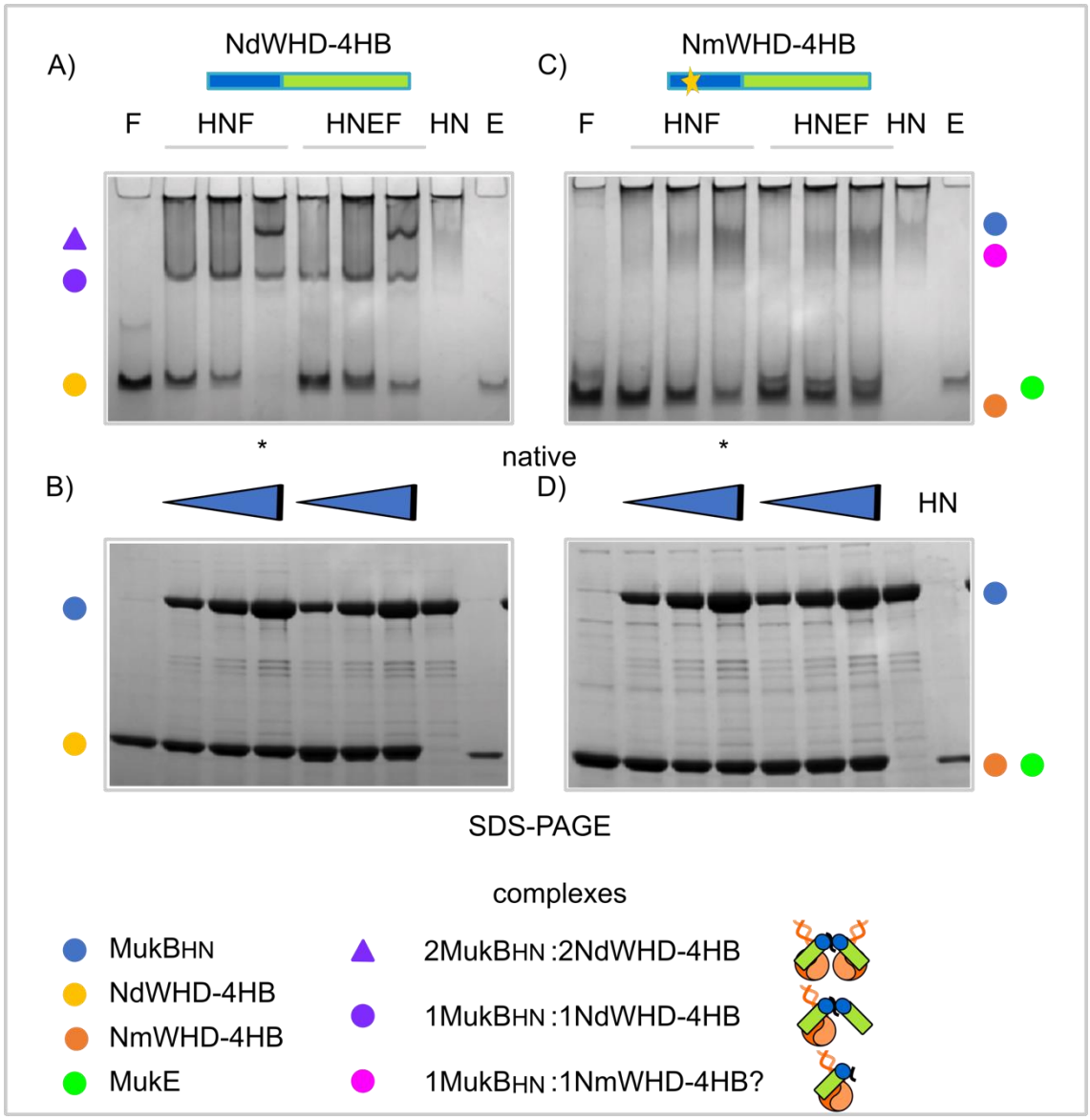

Figure 4.vi - 6% native PAGE analysing the binding of MukF variant to of $MukB_{HN}$ (HN) with increasing concentrations of $MukB_{HN}$.

A & B- SDS and native PAGE respectively of NdWHD4-HB showing complexes formed with increasing relative amount of $MukB_{HN}$ relative amounts 1:2, 1:2 and 2:1 (HN:F). **C & D**- SDS and native PAGE respectively showing the unstable complexes formed with the monomeric variant and increasing amounts of $MukB_{HN}$. An asterisk shows $MukB_{HN}$

in excess which allows for 100% of NdWHD4-HB and ~50% NmWHD-4HB to be bound. As expected, this variant does not bind MukE.

Electrophoresis of purified $MukB_{HN}$ on native PAGE gels showed that this variant runs as a diffuse band. Upon incubation with dimeric NWHD-4HB, sharp bands are resolved. The appearance of a second band on increasing $MukB_{HN}$ relative to NdWHD4-HB, suggested that these bands corresponded to either $1MukB_{HN}:2F_{NWHD\text{-}4HB}$ or the higher complex, $2MukB_{HN}:2F_{NWHD\text{-}4HB}$. This supported earlier conclusions drawn from the SEC-MALS data (Fig 4.v). Incubation with monomeric NmWHD-4HB did not form discrete bands, probably due to the unstable nature of NmWHD4-HB complex with $MukB_{HN}$. The relative binding ability was therefore assessed by quantification of unbound MukF variant in relation to increasing concentrations of $MukB_{HN}$. The assumption was made that this would equate to the formation of complex with $MukB_{HN.}$ It was estimated that NmWHD4-HB demonstrated an approximate reduction of 50% in binding to $MukB_{HN}$.

4.2.6 Binding to MukB of monomeric MukF variants with the middle flexible domain is stabilised in the presence of MukE

Interactions between MukF and MukB are stabilised by binding of dimeric MukE to MukF, and concomitantly, stimulation of MukB ATPase activity by dimeric MukF variants containing the Middle flexible linker (M) is inhibited (Zawadzka *et al.* 2018). Although DNA alone does not stimulate MukB ATPase activity as seen in *B. subtilis* (Hirano and Hirano, 2004) addition of DNA relieves MukE mediated inhibition of ATPase stimulation, suggesting that interplay between these

interactions may regulate MukBEF activity (Zawadzka *et al.* 2018). I therefore wanted to test whether monomeric variants containing the MukE binding domain had increased binding affinity to MukB (Fig 4.vii) and so were able to regulate MukBEF function.

Consistent with the SEC-MALS data previously described, binding of truncated monomeric MukF variants to $MukB_{HN}$ was unstable and higher-order complexes were only observed in the presence of MukE. Monomeric MukF variants lacking the C-WHD were more compromised in binding, again suggesting the C-WHD may act as an anchor when binding to MukB. Masses assigned to these dynamic complexes were highly variable, however higher order complexes were observed in the presence of MukE that may correspond to $MukB_{HN}$ binding with monomeric MukF variant and MukE. This supports previous data (Woo *et al.* 2009), suggesting interactions between the middle region of MukF and MukB in the presence of MukE.

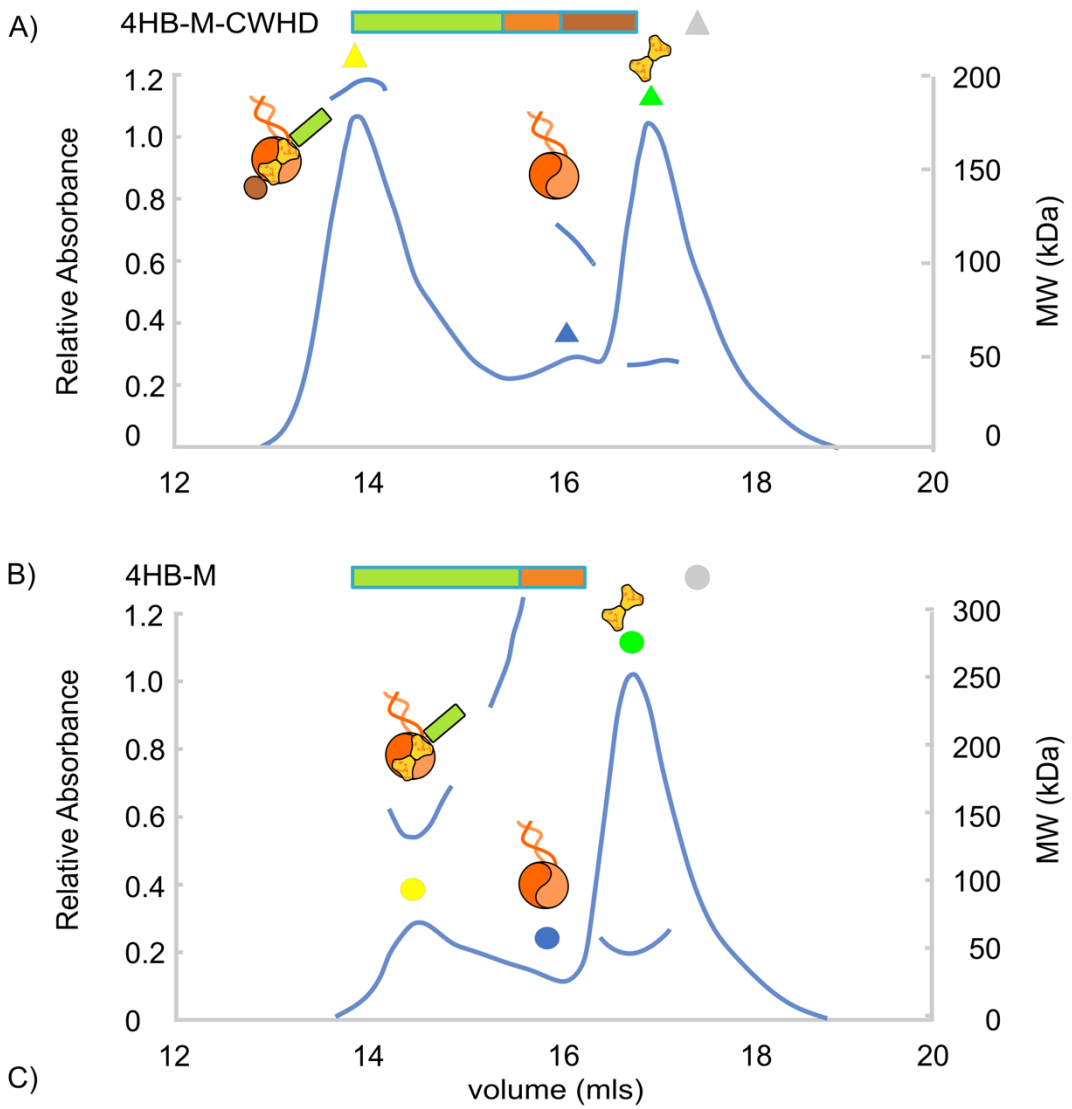

	Complex	Predicted (kDa)	Observed (kDa) ▲	Observed (kDa) ●
▲ ● MukE	2E	58 *	42	55
▲ ● $MukB_{HN}$	1HN	91.5	92	257?
▲ 4HB-M-CWHD	1HN-1F-2E	180.5 *	178	
● 4HB-M	1HN-1F-2E	170.5 *	143	

Figure 4.vii - Unstable binding of monomeric variants to $MukB_{HN}$ can be observed in the presence of MukE.

A & B- SEC-MALS traces of MukF variants 4HB-M-C-WHD and 4HB-M in the presence of $MukB_{HN}$ and MukE. **C**- Tabulated predicted and observed molecular weights. MukE

alone has not been shown to bind to MukB. *Due to the dynamic dimerisation of MukE, a mass of 47 kDa is assigned as determined by SEC-MALS for MukE despite an expected value of 58 kDa (Rajasekar *et al.* 2019; Gloyd *et al.* 2007). The higher value seen at the position where $MukB_{HN}$ was expected to elute in variant 4HB-M is most likely due to complex instability.

To further investigate the complexes observed in SEC-MALS, MukF variants were incubated (as described previously) with increasing concentrations of $MukB_{HN}$, with and without MukE, then resolved by native PAGE (Fig.4.viii). Monomeric MukF harbouring both the 4-helix bundle and C-WHD was found to bind to $MukB_{HN}$ with lower mobility complexes observed with increasing concentrations of $MukB_{HN}$ (Fig. 4.viii). This suggests two heads can be bound as seen with the full-length monomer (Rajasekar *et al.* 2019). In agreement with the results inferred from SEC-MALS (Fig. 4.vii), the variant lacking the C-WHD has reduced binding affinity and as expected was only able to bind one head domain via the 4-HB. Binding affinity of MukB to all monomeric variants carrying the MukE binding domain was increased in the presence of MukE. The severe defect in ATPase activity in variants lacking the C-terminal WHD was not affected by the presence of MukE, and levels of stimulation remained low. Any variation observed due to presence of MukE could not be statistically verified over experimental noise.

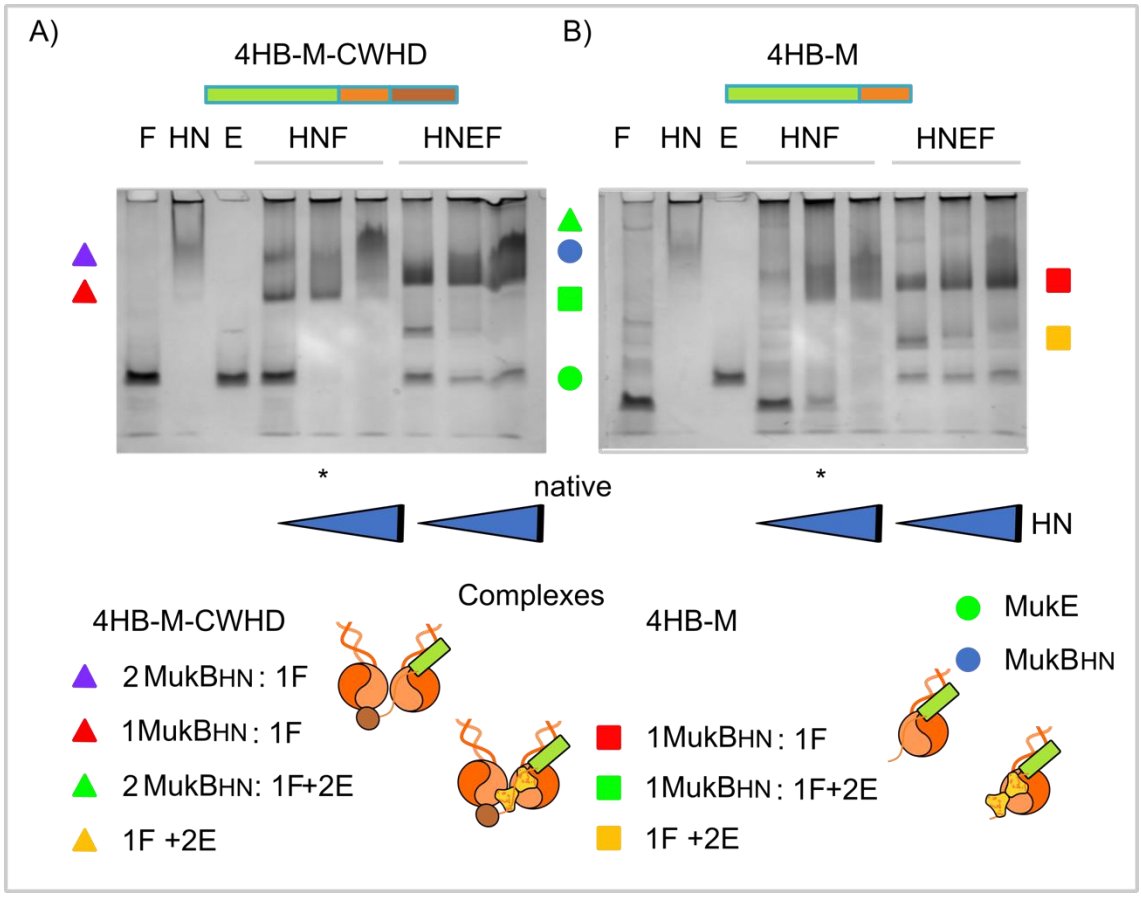

Figure 4.viii - Monomeric MukF variants with middle flexible region have increased affinity to $MukB_{HN}$ (HN) in the presence of MukE.

A- Native PAGE of MukF variant 4HB-M-C-WHD binding to $MukB_{HN}$ with and without MukE. **B**- Native PAGE of MukF variant M-C-WHD binding to $MukB_{HN}$ with and without MukE. In both cases relative increase in $MukB_{HN}$, with ratios of 1HN:2F, 1HN:1F, and 2HN:1F *$MukB_{HN}$ in excess allowing 100% of 4HB-M-C-WHD and ~50% 4HB-M to be bound.

To further confirm the effect of lack of C-WHD on monomeric variants a triple substitution on the NWHD-4HB-M variants was made. ATPase stimulation activity of the NdWHD-4HB-M variant, as seen in previous studies, is approximately 50% of WT MukF. Again, the monomeric variant (NmWHD-4HB-M) is severely compromised in ATPase activation of MukB, as seen with other

monomers with deleted CWHD (see above). Consistent with previous data, size exclusion chromatography also showed that binding to $MukB_{HN}$ was compromised with higher-order complexes only being seen in the presence of MukE. Native PAGE of NmWHD-4HB-M, showed complexes could be formed with $MukB_{HN}$ by the disappearance of the unbound MukF variant (Figure.4.ix). Binding levels were similar to those observed with the MukF variant deleted for both NWHD and CWHD. Diffuse bands suggested that the complexes were unstable, supporting SEC data (not shown). Binding to $MukB_{HN}$ was stabilised in the presence of MukE. MukF variants lacking the CWHD could only bind a single $MukB_{HN}$.

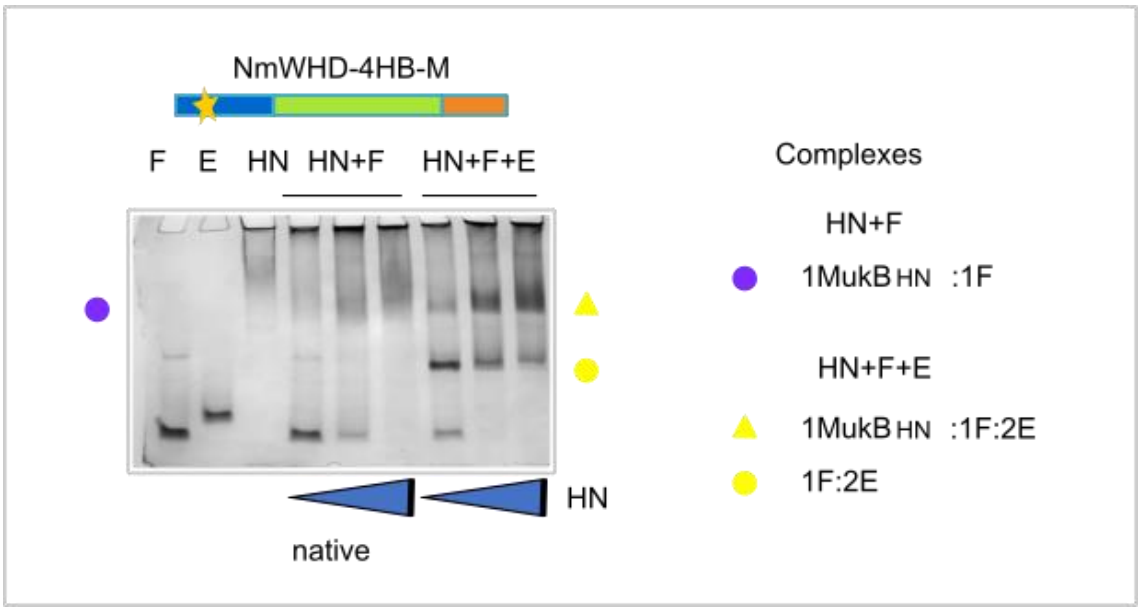

Figure 4.ix - Monomeric MukF lacking CWHD has reduced binding to $MukB_{HN}$ but not abolished.

Binding affinity to $MukB_{HN}$ is comparable to MukF variants with both the N- and C-WHD deleted.

The conclusions for this part of the work was that although compromised, binding to MukB by monomeric MukF variants which have the C-WHD deleted, was not completely abolished. The severe reduction in ATPase stimulation of MukB may therefore not be due to a reduced binding affinity alone, but also as a consequence of the monomeric 4-HB not being in a conformation that allows stable binding or activation of MukB ATP hydrolysis.

4.2.7 Monomeric NWHD-4HB does not bind to MukB *in vivo*

Overexpression of the MukF N-terminal WHD alone, carried on a multi-copy plasmid in wild type cells, led to loss of MukBEF clusters forming foci. This suggests that the MukF N-WHD disrupts endogenous MukF interaction with the neck and cap regions of MukB and is able to compete for binding, Subsequent complexes formed were unable to bind stably to the chromosome (Zawadzka *et al*. 2018).

In this study monomeric MukF N-WHD was overexpressed in cells carrying MukBmYpet from P*ara* promoter in pBAD24 by the addition of 0.2% arabinose. The presence of foci was then tracked by imaging every 20 minutes in cells grown with or without arabinose. As previously reported, loss of MukBEF clusters that form foci was rapid (Zawadzka *et al*. 2018), however in cells expressing NmWHD no loss of foci was observed, suggesting that monomeric interactions were too weak to out-compete endogenous MukF. Future experiments will investigate whether full-length monomeric MukF would have an effect.

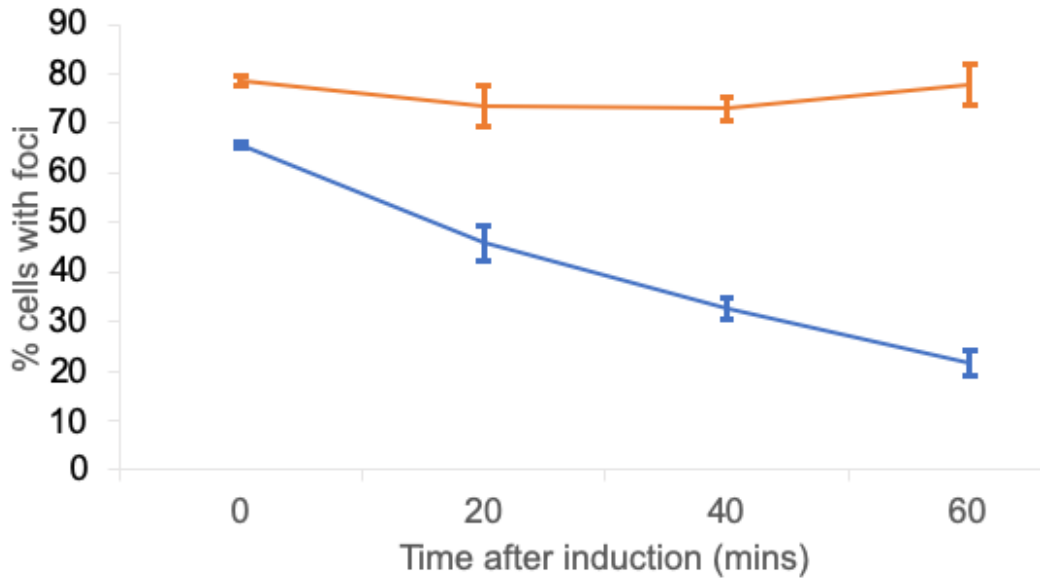

Figure 4.x - Monomeric 4HB is impaired in binding to MukB *in vivo*.

Monomeric MukF NWHD (orange) was overexpressed in cells carrying MukBmYpet from a P*ara* promoter in pBAD24 by the addition of 0.2% arabinose. Presence of foci was then tracked by imaging every 20 minutes and compared to dimeric MukF NWHD (blue).

4.3 Conclusions

Cells expressing monomeric MukF were temperature sensitive in growth on rich media and were unable to form stable MukBEF clusters on the chromosome. No stable or transient interactions of MukBEFm with DNA were observed *in vivo*. Evidence *in vivo* suggested that monomeric MukF lacking C-terminal WHD was unable to bind MukB and so unable to form functional MukBEF complexes. Although monomeric MukF was able to bind MukB *in vitro*, the affinity of this interaction increased in the presence of MukE. Monomeric variants lacking the C-terminal WHD bound weakly to MukB. All this evidence points towards the idea that MukF C-terminal domain may be essential in the conformational alignment of MukF 4HB, accounting for the severe reduction of ATPase stimulation of MukB in the absence of the C-terminal WHD (reported in chapter 3).

In the following chapter I raise the question of whether the MukF dimerisation domain can act as coordinator of MukBEF complexes.

Chapter 5

Will any dimerisation domain do?

5.1 Introduction

Homodimerisation plays a key role in many biological processes (Marianayagam *et al*. 2004). Intertwined homodimers can show conformational flexibility between domains which allows for the spatial positioning of recognition surfaces. Contacts between protomers may be maintained or broken and result in functional regulation.

The proposed ‘rope climber’ model (Badrinarayanan *et al*. 2012a) whereby MukBEF complexes ‘grab’ and ‘release’ distant segments of the chromosome may be stochastic (Ref. Fig 1.iv in introduction). The function of MukBEF may simply depend on the fact that simultaneous hydrolysis of four ATP molecules leading to the release of a complete dimer of dimers complex is less likely than the only 2 events required for the release of a single dimer complex. Or, could the dimerisation domain direct conformational changes that coordinate ATP hydrolysis events between MukBEF complexes? This in effect could lead to active translocation by the ‘rope climber’ model, whereby release of complex A allows for the entrapment of a new DNA segment whilst remaining attached by complex B (Badrinarayanan *et al*. 2012a). In this way, a staggered topological entrapment of DNA coupled with loop extrusion through the SMC kleisin interface could result in a step-based translocation of MukBEF complexes over large base-pair distances that would not need to follow the helical path of the DNA.

5.2 Results

Existing crystal structures of MukF provide no evidence for putative large-scale conformational changes that could be implicated in any molecular switch mechanisms. However, to test whether dimerisation of MukF behaves simply as

a structural tether or has a more dynamic role in the coordination between MukBEF complexes, an inducible synthetic dimerisation domain was introduced to full length MukFm and ΔN-terminal WHD variants. Upon dimerisation, cells were then analysed for rescue of the Muk^- phenotype observed when expressing monomeric MukF.

5.2.1 A synthetic dimer is only formed in the presence of rapamycin

Rapamycin (also known as sirolimus) is a macrolide with antifungal and antibacterial properties. It was first isolated from *Streptomyces hygroscopicus*, found in the soil of the Easter Island, Rapa Nui (Vézina *et al*.1975). This compound is widely used following organ transplant as an immunosuppressant (Buck 2006) but is also a commonly used tool in genetic and biochemical studies. Similar in structure to the immunosuppressant FK506, rapamycin binds a 12 kDa FKBP12 domain and the FRB domain of mTOR. In the absence of rapamycin, these polypeptides do not bind to each other, and rapamycin alone does not bind tightly to FRB (Banaszynski *et al*. 2005). Dimerisation only occurs when rapamycin binds to the FKBP12 domain. This establishes an interaction surface for the FRB domain to then form a tight ternary complex with a dissociation constant in the low nanomolar range (Chen *et al*. 1995). Competition for the FKBP12 site by FK506 allows for a controlled dimerisation of proteins tagged with either the FKBP12 or FRB domain (Fig 5.i).

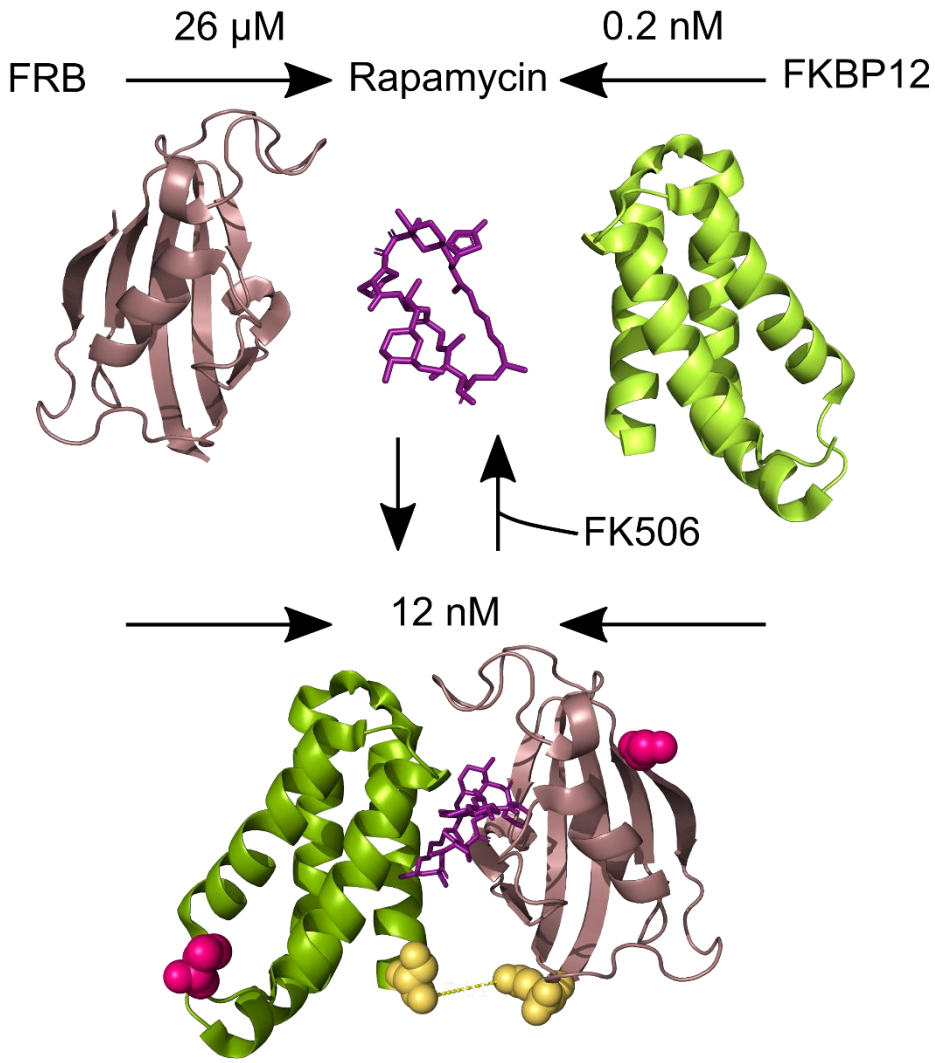

Figure 5.i - FRB and FKBP12 domains only bind in the presence of rapamycin.

The N-terminal of each peptide is coloured magenta. A C-terminal (yellow) fusion of both domains is tagged to MukF via a flexible linker. Rapamycin-induced dimerisation would equate to distance between the sites of conjugation on MukF of ~ 10.7 Å.

5.2.2 MukF function is not affected by fusion of the FKBP12 and FRB tags

FKBP12 and FRB domains that have been codon optimised for *E. coli* (Cui *et al*. 2014) were fused via a flexible linker onto full length MukF, full length monomeric MukF (MukFm) and a truncated variant 4HB-M-C-WHD that has the entire N-

terminal WHD deleted (Fig. 5.ii). Constructs with N-terminal FRB or FKBP12 tags (Ref. methods section 2.3.3) were then subcloned into pETDuet-1 where both genes were co-expressed by the T7 promoter. Proof of concept previously described in *E. coli* by bioluminescence (Cui *et al.* 2014), demonstrated intracellular rapamycin dependent dimerisation.

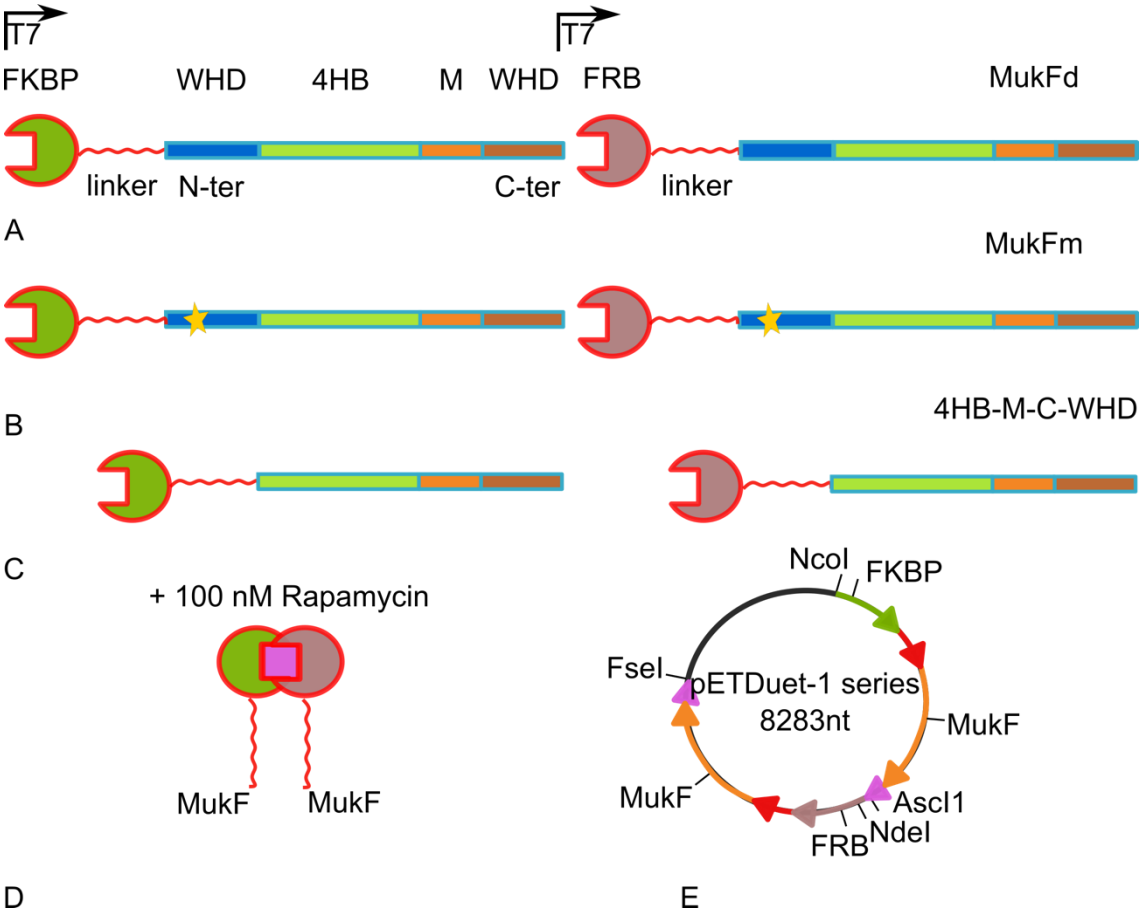

Figure 5.ii - Cartoon of MukF variants N-terminally tagged with either FKPB12 or FRB domains.

A- MukFd tagged with either FKBP12 or FRB. **B-** MukFm tagged with either FKBP or FRB. **C-** 4HB-M-C-WHD variant tagged with FKBP12 or FRB domain. **D-** FKBP12 and FRB domains only bind in the presence of rapamycin. **E-** Tagged MukF variants are cloned into vector pET Duet-1, designed to co-express two target genes. Two multiple cloning sites are preceded by a T7 promoter, lac operator and ribosome binding site.

To demonstrate that MukBEF complexes containing MukFd tagged with FRB or FKBP12 remained functional *in vivo,* cells were challenged with growth at 37˚C in rich media. In complementation assays previously described (see chapter 4), cells deleted for MukF expressing wild type tagged MukFd were able to grow at 37˚C, cell growth was not affected by the addition of 100 nM rapamycin to LB agar plates (Fig. 5.iii). This suggested that tagged MukFd was fully functional. Tagged monomeric MukF variants remained temperature sensitive in growth on rich media, cell growth was not affected by the addition of 100 nM rapamycin to LB agar plates when grown at permissive temperatures (Fig. 5.iii).

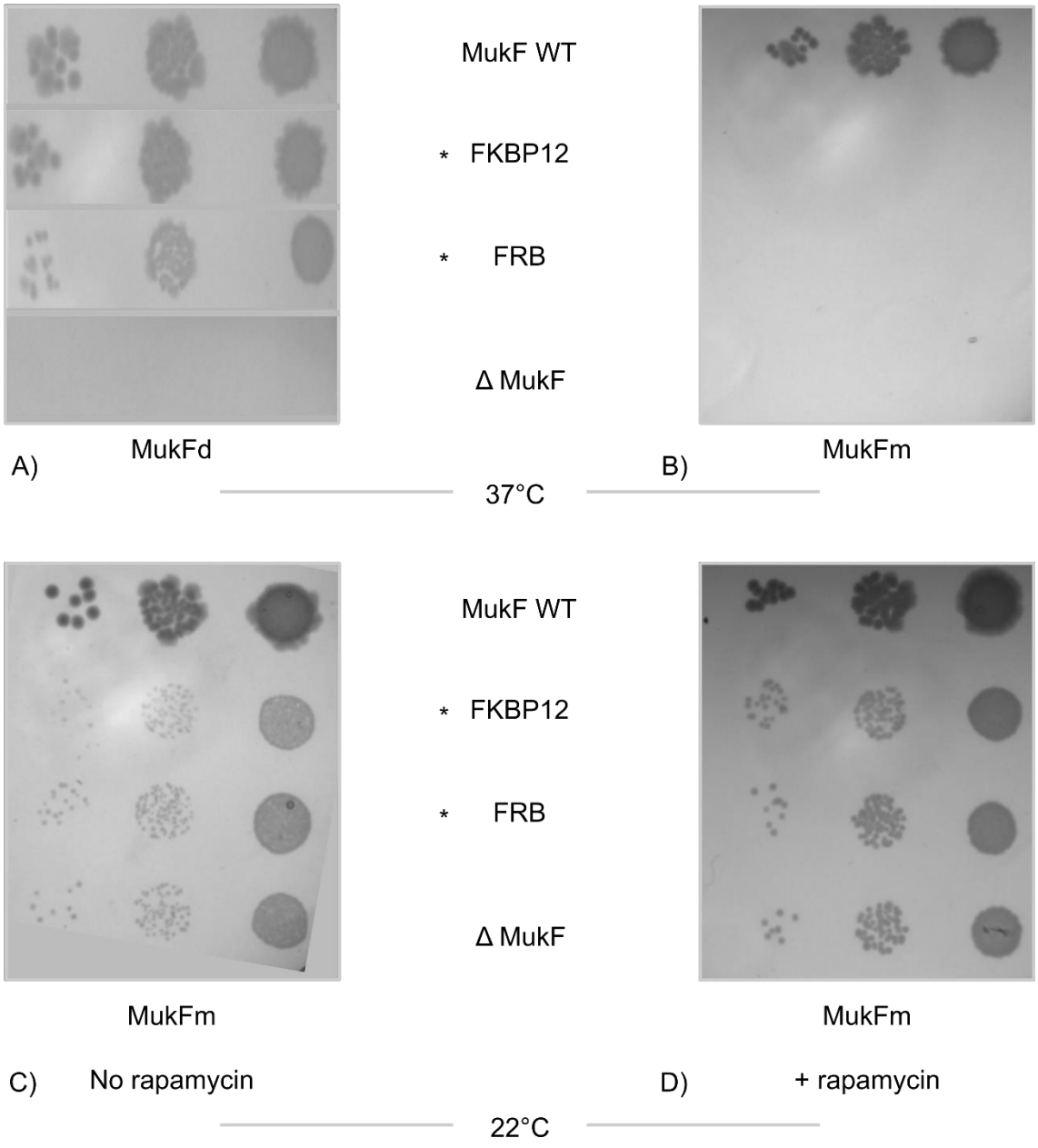

Figure 5.iii - Wild type MukF harbouring N-terminal tags remain functional.

A- Cells deleted for MukF expressing MukFd (WT) with FRB or FKBP12 domain tags (*) were able to grow at 37°C. **B-** Cells expressing tagged monomeric MukF remained temperature sensitive on rich media. **C & D**- Cells were unaffected by the presence of 100 nM rapamycin and able to grow at permissive temperature. Cells deleted for MukF were transformed with pET-21a carrying MukFd or empty vector in all plates to act as positive and negative controls, respectively.

Purification of the tagged MukF proteins over-expressed from the pETDuet-1 vector was carried out as described previously (see methods). Peptide ID by mass spectroscopy confirmed the presence of both the FRB and FKBP12 polypeptides (Fig. 5.iv). The 4HB-M-C-WHD MukF variant tagged with either FRB or FKBP12 hydrolysed 18.31 ±1.14 ATP molecules / MukB dimer / min. This corresponds to ~80% wild type levels and is equivalent to that measured for the untagged version of this variant, providing further evidence that the FRB or FKBP12 fusions did not interfere with function.

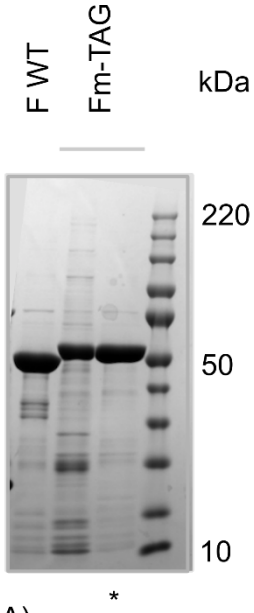

A)

B)

Peptide	Molecular weight kDa	% sequence coverage	Intensity Score
MukFm	50.58	69.1	2.74E+11
FKBP	12.05	61.5	2.48E+10
FRB	12.21	78.2	3.91E+09

Figure 5.iv - Mass Spectroscopy analysis shows MukFm tagged with either FRB or FKBP12 polypeptides are expressed.

A- SDS PAGE showing purification of tagged MukFm. The asterisk denotes purification of FRB-MukFm and FKBP-MukFm following an additional SEC step. Co-expressed FRB and FKBP tagged proteins are not separated as they are of similar size. **B-** Tabulated mass spectroscopy results from purified FRB or FKBP tagged MukFm.

5.2.3 Purified tagged proteins dimerise in the presence of rapamycin.

To test whether the FKBP or FRB domains fused to a monomeric variant of MukF allowed rapamycin dependent dimerisation, 4HB-M-C-WHD (Fig 5.ii) which is potentially equivalent to canonical kleisins, tagged with FRB or FKBP were purified separately. Mixed in equal concentrations, the purified proteins were incubated at room temperature for 10 minutes in varying NaCl concentrations and 100 nM rapamycin. Samples were also incubated with DMSO to confirm that dimerisation was rapamycin dependent. Upon resolution by native PAGE (Fig 5.v), a band shift was observed consistent with the dimeric molecule FRB-4HB-M-C-WHD:FKBP-4HB-M-C-WHD, this suggested that the long linker between the FRB or FKBP tag and 4HB-M-C-WHD MukF variant did not cause any conformational restrictions, so allowing for rapamycin dependent dimerisation of the domains FRB and FKBP12 *in vitro*.

Having ensured that rapamycin was not toxic to *E. coli* at concentrations sufficient to induce efficient dimerisation of MukF monomer *in vitro*, cells were grown in the presence of 100 nM rapamycin for the over-expression of both tagged variants co-expressed using the pETDuet system (Fig 5.ii). Following over-expression, cells were washed to remove rapamycin, all subsequent buffers for lysis and purification did not contain rapamycin. Assumptions were made that any dimerisation subsequently observed would have occurred within the cell (*in vivo*). The FKBP and FRB tagged 4HB-M-C-WHD MukF variants were then co-purified and assessed for dimerisation by native PAGE. Retarded bands equivalent to those seen *in vitro* were then analysed by mass spectroscopy. Both FRB and FKBP polypeptides were again detected with a high intensity score, suggesting

that rapamycin is able to permeate the cell and induce 'synthetic' dimerisation (Fig 5.iv).

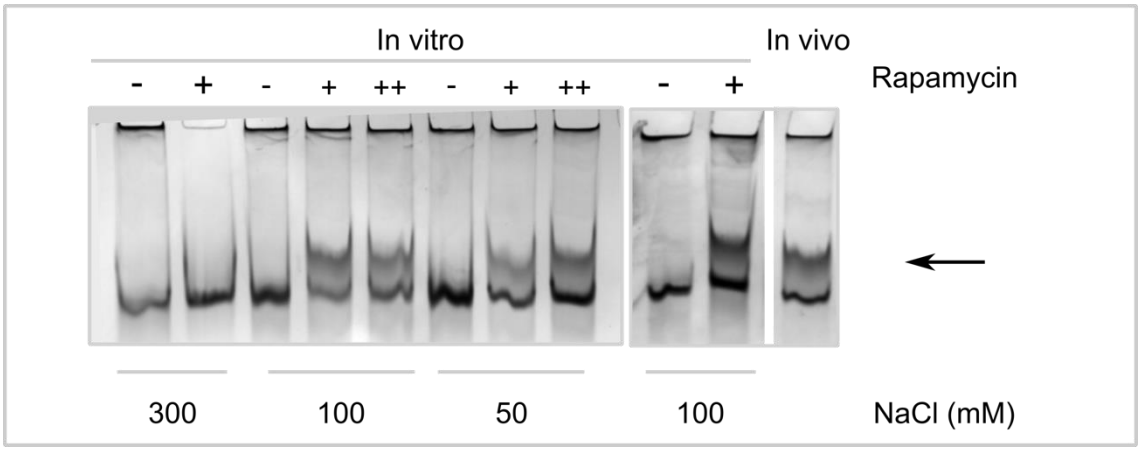

Figure 5.v - Rapamycin induced dimerisation *in vitro* and *in vivo.*

A MukF variant lacking the dimerisation domain (4HB-M-C-WHD) was tagged with FRB or FKBP. Rapamycin dependent dimerisation was observed *in vitro* at rapamycin concentrations of 100 nM (+) or 200 nM (++). DMSO (-) was added as a negative control. The arrow indicates dimeric band analysed by Mass Spectroscopy and confirmed to contain both FRB and FKBP domains, detected at an intensity score of 1.15E+12, FKBP at 1.4E+11 and FRB at 1.2E+11. Intracellular dimerisation (*in vivo*) was observed in cells grown in the presence of rapamycin (removed prior to purification see main text).100% dimerisation was not observed suggesting that the constructs may not be expressed equally by the pETDuet-1 expression vector.

5.2.4 Rapamycin dimerisation does not rescue Muk- phenotype.

To investigate whether the dimerisation domain of MukF simply acts as a structural tether, ΔMukF cells were transformed with pETDuet vector containing two copies of MukF variant each tagged with FKBP or FRB as previously described (Fig.5.ii). Basal expression levels sufficient to recover MukBEF

function was exploited as previously described (methods 2.5.2). Cells were spotted onto LB plates containing 100 nM rapamycin and challenged with growth at the non-permissive temperature of 37˚C. Cells basally co-expressing monomeric variants tagged either with FRB or FKBP remained temperature sensitive, suggesting that if MukBEF complexes were being made with synthetic MukF dimer and that these complexes were not functional.

Similarly cells co-expressing two copies of a MukF variant tagged with either FRB or FKBP were grown in M9 minimal media in the presence of rapamycin and imaged using PALM microscopy as described in Chapter 4. The estimated mean diffusion coefficients measured indicated that the fraction of immobile molecules was comparable to ΔMukF or MukFm cells. Therefore, it is evident that the complexes formed by synthetic dimerisation fail to associate stably with the chromosome (Fig 5.vi).

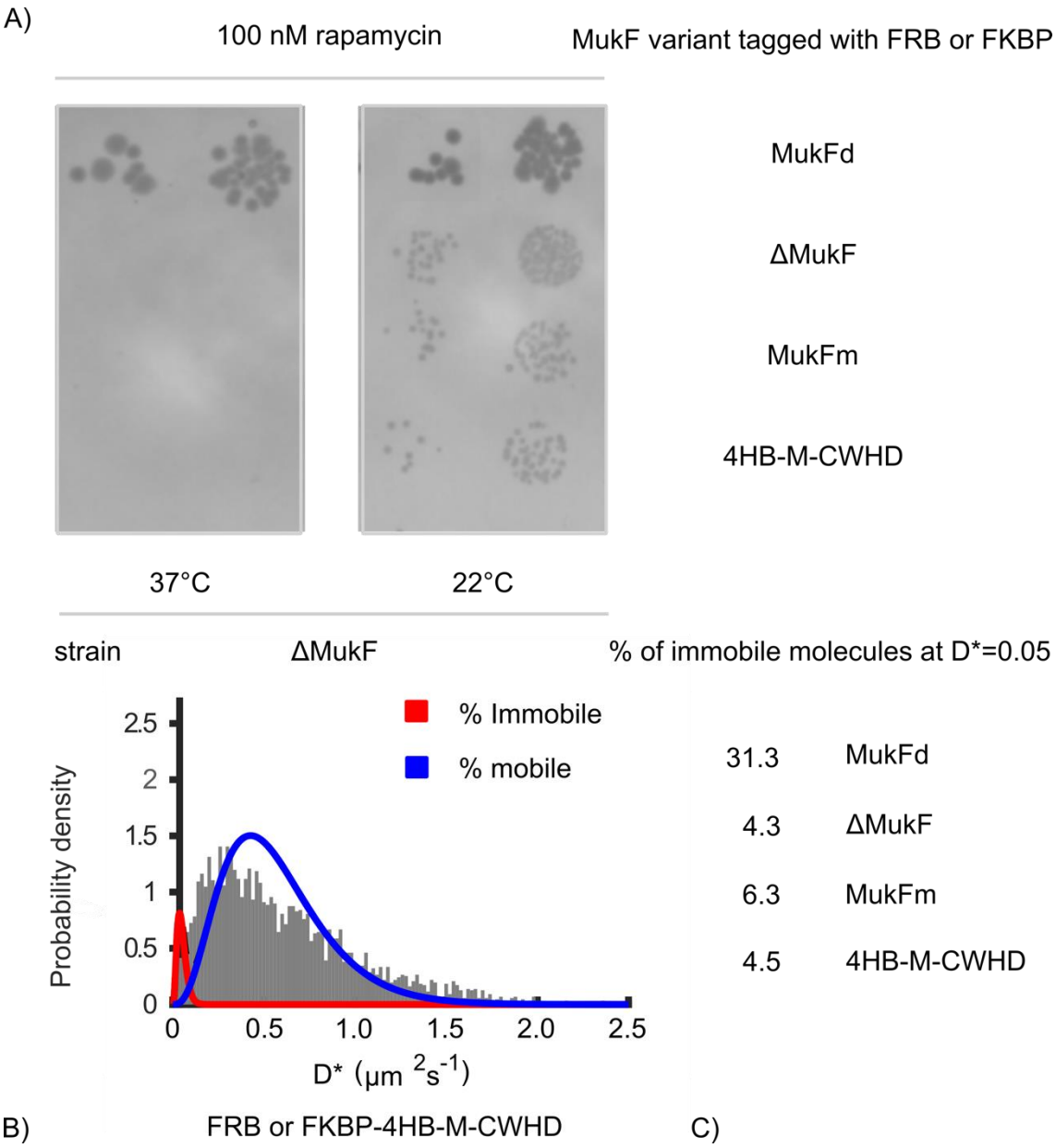

Figure 5.vi - ΔMukF cells expressing MukF variants tagged with FRB or FKBP have a Muk- phenotype.

A - ΔMukF cells carrying pETDuet carrying two copies of MukF variants one tagged with FRB the other with FKBP grown with and without rapamycin, (in both liquid and solid media) remained temperature sensitive if the variant was monomeric. **B** - PALM results. An example of mean diffusion coefficient of ΔMukF cells carrying petDUET carrying two copies of monomeric variant 4HB-M-C-WHD one tagged with FRB the other with FKBP in the presence of rapamycin. **C -** Percentage of immobile molecules with ΔMukF cells

carrying two copies of MukF variants each tagged with either FRB or FKBP in the presence of rapamycin.

5.3 Conclusions

Artificial dimerisation of MukF through a synthetic dimerisation domain failed to rescue the Muk$^-$ phenotype, consistent with the idea that MukF dimerisation domain may have a dynamic role in ‘cross-talk’ between the MukBEF dimer of dimers. The double domain swap between the MukF partners is such that the N-terminal WHD of one protomer cradles the 4-HB of its partner. This intimate interaction may be required for a coordinated ‘relay’ of information. Targeted residue substitutions that selectively disrupts these interactions may provide further insight into the mechanism of DNA transport by higher order MukBEF complexes mediated through the dimerisation of MukF. Alternatively, the synthetic dimerisation domain may not allow for the correct positioning of the 4-HB:MukB neck interaction required for stable DNA loading.

Chapter 6

Discussion and perspectives

6.1 Summary

The recent explosion of interest into the simple question of how DNA is packaged into cells in a manner that allows for efficient chromosome replication and segregation has resulted in a growing amount of evidence that points towards a common mechanism in all domains of life. In addition to the entropic effect of molecular crowding and DNA management by nucleoid-associated proteins (NAPS), the popular and elegant loop extrusion model, whereby a trapped loop is processively enlarged, is arguably the most efficient way of compacting DNA. This model allows for longitudinal order to be maintained and more importantly, individualisation of chromosomes (Nasmyth 2001).

Chromosome management ensures the faithful transfer of genetic material from mother to daughter. Eukaryotic cell division is temporally and spatially regulated, whereas prokaryotic proliferation is a continuous process with segregation occurring concomitantly with replication. Chromosome positioning and choreography of specific loci during the cell cycle is meticulously managed by SMCs and variation between species is reflected by the diversity of accessory factors that are involved (Haering and Gruber 2015). In many bacteria, chromosome organisation and segregation is managed by SMC homodimers and subunits ScpA and ScpB, whereas in *Escherichia coli* and other γ-proteobacteria, the condensin-like MukB, forms complexes with accessory factors MukF and MukE.

Atypically the kleisin MukF is dimeric allowing for the formation of functional multimers seen *in vivo* and *in vitro* (Matoba *et al*. 2005; Woo *et al.* 2009; Badrinarayanan *et al*. 2012a; Rajasekar *et al*. 2019) …the question is if and why is this important?

In this work, I identified conserved hydrophobic interactions involved in dimerisation of the *Escherichia coli* kleisin MukF. I have shown that monomeric MukF was able to stimulate MukB ATPase activity required for a cyclical interaction with DNA, but nevertheless, the dimerisation of MukF *in vivo* is essential for MukBEF function. I therefore propose that the dimerisation of MukF is a prerequisite for the formation of the higher order complexes that are known to be the minimal functional unit required for the management of chromosome organisation (Badrinarayanan *et al.* 2012a).

The question of whether all SMCs work as individual units or as oligomeric complexes is highly debated. *In silico* modelling has suggested that in order for efficient compaction and organisation of the chromosome, loops must be extruded symmetrically (Alipour *et al*. 2012, Goloborodko *et al.* 2016). This idea has been further strengthened by the *in vivo* data from Hi-C experiments (Wang et al. 2015). If back to back complexes extrude loops asymmetrically, ‘gaps’ of non-compacted DNA would be generated (Fig.6.i). If reeling in of DNA was unilateral from a single anchored complex would result in ‘stripes’ on Hi-C maps. Despite this, *in vitro* single molecule imaging of condensin complexes, demonstrate striking, asymmetric extrusion of loops (Ganji *et al.* 2018). To overcome problems of compaction, condensin has been shown to frequently dissociate from DNA and rebind in a random orientation (Walther et al. 2018). More recently it has also been suggested that condensin complexes are able to traverse one another. Time-lapse single molecule images show that a new type of loop termed the Z-loop is formed, whereby two condensin complexes tether three double stranded helices in parallel (Fig 6.i). The Z-loop provides another method of extruding loops symmetrically using an asymmetric ‘motor’ (Kim et al.

2019). In further ground-breaking experiments, the elusive cohesin has also been shown to extrude loops during interphase this time symmetrically and dependent upon ATPase activity and HAWK loading complexes NIPBL and MAU2 (Davidson *et al*. 2019).

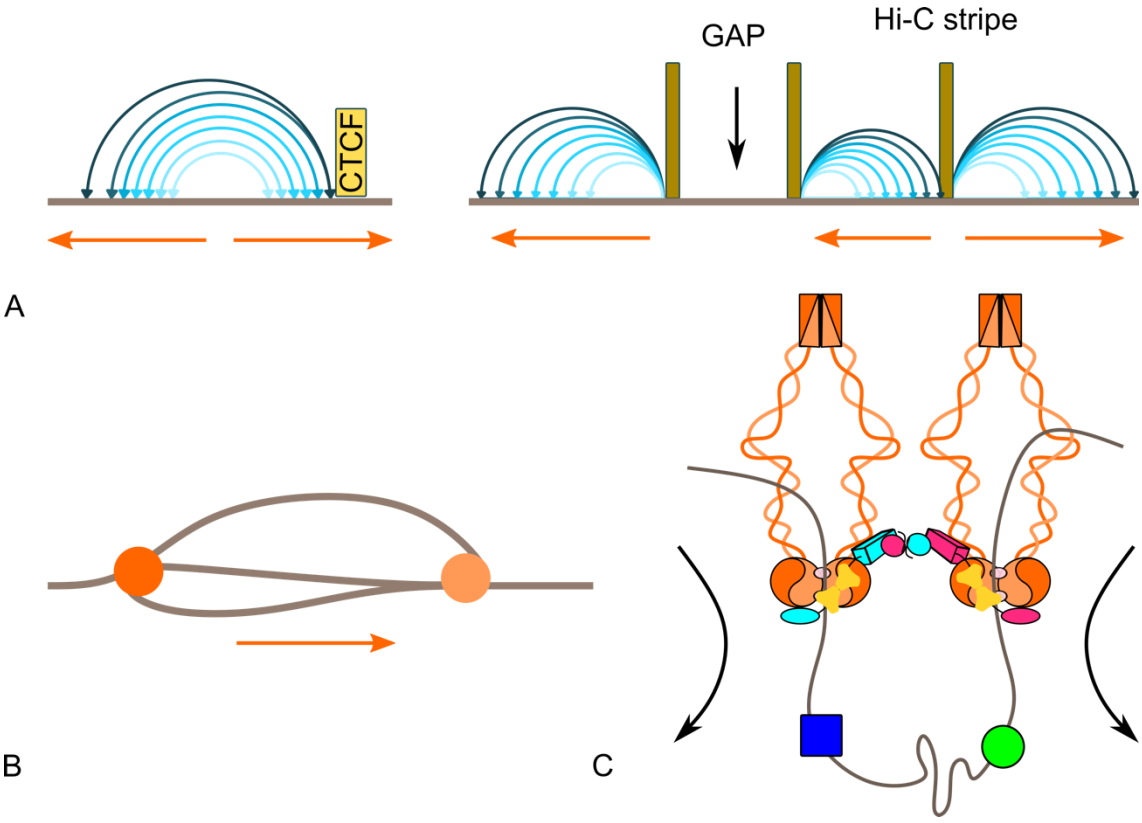

Figure 6.i - Asymmetric loop extrusion results in incomplete DNA compaction.

A- Schematic of symmetric loop extrusion by cohesin during interphase halted at CTCF insulation barriers reproducing TAD formation. Asymmetric extrusion demonstrating expected 'gaps' and 'stripes' (observed in Hi-C analysis) produced due to unfolded regions of DNA. (adapted from Hassler *et al*. 2018). **B-** Cartoon of Z-loops observed by time-lapse single molecule imaging of condensin (Kim *et al*. 2019). **C-** Cartoon of symmetric loop extrusion by dimeric MukBEF complexes.

The work described here suggests that conformational changes, directed by ATP hydrolysis, mediate long-range chromosome transport by a 'rock-climber'

mechanism, which requires multiple DNA contact points and coordination between dimer of dimers. Added to this, symmetrically extruding loops may be facilitated by ‘dimer of dimer’ complexes. This mechanism may be directed by the dimerisation domain of MukF (Fig. 6.i).

6.2 The importance of being a dimer

The dimerisation of proteins has essential biological significance in the regulation of key cellular processes. Heterodimerisation is relatively easy to explain in evolutionary terms, where variations between subunits in substrate binding affinities and recognition sights has advantages. More commonly, however, proteins form homodimers and within that group the most prevalent are those that have a two-fold symmetry (Garton *et al.* 2018). Whilst there is the potential advantage of reducing the genome size (Marianayagam *et al.* 2004), homodimers may be more sensitive to genetic error and also introduce the conundrum of functional regulation.

So why dimerise? Rapid *in vivo* dimerisation may be important for avoiding random association with other proteins so preventing aggregation. Studies have shown that interwoven double domain swaps, observed in MukF, despite possibly requiring a level of post-translational unfolding which could slow the dimerisation process down, contributing greatly to protein stability (MacKinnon *et al.* 2013).

Creating asymmetry within a symmetrical molecule is essential for regulation of function, even if this asymmetry is transient. MukBEF complexes, along with other SMCs, achieve this by the asymmetric binding of their cognate kleisin (Bürmann *et al.* 2013; Zawadzka *et al.* 2018). Allosteric regulation is common amongst homodimers, whereby binding of one domain results in conformational

changes that allow binding in another. This relies on local structural flexibility (Fig.6.i) seen in other systems such as regulation of enzymatic activity, for example, where small conformational changes within subunits can lead to significant changes in catalytic activity (Cui *et al.* 2008). As synthetic dimerisation of monomeric MukF did not form functional MukBEF complexes *in vivo* (See Chapter 5) MukBEF function may also rely on allosteric regulation. Dynamic inter-monomer interaction could regulate catalytic activity of MukB that in turn directs conformational changes essential for the transport of DNA by MukBEF complexes.

Dimer to monomer transition states can also act as molecular switches. The observation that a single mutation within MukF dimerisation domain does not totally abolish the ability to dimerise but disrupts *in vivo* activity suggests that monomerisation may not be an intermediate step required for function or regulation.

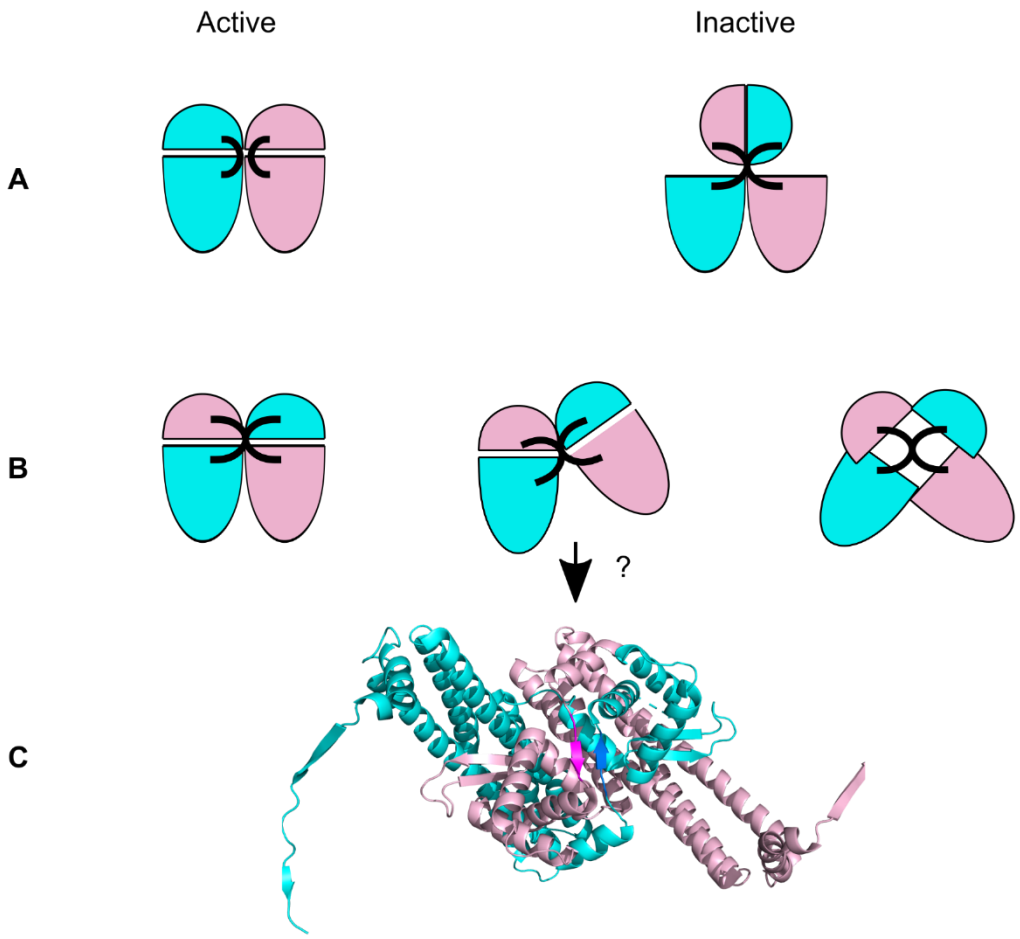

Figure 6.ii - Conformational flexibility allows for regulation of homodimers.

A & B-Examples of active (DNA bound) to inactive transitions of intertwined homodimers encountered in transcriptional regulator proteins (adapted from Garton *et al.* 2018). **C-** The crystal structure of MukF shows the entwined dimerisation (adapted from PDB: 3EUH, Woo *et al*. 2009)

6.3 Dimerise or Die! Monomerisation of MukF results in a Muk-phenotype

There has been some debate as to the whether MukF plays any part in chromosomal organisation by MukBEF complexes, as some *in vitro* studies have suggested that pre-assembled holocomplex is unable to bind DNA. The implication is that MukE and MukF disrupt MukB-DNA interactions (Petrushenko *et al* 2006a) and therefore act to dislodge MukB from the chromosome. MukB

alone was found to be able to bind single or double stranded DNA with equal affinity and promotes efficient supercoiling and catenation in the absence of either ATP or MukE and F. With this evidence, the inference has been drawn that MukB alone may be a key player required for chromosome organisation. (Petrushenko *et al.* 2006a: Bahng *et al*. 2014)

This is somewhat at odds with *in vivo* data, which showed that null mutations in any of the three genes result in a Muk^{-} phenotype and MukBEF localisation is reliant upon the ATPase activity of MukB stimulated only in the presence of MukF (Badrinarayanan *et al.* 2012b). Could the 'serendipitous' PALM result in which the hydrolysis deficient mutant, MukB^{EQ}, stably associated with DNA in the absence of MukF (See Chapter4) provide evidence *in vivo* supporting the above *in vitro* observations? I would suggest however, that this may be physiologically irrelevant. If MukB were able to manage DNA alone *in vivo* this would mean that transient interactions would be observed more frequently by the high resolution of PALM. In the absence of MukF, wild type MukB would also load onto DNA and not be released.

In this work I have established both by SEC-MALS and native PAGE that residue substitutions made within strand ß1 results in the monomerisation of MukF. This was true for both full length and all truncated variants containing the N-terminal WHD. Upon expression of monomerised full length MukF, cells deleted for MukF were temperature-sensitive so displaying the well-documented Muk- phenotype (Nikki *et al*. 1991). This provides (at a simplistic level) a demonstration that MukF has a key role in chromosome management with dimerisation being essential for MukBEF function. This perhaps poses further questions into the mechanistic role of MukF.

I have demonstrated that monomeric MukF is able to bind to MukB (See Chapter 4). This binding is stabilised by MukE and supports recently published work that has shown that monomeric MukF can bind two MukB heads both in the engaged state and in the presence of ADP when MukB heads are assumed to be driven apart (Rajasekar *et al.* 2019). Dimer of dimer complexes (4B:4E:2F) are only detected in the presence of dimeric MukF and furthermore there is a conversion to the MukBEF stoichiometry of 2:4:2 in the presence of ATP. Both forms have been observed *in vivo* (Badrinarayanan 2012a), which would suggest that interconversion between oligomeric states is a functional pathway leading to chromosome management.

I suggest that the function of the kleisin MukF is not simply to act as a bridge, bringing together distant segments of DNA (See Chapter 5). Preliminary evidence points to the fact that dimerisation of MukF may play a role in conformational changes within the MukBEF complex, fuelled by the hydrolysis of ATP. Note that in the absence of C-WHD, binding of monomeric N-terminal domain is severely perturbed with complete loss of function. Perhaps by dimerising, MukF is therefore conformationally restrained with respect to binding to MukB 'neck'. As 100% rapamycin dependent dimerization of MukF variants tagged with FRB or FKBP12 was not achieved either within the cell or *in vitro,* potential problems with uneven expression may have been identified, future analysis by western blotting would compare expression levels to WT MukF.

Disruption in MukF dimerisation (even transiently) results in temperature sensitivity of cells grown in rich media, yet MukFm remains active in stimulation of MukB ATPase. This occurs even in the absence of the entire dimerisation domain (See Chapter 3). By uncoupling ATPase activity with *in vivo* function, the

preliminary evidence presented here shows that dimeric MukF may have a role in both the bridging of DNA and the mediation of conformational changes within the MukBEF complex. Thus, MukF not only establishes oligomeric MukBEF complexes allowing for symmetric loop extrusion but could also coordinate the activity between these complexes.

6.4 Dimerisation of MukF is essential for the formation of 'Dimer of dimers' which is the minimal unit required for chromosome organisation by MukBEF complexes.

From data obtained from quantitative fluorescent microscopy, it has been estimated that there are ~200 dimeric MukBEF complexes per *E. coli* cell, (Badrinarayanan *et al.* 2012a) and of these approximately 50% associate tightly with the chromosome. Out of this sub-population, around 30-50% form clusters with a stoichiometry of 4B:4E:2F. The formation of these localised foci is reliant upon two ATP molecules being sandwiched, *in trans*, at the MukB head dimer interface by the highly conserved Walker A motif of one subunit and the signature motif of the opposite head. Head dimerisation leads to steric expulsion of the C-terminal WHD of MukF and engagement allows MukBEF complexes to associate with the chromosome. Stimulated by MukF, the composite MukB head becomes catalytically active, ATP hydrolysis drives the heads apart, and the separation allows MukBEF complexes to be released from the DNA (Badrinarayanan *et al*. 2012a).

The ATP binding and hydrolysis cycle of events is central to chromosome management but although precise mechanisms and relevance of interplay between complexes with 2:4:2 and 4:4:2 remains unclear, the formation of dimer

of dimers seems to be an essential intermediate for MukBEF function. Once again, this raises a further question, are these oligomeric complexes formed only through the dimerisation of MukF or could MukE provide the glue?

The KITE protein MukE binds avidly as a dimer to the middle region of MukF, transitioning this flexible linker from a disordered to ordered state. Binding of MukF to MukB is stabilised by MukE. By elongating the molecule, interactions are only able to form *in trans*, i.e. the C-terminal WHD and 4-BH of one MukF molecule binds two separate MukB heads (Rajasekar *et al*. 2019). Upon binding of MukE, the ATPase stimulation of MukB is reduced in the presence of DNA, full activity is restored. MukE is therefore thought to have a regulatory role. Unlike MukF, MukE exhibits reversible dimerisation, complexes with stoichiometries of F2E2 and F2E4 have been observed and it is thought that both these forms of complexes are present *in vivo* (Gloyd *et al.* 2007). Could multimerisation of MukBEF complexes be mediated by through the dimerisation of MukE as postulated by Gloyd *et al*. (2007)?

In cells expressing monomeric MukF, the number of cells with foci were at levels similar to cells deleted for MukF. The inability of MukBEF complexes to form clusters with a stoichiometry of 4:4:2 (Badrinarayanan *et al.* 2012a) implies that dimer of dimers are not formed in the presence of monomeric MukF. This gives further support to *in vitro* data (Rajasekar *et al.* 2019) showing that the formation of MukBEF dimer of dimers is dependent upon MukF itself being dimeric. In addition, functional interactions of both MukF 4HB and C-terminal WHD with neck and cap of MukB respectively also proved crucial to the formation of higher order complexes. As monomerisation of MukF induces a Muk- phenotype, this would suggest that the formation of higher order complexes is not only an important

intermediate for MukBEF function but is also dependent upon the dimerisation domain of MukF. This may not be the case for MukE.

6.5 Climbing the ropes.

Fluorescence Recovery After Photobleaching (FRAP) data indicated that MukBEF complexes had dwell times of ~50 seconds. (Badrinarayanan *et al.* 2012a). MukB dimers hydrolyse ~20 molecules of ATP per minute in the presence of MukF and this implies that there may be multiple rounds of ATP hydrolysis occurring without complexes being released from the DNA. This would indicate that somehow a MukBEF dimer is being tethered to the DNA despite hydrolysis driving the heads apart. Together with the MukBEF stoichiometry of 4:4:2 observed in the localised foci, it was proposed that asynchronous and coordinated ATP hydrolysis between multimeric MukBEF complexes would result in reduced turn-over rates (Badrinarayanan *et al.* 2012a). This has supported the 'rope-climber' model discussed earlier, where a step-wise translocation along DNA would result from stochastic grabbing and release of distant segments of DNA (Fig 6.iii).

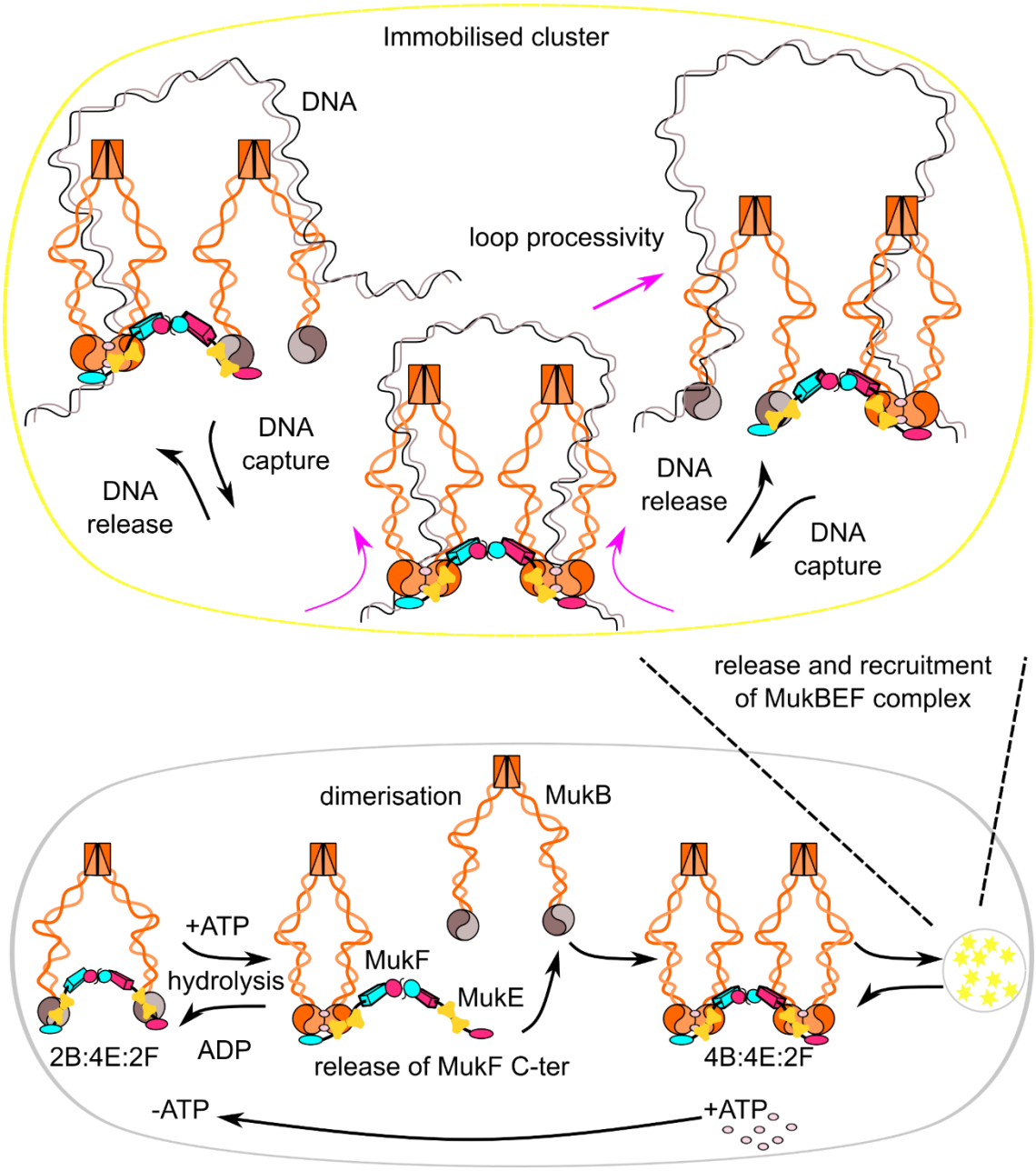

Figure 6.iii - Schematic of MukBEF recruitment to DNA to form clusters of oligomers that direct organisation of the chromosome by the 'rope-climber' model

ATP bound MukB heads shown in orange and ADP bound MukB or -ATP in fawn. (adapted from Badrinaraynan *et al.* 2012a; Mäkelä and Sherratt 2019). Dimeric MukE shown in yellow and dimeric MukF shown with one protomer in cyan and its partner in magenta.

Transient or constant disruption of MukF dimerisation has been shown to be catastrophic for *in vivo* function of MukBEF (See Chapter 4). This supports previous work that the mechanism for transport or organisation of DNA by the 'rope-climber' model is dependent upon the ability to form higher order complexes (Badrinarayanan *et al.* 2012a) and this is mediated through the obligate dimerisation of MukF.

6.6 Safety belt or anchor? Monomeric MukF N- terminal domain interaction with MukB neck is dependent upon C-terminal interaction with MukB cap

Observations made from single molecule tracking in cells expressing monomeric MukF estimated that the percentage of mobile molecules was similar to that in cells deleted for MukF, indicating that any interactions with DNA are disrupted and too transient to be detected. MukFm is able to stimulate ATPase activity of MukB to wild type levels in steady state assays and therefore upon ATP binding, heads dimerise and MukFm is able to direct head engagement. Both of these actions are known to be a requirement for DNA 'loading' (Badrinarayanan *et al*. 2012a), but this raises another question. Why is no DNA interaction detected by PALM with complexes formed by monomeric MukF?

To date there is no conclusive evidence to show whether MukBEF complexes interact with DNA in a topological manner. However, MukF dimers could be acting as a safety belt, stabilising interactions between MukBEF complexes and DNA in order for loops to be processively enlarged in an ATP-dependent manner. There is evidence of this in the eukaryotic condensin complex, whereby transient opening of the kleisin/SMC interface entraps DNA, which is wrapped around the kleisin to prevent dissociation (Kschonsak *et al.* 2017). Low affinity interactions

allow DNA to slide through the Ycg1/Brn1 groove, so forming loops. The hypothesis was later supported by real time imaging showing a single condensin complex reeling in DNA and extruding loops asymmetrically at a rate of up to 1500 bp/s (Ganji *et al*. 2018)

Whether MukF and E form a contact groove that could bind or wrap DNA alone is not known, however MukF dimer has four independent contact points with MukB and this conceivably could result in the formation of two compartments within the SMC ring, between the hinge and head of MukB (S compartment), and between MukB head and MukF (K compartment). Further investigation into binding and ATPase activity of truncated monomeric MukF provided evidence that in addition to being central for the formation of dimer of dimers, dimerisation of MukF stabilizes binding to MukB which could be crucial for the integrity of the MukBEF 'ring'.

As with other kleisins (Bürmann *et al*. 2013; Gligoris *et al.* 2014; Huis in't Veld *et al.* 2014), MukF bridges MukB by binding asymmetrically. The C-terminal WHD interacts with MukB cap and the 4-helix bundle proximal to the N-terminal WHD interacts with MukB neck. Both domains are able to stimulate MukB ATPase activity independently (Zawadzka *et al.* 2018). Upon ATP binding, the MukB heads dimerise resulting in steric expulsion of MukF C-terminal domain and head engagement (Woo *et al.* 2009). This in turn may also result in a reversion to dimeric MukBEF, so switching between oligomeric states (Rajasekar *et al.* 2019). Both full length MukF monomer and the variant deleted for the N-terminal dimerisation domain were able to stimulate MukB ATPase activity to WT levels. However, truncated monomeric variants lacking the C-terminal WHD domain were severely perturbed. Dimeric MukF with C-terminal deletions stimulate MukB

activity to approximately 50% of WT suggesting that C-terminal domain becomes essential in anchoring or positioning the 4HB into an active configuration when lacking a functional dimerisation domain. The reduction in binding to MukB observed by PAGE was reduced but not abolished suggesting that the C-terminal domain has a role in conformational alignment of the 4-HB with MukB neck. This view was supported by further investigation into full length monomeric MukF with MukB mutants that were perturbed in both neck and cap interactions.

In vivo overexpression of the N-terminal and C-terminal MukF truncations results in the disruption of endogenous MukF interactions with MukB neck and cap. The resulting loss of localised foci over time in cells carrying MukB-GFP (Zawadzka *et al.* 2018) inferred that “opening” of the MukBEF ring promotes the dissociation of complexes from DNA. Overexpression of C-terminal domain resulted in a slower loss of foci with a turnover rate estimated to be ~5 fold slower than the N-terminal domain implying that the interaction formed between MukF 4HB and MukB neck may be more dynamic. Thus, cycles of ATP hydrolysis may result in neck disengagement more frequently than cap disengagement, leading to release of DNA.

In similar experiments where monomeric N-terminal WHD-4HB was overexpressed, no loss of foci was observed. This supported the view that monomeric variants lacking the C-terminal were severely deficient in MukB binding and so unable to compete with endogenous MukF. This disparity in binding gives further support to the idea that the kleisin N-terminal and SMC neck may function as a DNA entry or exit gate. A similar mechanism has been proposed in yeast and human cohesin complexes (Huis in’t Veld *et al.* 2014; Beckouët *et al.* 2016).

Disruption of MukF dimerisation resulting in a Muk- phenotype may be a consequence of an inability to anchor or trap DNA within the K chamber. In variants lacking the C-WHD this is more pronounced. The mechanisms by which MukBEF complexes transport or organisation of DNA may therefore be dependent upon the ability of dimeric MukF to form dynamic, robust interactions with MukB neck and cap in addition to allowing for the formation higher order complexes.

6.7 Dimeric MukF is more than a structural bridge

Chromosome organisation cannot rely on random topological entrapments formed by stochastic ‘grabbing’ of distant segments DNA. Random events would result in *trans* interactions that could prevent chromosome segregation. The observation that SMCs localise suggests either specific binding sights or an ability to translocate.

Endogenous overexpression of fluorescently labelled MukBEF complexes shows the decorated DNA to be organised into loops with a thin filamentous axial core, depleted at *ter* in the presence of MatP (Mäkelä and Sherratt 2019). This level of chromosomal organisation provides further evidence that DNA cannot be efficiently managed by stochastic DNA interactions alone. Whilst an increase in occupancy of complexes was observed, dwell times of ~50s remained the same as previously reported (Badrinarayanan *et al*. 2012a), suggesting that dimer of dimers are again central to the formation of stable foci. Furthermore, *in silico* modelling indicates that for loop extrusion to be efficient, it must be bi-directional (Banigan and Mirny, 2019), which in turn implies that if the kleisin acts as an

anchor for unilateral ‘reeling’ of DNA, MukBEF (and maybe other SMCs), must function as a multimeric unit.

Although this reinforces the importance of oligomeric MukBEF complexes through the dimerisation of MukF, it may also point to the importance of MukF in a more dynamic role in coordinating ATP hydrolysis events between complexes.

6.7.1 The MukF dimerisation domain may coordinate between MukBEF complexes

I have provided evidence to support previous data that in order to organise the *E.coli* chromosome efficiently MukBEF complexes function as multimers. Whether multimerisation is unusual to MukBEF is still a matter for debate; however, the obligate dimerisation of MukF may suggest a level of coordination unique to MukBEF complexes that could result in a directed stepwise transport of DNA. Curtains experiments (For method description, Collins *et al.* 2014) have shown that the direction of condensin translocation is random but once translocation commenced, translocation was unidirectional with reversal events being rare (Terawaka *et al*. 2017).

In order to provide the ‘structural bridge’ required for formation of dimer of dimers, a synthetic, inducible dimerisation domain was fused to monomeric MukF variants (See. Materials and Methods). I established that the dimerisation of a variant lacking the N-WHD domain occurred in the cell in the presence of rapamycin (See Chapter 6), however this did not rescue the Muk- phenotype demonstrated in cells expressing monomeric MukF. This preliminary data may infer that the dimerisation domain has a dynamic role in coordination between MukBEF complexes.

Further work is in progress to pinpoint residues that may be involved in intermonomer contacts, which in combination with a heterodimer MukB, could establish a mechanism whereby a signal is ‘relayed’ between MukBEF complexes.

6.8 Are ATP hydrolysis events sequential?

The asymmetric binding of MukF to MukB raises the possibility that each MukB monomer has an exclusive role mediated by non-simultaneous ATP events, a mechanism that is common amongst Walker ATPases (Hopfner 2016). Asymmetric activity between sites has been demonstrated in cohesin whereby ATP hydrolysis at the Smc1A site activated by the C-WHD of Rad21 (kleisin) triggers activity at the Smc3 site (Marcos-Alcade *et al.* 2017). Asymmetric ATPase activity has also been demonstrated in condensin. ATP binding to the Smc4 head induces a conformational change, which promotes head engagement. This enables nucleotide binding to the second active site and disengages the Brn1 N-terminal from Smc2, so opening the condensin ring (Hassler *et al*. 2019). Functionally this asymmetry has led to the observation that both ATPase sites contributed to DNA loading but release was dependent upon one site (Elbatsh *et al.* 2016).

Although the ATP-induced rotation of heads observed in condensin has not been demonstrated in with MukB heads, investigations into truncated monomeric MukF variants has highlighted possible differences in both binding affinity to the neck and cap of MukB, and ATPase activity stimulated by the N-and C-terminal domains. In a system where the SMC units are heteromeric, roles of individual subunits can be analysed by residue substitution, further work is underway to

construct a ‘heteromeric’ MukB molecule by fusing each partner with a different chromatography affinity tag. Residue substitutions made in a monomer with a specific tag would allow us to purify ‘heterodimeric’ MukB molecules and would provide us with an invaluable tool to further demonstrate asymmetrical regulation of MukBEF function.

6.9 Do MukBEF complexes just climb-ropes?

The step-wise translocation observed in single molecule assays with indicate that the stride length may be related to the length of the coiled-coil polypeptide that separates the hinge and head of SMCs (Terawaka *et al.* 2017; Ganji *et al.* 2018). Investigations in to MukBEF indicate that there are discontinuities within the coiled- coil that could allow for conformational flexibility. Negative stain electron microscopy (EM) revealed that MukBEF complexes were folded at a kink or ‘elbow’ midway along coiled-coil, thus bringing about the juxtaposition of MukB hinge with head (Bürmann *et al.* 2019).

Discontinuities and folded structures have also been observed in cohesin complexes (Anderson *et al*. 2002; Haering *et al*. 2002) and further investigation described by Bürmann *et al.* (2019) predicted a common ‘elbow’ in all SMCs sampled. The ability of the coiled-coil to bend that may result from an opposing twist of arms could be fundamental to the ATP dependent mechanism for transport of DNA (Fig 6.iii). The asymmetric twist is conceivably a consequence of the asymmetric binding of the kleisin to SMC heads. This ‘inchworm’ mechanism also relies on one complex acting as the DNA binding site (and is tethered) whilst the other acts as a grapple. The model therefore does not exclude

the idea that oligomeric MukBEF complexes act in concert directed through the dimerisation domain of MukF.

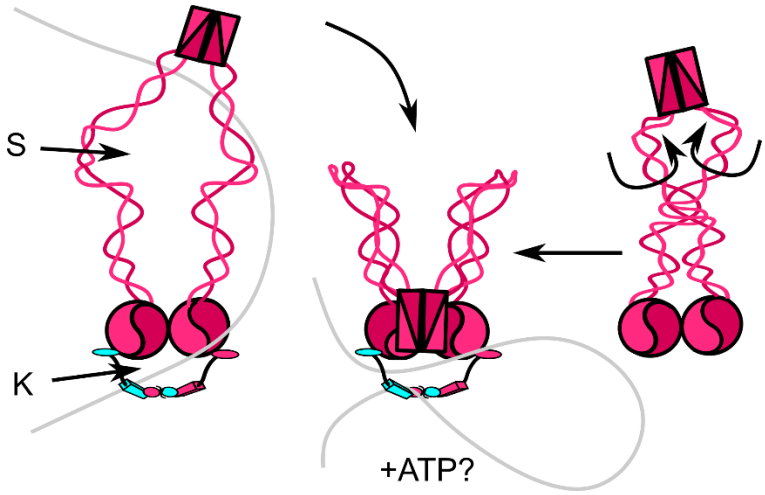

Figure 6.iv - A discontinuity in coiled-coils may be fundamental to the transport of DNA.

Examples of how hinge and heads could be juxtaposed by conformational changes through the coiled-coil. Putative DNA binding sites have been described at hinge and head domains proximal to coiled-coils (Woo *et al*. 2009). (Adapted from Burmann *et al*. 2019).

6.10 Summary and future perspectives

Dimerisation of MukF is required for MukBEF function. To further establish whether the dimerisation domain acts as a dynamic switch that drives conformational changes required for directed transport of DNA, other dimerisation domains have been considered such as those in LexA or TetR. *In vivo* cross-linking at present has proved intractable due to toxicity, however photoactivatable cross-linking could be an option as with the eukaryotic system 'Lovetrap' or 'Ilid' (Guntas *et al.* 2015; Wang *et al.* 2016).

Recent collaborations and advances in our laboratory have been made with the hope that direct single molecule *in vitro* assays, which thus far have proven elusive, will demonstrate DNA translocation and symmetric loop extrusion by MukBEF complexes. With this I will aim to provide further support to the idea that chromosome organisation by MukBEF complexes is dependent upon the stable dimerisation of MukF.

References

Adams D. The Hitchhiker's guide to the galaxy**. Pan Books 1979.**

Alipour E and Marko J.F. Self organisation of domain structures by DNA-loop-extruding enzymes. **Nucleic Acid Res. 2012 40:11202-11212.**

Anderson, D.E, Losada, A, Erickson, H.P, and Hirano, T. Condensin and cohesin display different arm conformations with characteristic hinge angles. **J. Cell Biol. 2002 156:419-424.**

Arumugam P, Gruber S, Tanaka K, Haering C.H, Mechtler K and Nasmyth K. ATP hydrolysis is required for cohesin's association with chromosomes. **Curr. Biol. 2003 13:1930-1940.**

Arumugam P, Nishino T, Haering C.H, Gruber S, Nasmyth K. Cohesin's ATPase Activity is Stimulated by the C-Terminal Winged-Helix domain of its Kleisin subunit. **Current Biol. 2006 16:1998-2008.**

Bachmann B.J. Pedigrees of some *E.coli* K-12. **Bacteriol. Rev. 1972 36:525-557**

Badrinarayanan A, Reyes-Lamothe R, Uphoff S, Leake M.C and Sherratt D.J. *In vivo* Architecture and Action of Bacterial Structural Maintenance of Chromosome Proteins. **Science 2012(a) 26:338(6106).**

Badrinarayanan A, Lesterlin C, Reyes-Lamothe R and Sherratt D.J. The *Escherichia coli* SMC complex, MukBEF, shapes nucleoid organization independently of DNA replication. **J. Bacteriol. 2012(b) 194:4669-4676.**

Banaszynski L.A, Liu C.W, and Wandless T.J. Characterization of the FKBP, Rapamycin, FRB Ternary Complex. **J. Am. Chem. Soc. 2005 127:4715-4721**

Banigan E.J and Mirny L.A. Limits of chromosome compaction by loop extruding motors**. Phys. Rev. 2019 X9, 03100.**

Bahng. S, Hayama R, Marians K. MukB-mediate catenation of DNA is ATP and MukEF independent. **J. Biol. Chem. 2016 291 (46):23999-24008.**

Beckouët F, Srinivasan M, Roig M.B, Chan K.L, Scheinost J.C, Batty P, Hu B, Petela N, Gligoris T, Smith A.C, Strmecki L, Rowland B.D, Nasmyth K. Releasing activity disengages cohesin's Smc3/Scc1 interface in a process blocked by acetylation. **Mol. Cell 2016 61:563–574.**

Britton R.A, Lin C-H & Grossman A.D. Characterization of a prokaryotic SMC protein involved in chromosome partitioning. **Genes Dev. 1998 12:1254-1259.**

Browning D.F, Grainger D.C, Busby S.J. Effects of nucleoid-associated proteins on bacterial chromosome structure and gene expression. **Curr. Opin. Microbiol. 2010 13:773-780.**

Buck ML. Immunosuppression with Sirolimus after solid organ transplantation in children. **Paediatric Pharmacotherapy 2006 12 (2).**

Bürmann F, Shin H-C, Basquin J, Soh Y-M, Gimenez-Oya V, Kim Y-G, Oh B-H, Gruber S. An asymmetric SMC- kleisin bridge in prokaryotic condensin. **Nat. Struct. Mol. Biol. 2013 20:371-379**

Bürmann F, Lee B-G, Than T, Sinn L, O'Reilly F.J, Yatskevich S, Rappsilber J, Bin Hu, Nasmyth K and Löwe J. A folded conformation of MukBEF and cohesion. **Nat. Struct. Mol. Biol. 2019 26:227-236.**

Chapard C, Jones R, van Oepen T, Scheinost. J.C, Nasmyth K. The topology of DNA entrapment by cohesin rings. **bioR*X*iv Dec. 13, 2018.**

Chen J, Zheng X-F, Brown E.J, Schreiber S.L. Identification of an 11-kDa FKBP12-rapamycin-binding domain within the 289-kDa FKBP12-rapamycin-associated protein and characterization of a critical serine residue. **PNAS 1995 92:4947- 4951.**

Cobbe N, and Heck M.M. The evolution of SMC proteins: phylogenetic analysis and structural implications. **Mol. Biol. Evol. 2004 21:332-347.**

Collins. B.E, Ye L-F, Greene E.C. DNA curtains: novel tools for imaging protein-nucleic acid interactions at the single-molecule level. **Methods in Cell Biology 2014 123:217-234**

Cui B, Wang Y, Song Y, Wang T, Li C, Wei Y, Luo Z-Q, Shena X. Bioluminescence Resonance Energy Transfer System for Measuring Dynamic Protein-Protein Interactions in Bacteria. **mbio.asm.org 2014 5(3): e01050-14**

Cui Q, Karplus M. Allostery and cooperativity revisited. **Protein Sci. 2008 17: 1295-1307.**

Ciu.Y, Petrushenko Z.M Rybenkov MukB acts as a macromolecular clamp in DNA condensation. **Nat. Struct. Mol. Biol. 2008 5:411-418.**

Danilova O, Reyes-Lamothe R, Pinskaya M, Sherratt D.J, Possoz C. MukB colocalizes with the oriC region and is required for organization of the two *Escherichia coli* chromosome arms into separate cell halves. **Mol. Microbiol. 2007 65:1485-1492.**

Datsenko K.A, Wanner B.L, One-step inactivation of chromosomal genes in *Escherichia coli* K-12 using PCR products **PNAS 2000 97(12):6640-6645.**

Davis J.H, Baker T.A and Sauer R.T. Small-molecule control of protein degradation using split adaptors. **ACS Chem. Biol. 2011 6(11):1205-1213.**

Davidson I.F, Bauer B, Goetz D, Tang, W, Wutz G, Peters J-M. DNA loop extrusion by human cohesin. **Science 2019 10.1126/Science.aaz3418.**

Diebold-Durand M-L, Lee H, Ruiz Avila L.B, Noh H, Shin H-C, Im H, Bock F.P, Bürmann F, Durand A, Basfield A, Sihyun H, Basquin J, Oh B-H, Gruber S. Structure of Full-Length SMC and Rearrangements Required for Chromosome Organization. **Mol. Cell 2017 271:2309-2328.**

Elbatsh A.M.O, Haarhuis J.H.I, Petela N, Chapard C, Fish A, Patrick H, Celie P.H, Stadnik M, Ristic D, Wyman C, Medema R.H, Nasmyth K, Rowland B.D. Cohesin Releases DNA through Asymmetric ATPase- Driven Ring Opening. **Mol. Cell 2016 61: 575–588,**

Fennell-Fezzie R, Gradia S.D, Akey D and Berger J.M. The MukF subunit of *Escherichia coli* condensin: architecture and functional relationship to kleisins. **EMBO J. 2005 24:1921-1930.**

Garton M, MacKinnon S.S, Malevanets A, Wodak S.J. Interplay of self-association and conformational flexibility in regulating protein function. **Phil. Trans. R. Soc. B. 2018 373 (1749):20170190.**

Ganji M, Shaltiel I.A, Bisht S, Kim E, Kalichava A, Haering C.H, Dekker C. Real-time imaging of DNA loop extrusion by condensin. **Science 2018 360 (6384): 102-105.**

Graham J.E, Sherratt D.J, and Szszelkun M.D. Sequence-specific assembly of FtsK hexamers establishes directional translocation on DNA. **PNAS 2010 107:20263-20268**.

Gligoris TG, Scheinost JC, Bürmann F, Petela N, Chan K-L, Uluocak P, Beckouët F, Gruber S, Nasmyth K, Löwe J. 2014. Closing the cohesin ring: structure and function of its Smc3-kleisin interface. **Science 2014 346:963-967.**

Gligoris T, Löwe J. Structural insights into ring formation of cohesin and related Smc complexes. **Trends Cell Biol. 2016 26:680-693.**

Gloyd. M, Ghirlando R, Matthews L. A, Alba G. MukE and MukF Form Two Distinct High Affinity Complexes. **J. Biol. Chem. 2007 282(19): 14373-8.**

Golodborodko A, Marko J.F, Mirny L.A. Chromosome compaction by active loop extrusion. **BioPhys. J. 2016 110:2162-2168**

Gruber S, Haering C.H, Nasmyth K. Chromosomal cohesin forms a ring. **Cell 2003 112:765-777.**

Guntas G, Hallett RA, Zimmerman S.P, Williams T, Yumerefendi H, Bear J.E, Kuhlman B. Engineering an improved light-induced dimer (iLID) for controlling the localization and activity of signalling proteins. **PNAS 2015 112:112-117.**

Guzman LM, Beli D, Carso M.J, Beckwith J. Tight regulation, modulation, and high-level expression by vectors containing the arabinose pBAD promoter. **J. Bacteriol. 1995 177(14):4121-30.**

Haering, C.H., Löwe, J., Hochwagen, A., and Nasmyth, K. Molecular architecture of SMC proteins and the yeast cohesin complex. **Mol. Cell 2002 9, 773-788.**

Haering C.H Farcas A.M, Arumugam P, Metson J, Nasmyth K. The cohesin ring concatenates sister DNA molecules. **Nature 2008 454: 297-301.**

Haering C.H and Gruber S SnapShot: SMC Protein Complexes Part I. **Cell 2016 164.**

Hassler M, Shaltiel I.A, Haering C.H. Towards a unified model of SMC complex function. **Curr. Biol. 2018 28:1266-1281.**

Hassler M, Shaltiel I.A, Kschonsak M, Bernd S, Merkel F, Thärichen L, Bailey H.J, Macošek J, Bravo S, Metz J, Hennig J, Haering C.H. Structural Basis of an Asymmetric Condensin ATPase Cycle. **Mol. Cell. 2019 74:11751188.**

Hayama R, Marians K.J. Physical and functional interaction between the condensin MukB and the decatenase topoisomerase IV in *Escherichia coli*. **PNAS 2010 107:18826-18831.**

Hirano T. SMC-mediated chromosome mechanics: a conserved scheme from bacteria to vertebrates? **Genes Dev. 1999 13:11-19.**

Hirano T. The ABCs of SMC proteins: two armed ATPases for chromosome condensation, cohesion and repair. **Genes Dev. 2002 16:399-414.**

Hirano T. At the heart of the chromosome: SMC proteins in action. **Nat. Rev. Mol. Cell. Biol. 2006 15:311-322.**

Hirano T. Condensins: universal organizers of the chromosome with diverse functions. **Genes Dev. 2012 26:1659-1678.**

Hirano T, Anderson, D.E, Erickson H.P, Hirano T, Bimodal activation of SMC ATPase by intra- and inter- molecular interactions. **EMBO J. 2001 20:3238-3250.**

Hirano M, Hirano T. Hinge-mediated dimerization of SMC protein is essential for its dynamic interaction with DNA. **EMBO J. 2002** 21**:5733-5744**

Hirano M, Hirano T. Positive and negative regulation of SMC–DNA interactions by ATP and accessory proteins. **EMBO J. 2004 23:2664-2673.**

Hirano T and Mitchison T.J. A heterodimeric coiled-coil protein required for mitotic chromosome condensation *in vitro* **Cell 1994 79:449-458.**

Hofmann A, Mäkelä J, Sherratt D.J, Heermann D and Murray S.M. Self-organised segregation of bacterial chromosomal origins. **eLife 2018 doi:10.7554/eLife.46564.**

Hopfner, K.P. Architectures and mechanisms of ATP binding cassette proteins. **Biopolymers 2016 105:492-504.**

Huis in ’t Veld P.J, Herzog F, Ladurner R, Davidson I.F, Piric S, Kreidl E, Bhaskara V, Aebersold R, Peters J.M. Characterization of a DNA exit gate in the human cohesin ring. **Science 2014 346:968-972.**

Ivanov F, Nasmyth K. A toplogical interaction between cohesin rings and a minichromosome. **Cell 2005 122:849-860.**

Jensen R.B and Shapiro L. The *Caulobacter crescentus smc* gene is required for cell cycle progression and chromosome segregation**. PNAS 1991 96:10661-10666.**

Jensen R.B and Shapiro L. Cell-Cycle-regulated expression and subcellular localization of the *Caulobacter crescentus* SMC chromosome structural protein. **J. Bacteriol. 2003 185:3068-3075.**

Jeppsson K, Carlborg K.K, Nakato R, Berta D.G, Lilienthal I, Kanno T, Lindqvist A, Brink M.C, Dantuma N.P, Katou Y, Shirahige K, Sjögren C. The chromosomal association of the Smc5-6 complex depends on cohesion and predicts the level of sister chromatid entanglement. **PLoS Genet. 2014 10(10):e1004680.**

Kapanidis A.N, Uphoff S and Stracy. M. Understanding Protein Mobility in Bacteria by Tracking Single Molecules. **J. Mol. Bio. 2018 430(22):443-4455.**

Kavenhoff R and Bowen C. Electron microscopy of membrane-free folded chromosomes from *Escherichia coli.* **Chromosoma 1976 16;59(2):89-101.**

Kim E, Kerssemakers J, Shaltiel I.A, Haering C.H, Dekker C.DNA-loop extruding condensin complexes can traverse one another**. https://doi.org/10.1101/682864.**

Kschonsak M, Merkel F, Bisht S, Metz J, Rybin V, Hassler M, Haering C.H. Structural Basis for a Safety-Belt Mechanism That Anchors Condensin to Chromosomes. **Cell 2017 171(3): 588-600**

Lehmann A.R, Walicka M, Griffiths D.J, Murrau J.M, Watts F.Z, McCready S, Carr, A.M. The *rad18* gene of *Schizosaccharomyces pombe* defines a new subgroup of the SMC superfamily involved in DNA repair. **Mol. Cell. Biol. 1995 12:7067-80**

Lim H-S, Kim J-S, Park Y-B, Gwon G-H, Cho Y. Crystal structure of the Mre11Rad50 ATPγS complex: understanding the interplay between Mre11 and Rad50. **Genes Dev. 2011 25:1091-1104.**

Lindow J.C, Britton R.A and Grossman A.D Structural maintenance of chromosomes protein of *Bacillus subtilis* affects supercoiling *in vivo***. J. Bacteriol. 2002 184:5317-5322.**

Lioy V.S, Cournac A, Marbouty M, Espe´li O, Boccard F, Koszul R. Multiscale Structuring of the *E. coli* Chromosome by Nucleoid-Associated and Condensin Proteins. **Cell 2018 172:771-783.**

MacKinnon S.S, Malevanets A, Shoshana J and Wodak S.J. Intertwined Associations in Structures of Homo-oligomeric Proteins. **Structure 2013 21:638-649.**

Mäkelä J and Sherratt D.J. The SMC complex, MukBEF, organizes the *Escherichia coli* chromosome by forming an axial core. **bioR*X*iv 2019 doi.org/10.1101/696872**.

Mascarenhas, J, Soppa, J, Strunnikov, A.V, Graumann P.L. Cell cycle-dependent localisation of two novel prokaryotic chromosome segregation and condensation proteins in *Bacillus subtilis* that interact with SMC protein. **EMBO. J. 2002 21:3108-3118.**

Marcos-Alcalde I, Mendieta-Moreno J.I , Puisac B, Rodríguez M.C, Hernández-Marcos M, Soler-Polo D, Feliciano J. Ramos, Ortega F.J.J , Pié J, Mendieta J and Gómez-Puertas P. Two-step ATP-driven opening of cohesin head. **Scientific Reports 2017 7:3266.**

Marianayagam N.J, Sunde M and Matthews J.M. The power of two: protein dimerization in biology. **Trends Biochem. Sci. 2004 29:618-625.**

Matoba K, Yamazoe M , Mayanagi K, Morikawa K , Hiraga S. Comparison of MukB homodimer versus MukBEF complex molecular architectures by electron microscopy reveals a higher-order multimerization. **Biochemical and Biophysical Research Communications 2005 333:694-702.**

Mercier R, Petit M.A, Schbath S, Robin S, El Karoui M, Boccard F, Espéli O. The MatP/matS site-specific system organizes the terminus region of the E. coli chromosome into a macrodomain. **Cell 2008 135(3):475-85.**

Merkenschlager, M and Nora, E.P. CTCF and cohesin in genome folding and transcriptional gene regulation. **Annu. Rev. Genomics Hum. Genet. 2016 17:17-42**

Melby T.E, Ciampagnolo C.N, Briscoe. G, Erickson H.P The symmetrical structure of structural maintenance of chromosomes (SMC) and MukB proteins: long, antiparallel coiled-coils folded at a flexible hinge. **J. Cell Biol. 1998 142:1595-1604**

Michaelis C, Ciosk R and Nasmyth K. Cohesins: chromosomal proteins that prevent premature separation of sister chromatids. **Cell 1997 3;91(1):35-45**

Minnen A, Bürmann F, Wilhelm L, Anchimuik A, Diebold-Durand M.L, Gruber. S. Control of SMC coiled-coil architecture by the ATPase heads facilitates targeting to chromosomal ParB/ parS and release onto flanking DNA. **Cell Rep. 2016 14:2003-2016.**

Möckel C, Lammens K, Schele A, Hopfner KP. ATP driven structural changes of the bacterial Mre11:Rad50 catalytic head complex. **Nucleic Acids Res. 2012 40:914-927.**

Moody J, Millen L, Bonns D. Huntl J.F, Thomas P.J. Cooperative ATP-dependent Association of the Nucleotide Binding Cassettes during the Catalytic Cycle of ATP-binding Cassette Transporters. **J. Biol. Chem. 2002 277:21111-21114.**

Moriya S, Tsujikawa E, Hassan A.K.M, Asai K, Kodama T, Ogasawara N. A *Bacillus subtilis* gene-encoding protein homologous to eukaryotic SMC motor protein is necessary for chromosome partition. **Mol. Microbiol. 1998 29:179-187.**

Murray S.M *and* Sourjik V. Self-organization and positioning of bacterial protein clusters*.* ***Nat Phys.*** **2017 13*:*1006-1013*.***

Nasmyth K. Disseminating the genome: joining, resolving, and separating sister chromatids during mitosis and meiosis. **Annu. Rev. Genet. 2001 35:673-745.**

Nasmyth K and Haering C.H. The structure and function of SMC and kleisin complexes. **Ann. Rev. Bioch. 2005 74: 595-648.**

Nicolas E, Upton A.L, Uphoff S, Henry O, Badrinarayanan, A, Sherratt D.J. The SMC complex MukBEF recruits topoisomerase IV to the origin of replication region in live Escherichia coli **mBio. 2014 5:e01001-13.**

Niki H, and Hiraga S. Polar localisation of the replication origin and terminus in *Escherichia coli* nucleoids during chromosome partitioning. **Genes and Dev. 1998 12:1036-1045.**

Niki H, Jaffe A, Imamura R, Ogura, T. and Hiraga S. The new gene *mukB* codes for a 177 kd protein with coiled-coil domains involved in chromosome partitioning of E. coli. **EMBO J. 1991 10:183-193.**

Niki H, Imamura R, Kitaoka M, Yamanaka K, Ogura T. and Hiraga S. *E. coli* MukB protein involved in chromosome partition forms a homodimer with a rod-and-hinge structure having DNA binding and ATP/GTP binding activities. **EMBO J. 1992 11:5101-5109.**

Niki H, Yamaichi Y and Hiraga S. Dynamic organisation of chromosomal DNA in *Escherichia coli*. **Genes and Dev. 2000 14:212-223.**

Nolivos S. and Sherratt D.J. The bacterial chromosome: Architecture and action of bacterial SMC and SMC-like complexes. **FEMS Microbiol. Rev. 2014 38:380-392.**

Nolivos S, Upton A.L, Badrinarayanan A, Müller, J, Zawadzka K, Wiktor J, Gill A, Arciszewska L, Nicolas E, Sherratt D.J. MatP regulates the coordinated action of topoisomerase IV and MukBEF in chromosome segregation. **Nat. Comm. 2016 7:10466.**

Ohsumi K, Yamazoe M and Hiraga S. Different localisation of SeqA-bound nascent DNA clusters and MukF-MukE-MukB complex in *Escherichia coli* cells. **Mol. Microbiol. 2001 40:835-845.**

Ono T, Losada A, Hirano M, Myers, M.P, Neuwald A.F, Hirano T. Differential contributions of condensin I and condensin II to mitotic chromosome architecture in vertebrate cells. **Cell 2003 115(1):109-21.**

Palecek, J.J and Gruber, S. Kite proteins: a superfamily of SMC/kleisin partners conserved across bacteria. Archaea and eukaryotes. **Structure 2015 23:2183-2190.**

Peterson C.L. The SMC family: novel motor proteins for chromosome condensation? **Cell 1994 79:389-392.**

Petrushenko Z.M, Lai C-H and Rybenkov V.V. Antagonistic interactions of kleisins and DNA with bacterial Condensin MukB. **J Biol. Chem. 2006(a) 281:34208-34217.**

Petrushenko Z.M, She W & Rybenkov V.V. A new family of bacterial condensins. **Mol. Microbiol. 2011 81: 881-896.**

Rajasekar K, Baker R, Fisher G.L.M, Bolla J.R, Mäkelä J, Tang M, Zawadzka K, Koczy O, Wagner F, Robinson C.V, Arciszewska L.K and Sherratt D.J. Dynamic architecture of the *Escherichia coli* structural maintenance of chromosomes (SMC) complex, MukBEF. **Nucleic Acids Res. 2019 doi: 10.1093/nar/gkz696.**

Ryu J-K, Katan A.J, van der Sluis E.O, Wisse T, de Groot R, Haering C, Dekker C. AFM image of open and collapsed states of yeast condensin suggest a scrunching model for DNA loop extrusion. **Molecular Cell submitted 2019.**

Saitoh N, Goldberg I and Earnshaw W.C. The SMC proteins and the coming of age of the chromosome scaffold hypothesis. **Bioessays 1995 9:759-66.**

Schleiffer A, Kaitna S, Maurer-Stroh, Glotzer M, Nasmyth K, Eisenhaber F. Kleisins: a superfamily of bacterial and eukaryotic SMC protein partners. **Mol. Cell 2003 11(3):571-5**.

Schwartz M.A and Shapiro L. An SMC ATPase mutant disrupts chromosome segregation in *Caulobacter*. **Mol. Microbiol. 2011 82:1359-1374.**

Seifert F.U, Lammens K, Stoehr, Kessler, Hopfner K.P. Structural mechanism of ATP-dependent DNA binding and DNA end bridging by eukaryotic Rad50. **EMBO J. 2016 1:35(7):759-72.**

Soppa J, Kobayashi K, Noirot-Gros, M.F, Oesterhelt, D, Ehrlich, S.D, Dervyn, E, Ogasawara N, Moriya S. Discovery of two novel families of proteins that are

proposed to interact with prokaryotic SMC proteins, and characterisation of the *Bacillus subtilis* family members ScpA and ScpB. **Mol. Microbiol. 2002 45:59-71.**

Stracy M, Wollman A.J.M, Kaja E, Gapinski J, Lee J-E, Leek V.A, McKie S.J, Mitchenall L.A, Maxwell A, Sherratt D.J, Leake M.C, Zawadzki P. Single-molecule imaging of DNA gyrase activity in living *Escherichia coli.* **Nucleic Acids Res. 2019 47:210-220.**

Strunnikov A.V, Larinov V.L and Koshland D. *SMC1*: An essential yeast gene encoding for a putative head-rod-tail protein is required for nuclear division and defines a new ubiquitous protein family. **J. Cell Biol. 1993 123:1635-1648.**

Stylianidou S, Brennan C, Nissen S.B, Kuwada N.U, Wiggins P.A. Supersegger: Robust image segmentation, analysis and lineage tracking of bacterial cells. **Mol. Microbiol. 2016 102:690-700.**

Terawaka T, Bisht S, Eeftens J.M, Dekker C, Haering C.H, Greene E.C**.** The condensin complex is a mechanochemical motor that translocates along DNA**. Science 2017 358(6363):672-676.**

Thadani R, Uhlmann F and Heeger S. Condensin, chromatin cross barring and chromosome condensation. **Curr. Biol. 2012 22 (23) R1012-21.**

Uhlmann F. SMC complexes: from DNA to chromosomes. **Nat. Rev. Mol. Cell Biol. 2016 17:399-412.**

Vazquez Nunez R, Ruiz Avila L.B, Gruber S. Separate Compartments for Chromosome Entrapment and DNA Binding during SMC translocation. Rearrangements Required for Chromosome Organization. **Mol Cell. 2017 67(2):334-347.**

Vézina C, Kudelski A and Sehgal S.N. Rapamycin (AY-22,989), a new antifungal antibiotic. I. Taxonomy of the producing streptomycete and isolation of the active principle. **J. Antibiot. 1975 28(10):721-6.**

Vian L, Pękowska A.P, Rao S.S.P, Kieffer-Kwon K-R, Jung S, Baranello L, Huang S.C, El-Khattabi L, Dose M, Pruett N, Sanborn A.L, Canela A, Maman Y, Oksanen A, Resch W, Li X, Lee B, Kovalchuk A.L, Tang Z, Nelson S, Di Pierro M, Cheng R.R, Machol I, St Hilaire B.G, Durand N.C, Shamim M.S, Stamenova E.K, Onuchic J.N, Ruan Y, Nussenzweig A, Levens D, Aiden E.L, Casellas R. The energetics and physiological impact of cohesin extrusion. **Cell 2018 173(5):1165-1178.**

Walther N, Hossain M.J, Politi A.Z, Koch B, Kuelbeck M, Ødegård-Fougner Ø, *et al.* A quantitative map of human condensins provides new insights into mitotic chromosome architecture. **J Cell Biol. 2018 271:2309-2328.**

Wang H, Vilela M, Winkler A, Tarnawski M, Schlichting I, Yumerefendi H, Kuhlman B, Liu R, Danuser G and Hahn KM. LOVTRAP: an optogenetic system for photo-induced protein dissociation. **Nat. Methods 2016 13:755-8.**

Wang X, Possoz C, and Sherratt D.J. Dancing around the divisome: asymmetric chromosome segregation in *Escherichia coli.* **Genes and Dev. 2005 19:2367-2377.**

Wang, X, Tang, O.W, Riley, E.P, Rudner, D.Z. The SMC condensin complex is required for origin segregation in *Bacillus subtilis.* ***Curr. Biol. 2014* 24*:* 287-292.**

Wang X, Le B.K Lajoie B,R, Dekker J, Laub M.T, Rudner D.Z. Condensin promotes the juxtaposition of DNA flanking its loading site in *Bacillus subtilis.* ***Genes Dev.* 2015 29*:* 1661-1675.**

Wang X, Brandäo H.B, Le T.B.K, Lau M.T and Rudner D.Z. *Bacillus subtilis* SMC complexes juxtapose chromosome arms as they travel from origin to terminus. **Science 2017 355:524-527.**

Weitzer S, Lehane C, and Uhlmann F. A Model for ATP Hydrolysis-Dependent Binding of Cohesin to DNA. **Curr. Biol. 2003 13:1930-1940.**

Wells J.N, Gligoris T.G, Nasmyth K.A, Marsh J.A. Evolution of condensin and cohesin complexes driven by replacement of Kite by Hawk proteins. **Curr. Biol. 2017 27:1-18.**

Wilhelm L., Bürmann F, Minnen A, Shin H-C, Toseland C.P, Oh B-H, Gruber S. SMC condensin entraps chromosomal DNA by an ATP hydrolysis dependent loading mechanism in *Bacillus subtilis*. **eLife 2015:4:e06659**

Whitmore L, Wallace BA Protein secondary structure analyses from circular dichroism spectroscopy: methods and reference databases. **Biopolymers. 2008 89 (5):392-400.**

Woo J-S, Lim J-H, H Shin H-C, Suh M-K, Ku B, Lee K-H, Joo K, Robinson H, J Lee J, S S-Y, Ha N-C, and Oh B-H. Structural Studies of a Bacterial Condensin Complex Reveal ATP-Dependent Disruption of Intersubunit Interactions. **Cell 2009 136:85-96.**

Yamanaka K, Ogura T, Niki H, Hiraga S. Identification of two new genes, *mukE* and *mukF*, involved in chromosome partitioning in *Escherichia coli***. Mol. Gen. Genet. 1996 25;250(3):241-245.**

Yamazoe M, Onogi T, Sunako Y, Yamanaka K, Ichimura T, Hiraga S. Complex formation of MukB, MukE and MukF proteins involved in chromosome partitioning in *Escherichia coli*. **EMBO J. 1999 1;18(21):5873-84.**

Zhao H, Clevenger A.L, Ritchey J.W, Zgurskaya H.I, Rybenkova V.V. *Pseudomonas aeruginosa* Condensins Support Opposite Differentiation States. **J. Bact. 2016 198:2936-2944.**

Zawadzka K, Zawadzki P, Baker R, Rajasekar K.V, Wagner F, Sherratt D.J, Arciszewska L.K. MukB ATPases are regulated independently by the N- and C-terminal domains of MukF kleisin. **eLife 2018;7:e31522.**

Zawadzki P, Stracy M, Ginda K, Zawadzka K, Lesterlin C, Kapanidis A.N, Sherratt D.J. The localization and action of topoisomerase IV in *Escherichia coli*

chromosome segregation is coordinated by the SMC complex, MukBEF. **Cell Reports 2015 13:2587-2596.**